OXIDATIVE MODULATION OF TRANSIENT POTASSIUM CURRENT BY ARACHIDONIC ACID IN BRAIN CENTRAL NEURONS

D i s s e r t a t i o n

zur Erlangung des akademischen Grades
d o c t o r r e r u m n a t u r a l i u m
(Dr. rer. nat.)

im Fach Biophysik
eingereicht an der

Mathematisch-Naturwissenschaftlichen Fakultät I
der Humboldt-Universität zu Berlin

von
Dipl. Mol. Biol. Plamena Angelova
geboren am 4. Juli 1977 in Varna, Bulgarien

Präsident der Humboldt-Universität zu Berlin
Prof. Dr. Christoph Markschies

Dekan der Mathematisch-Naturwissenschaftlichen Fakultät I
Prof. Dr. Christian Limberg

Gutachter:

1. Prof. Dr. Andreas Elepfandt
2. Prof. Dr. Uwe Heinemann
3. Prof. Dr. Dietmar Schmitz

Tag der mündlichen Prüfung: 23.04.07

ABSTRACT

Oxidative stress and dysfunction of potassium channels are believed to play a role in neuronal death in a number of CNS diseases (e.g. Alzheimer's disease, epilepsy).
The present study addresses selective neuronal vulnerability to oxidative stress by studying oxidative modulation of potassium channels in entorhinal cortex (EC) layer II stellate neurons (cell loss early in AD) and layer III pyramidal neurons (early damage in TLE), in comparison to hippocampal CA1 pyramidal neurons (late damage in TLE and AD). Using whole-cell patch-clamp, differential inhibition of transient I_A and delayed rectifier K^+-currents $I_{K(V)}$ by arachidonic acid (AA) and H_2O_2 was demonstrated.
Intracellular AA (1 pM) reduced I_A in EC neurons significantly stronger than in CA1 neurons. AA affected the voltage dependence of steady-state inactivation as well. ETYA mimicked the effect of AA, excluding its metabolites as mediators of I_A modulation. Neither AA nor ETYA reduced $I_{K(V)}$. In contrast, a non-lipid oxidizing agent, H_2O_2 reduced I_A more effectively and robustly attenuated $I_{K(V)}$ in CA1, compared to EC neurons. AA-mediated reduction of I_A was blocked by free radical scavengers (glutathione, ascorbic acid, Trolox).
Antioxidants did not simply inhibit AA and H_2O_2 effects. In particular, they even enhanced AA effects, suggesting more complex modulation of these currents in slices, compared to culture. Moreover, intracellular antioxidants, themselves, influenced maximal conductance and voltage-conductance characteristics of I_A and $I_{K(V)}$. This should be considered in design of anti-oxidative therapies in AD and TLE.
Heterologous expression of Kv1.4 and of Kv4.2 cDNA in HEK-293 cells formed functional channels and elicited A-type currents, which shared similar biophysical characteristics with native I_A from the hippocampus. These currents were strongly decreased upon administration of 1pM AA, demonstrating that at least one of multiple sites for AA action is situated on the pore-forming alfa-subunit of the A-channel.
In conclusion, beside contribution to cell damage, ROS may regulate physiological processes by acting on different signalling pathways. Since voltage-gated K^+-channels underlie many important cellular functions modulation of these channels by ROS would represent a mechanism for fine tuning of cellular processes.

ZUSAMMENFASSUNG

Der neuronale Zelluntergang bei einer Vielzahl von Krankheiten des ZNS, wie z.B. Morbus Alzheimer (AD) und Temporallappenepilepsie (TLE), wird mit oxidativem Stress sowie Fehlfunktionen von Kaliumkanälen in Verbindung gebracht. In dieser Studie soll die selektive neuronale Sensitivität auf oxidativen Stress durch die Messung der oxidativen Modulation von Kaliumströmen untersucht werden. Dabei werden sternförmige Neuronen der zweiten Schicht des entorhinalen Kortex (EC) (bei AD bereits früh geschädigt) mit pyramidalen Neuronen der dritten Schicht des EC (früh geschädigt bei TLE) sowie hippocampalen pyramidalen Neuronen der CA1 Region (bei AD und TLE erst spät geschädigt) miteinander verglichen.
Mittels patch-clamp Ganzzellmessung zeigt diese Studie die differentielle Hemmung spannungsabhängiger transienter (I_A) und „delayed-rectifier" K^+-Ströme ($I_{K(V)}$) durch Arachidonsäure (AA) und Wasserstoffperoxid (H_2O_2). Die intrazelluläre Applikation von AA (1 pM) reduzierte I_A in Neuronen des entorhinalen Kortex signifikant stärker verglichen mit Neuronen des CA1.
ETYA imitiert diesen Effekt, dies schliesst die Metabolite der AA als Mediatoren des Effekts auf Kaliumkanäle aus. Weder AA noch ETYA reduzierten $I_{K(V)}$. Im Gegensatz dazu reduzierte H_2O_2 I_A in Neuronen des CA1 effektiver als in Neuronen der Schichten II und III des entorhinalen Kortex. Die Reduktion des I_A, vermittelt durch AA, wurde durch Radikalfänger (Glutathion, Ascorbinsäure, Vitamin E Analogon Trolox) blockiert. Dabei verstärkten manche dieser Antioxidantien den Effekt der AA, dies legt eine komplexere Modulation dieser Ströme in Schnitten verglichen mit Kulturen nahe. Dies sollte bei der Entwicklung antioxidativer Therapien von AD und TLE berücksichtigt werden.
Bei der heterologer Expression von Kv1.4 und Kv4.2 in HEK-293 Zellen wurden funktionelle Kanäle gebildet und A-Typ Ströme ausgelöst. Diese Ströme wurden nach der Applikation von 1 pM AA stark reduziert.
ROS scheinen neben ihrer zellschädigenden Wirkung physiologische Prozesse zu regulieren, indem sie eine Reihe von Signalwegen beeinflussen. Da spannungsabhängige Kaliumkanäle vielen wichtigen zellulären Funktionen zugrundeliegen, könnte die Modulation dieser Kanäle durch ROS einen Mechanismus für die Feinabstimmung zellulärer Prozesse darstellen.

List of Abbrevations

AA- **A**rachidonic **a**cid; 5,8,11,14-eicosatetraenoic acid

ACSF- **A**rtifical **C**erebro-**S**pinal Fluid

AD - **A**lzheimer's **d**isease

CA1- area **C**ornu **A**monis **1**

Ca^{2+}-**ca**lcium ion

CNS-**c**entral **n**ervous **s**ystem

DMSO- **d**i**m**ethyl **s**ul**f**o**x**ide

ETYA- 5,8,11,14-**e**icosa**t**etra**y**noic **a**cid

GSH- reduced form of glutathione

H_2O_2 - hydrogen peroxide

HEK293 - **h**uman **e**mbryonal **k**idney cell line

I_A- transient potassium current; A-current

$I_{K(V)}$ -delayed rectifier potassium current

IR-DIC-**I**nfra- **R**ed **D**ifferential **I**nterference **C**ontrast

K^+- potassium ion

Kv channels-voltage dependent potassium channels

LTP – **l**ong **t**erm **p**lastisity

mEC- **m**edial **e**ntorhinal **c**ortex

P/S – **p**enicillin-**s**treptomycin mixture

pM - picomol/liter =$1x10^{-12}$ mol/liter

PUFAs-**p**oly**u**nsaturated **f**atty **a**cids

ROS – **r**eactive **o**xygen **s**pecies

RMP - **r**esting **m**embrane **p**otential

SEM-**s**tandard **e**rror of the **m**ean

τ – characteristic time constant

TLE - **t**emporal **l**obe **e**pilepsy

TTX-**t**etrodo**t**o**x**in

List of Tables

List of Figures

INDEX

INTRODUCTION

Voltage-gated potassium currents

Voltage-gated potassium currents were among the first membrane currents to be recognized and investigated for their important roles in neuronal signaling, particularly in the repolarization of the action potential (Hodgkin and Huxley, 1952). The first K^+-current characterized by Hodgkin and Huxley was termed delayed rectifier to describe kinetic that is characterized by delayed onset of activation (compared to the sodium current), followed by little or no inactivation, and outward rectification, i.e. a deviation from the linear current-voltage relationship of Ohm's law.

Almost 20 years later a second type of voltage gated K^+-current has been detected: the transient A-current (I_A) presents with rapid, transient activation in the subthreshold range of membrane potentials (-60 mV to -45 mV), fast inactivation, and fast recovery from inactivation (Connor and Stevens, 1971; Neher, 1971). These features suggest strong contribution to action potential or spike repolarization, and contribute to the regulation of the frequency of the repetitive firing (Baxter and Byrne, 1991; Connor and Stevens, 1971; Hille, 1992; Liss and Roeper, 2001; Rudy, 1988). I_A contributes also to the resting membrane potential (RMP) by the so-called window current (an overlap in the voltage range of current activation and inactivation), and therefore I_A-channels exert a strong influence on steady state inactivation of Na^+-channels. Thereby the A-current plays an important role in the signal processing in the dendrites, including the integration of the synaptic inputs, the filtering of fast synaptic potentials, the temporal regulation of action potential back-propagation from the soma into the dendrite, that is important for the induction of long-term potentiation by its voltage effect on Ca^{2+}-permeation through NMDA receptors (Hoffman et al., 1997; Johnston et al., 2000; Schoppa and Westbrook, 1999; Watanabe et al., 2002). Influencing action potential duration, I_A-channels strongly affect presynaptic Ca^{2+}-influx and transmitter release (Pongs, 1999), affecting synaptic and network excitability (Muller and Misgeld, 1990; Muller

and Misgeld, 1991). The importance of the somatodendritic A-current in regulating firing frequency was recently highlighted by the demonstration that the pacemaker activity of individual dopaminergic neurons in the *substantia nigra,* and hence the level of dopamine release, is directly correlated with the density of the A-current (Liss and Roeper, 2001). For the investigation of function of those and other K^+-currents (leak, Ca^{2+}-dependent, etc.), availability of specific blockers (TEA, 4-AP, Cs^+, dendrotoxin, charibdotoxin etc.) was crucial.

Molecular basis of voltage-gated potassium currents

Fast development of molecular biology, cloning and expression of K^+-channels in the past 20 years made possible a better understanding of K^+-channel physiology and pathophysiology. These studies have demonstrated that potassium channels constitute a very diverse subfamily of ion channels and are composed of variable combinations of subunits encoded in large multigene families. The Kv family of genes encodes subunits of tetrameric voltage-gated potassium channels and is divided into several subfamilies, based on sequence similarities and evolutionary relationship (Coetzee et al., 1999; Cooper et al., 1998; Hille, 1992; Jan and Jan, 1990; Pongs, 1992; Pongs, 1999; Rudy, 1988). This diversity contributes to the ability of specific neurons to respond uniquely to different inputs. Most of the cloned voltage-dependent channels appear to be members of four gene families. Simultaneous research on drosophila and rat resulted in two nomenclatures: voltage-gated potassium channel families can be identified by their Drosophila gene homologue (*Shaker, Shab, Shaw* and *Shal*) or by an alternative nomenclature (Kv1, Kv2, Kv3 and Kv4) (Wei et al., 1990). This classification has physiological consequences, because different subunits of the same family could combine to form functional tetrameric channel (Covarrubias et al., 1991; Salkoff et al., 1992).

Among Kv-α-subunit genes that encode the transient outward Kv channels (I_A) are Kv1.4, Kv3.3, Kv3.4, Kv4.1, Kv4.2 and Kv4.3.

Principal subunits

Kv4.2

Kv4.2 (KCND2, *Shal* family) protein is strongly expressed across the somatodendritic axis of hippocampal CA1 pyramidal neurons (Maletic-Savatic et al., 1995; Sheng et al., 1992), and evidence suggests that the predominant A-type transient current throughout principal neurons of the CNS arises from channels formed by Kv4.2 (Serodio et al., 1994). By Northern blot analysis, (Isbrandt et al., 2000; Zhu et al., 1999) expression of a 6.8-kb transcript was detected only in brain, particularly in the amygdala, caudate nucleus, cerebellum, hippocampus, *substantia nigra*, and thalamus. Heterologous expression determined that KCND2 mediates the rapidly inactivating, A-type outward potassium current which is not under the control of the N-terminus as it is in Kv1 (*Shaker*) channels (Zhu et al., 1999). The somatodendritic A-type (Kv4.2) channels rapidly inactivate close to the action potential firing threshold and recover from inactivation in the millisecond time range (Pak et al., 1991; Serodio et al., 1994). In 2001, Bähring and co-workers suggested that Kv4.2 channels in response to membrane depolarization accumulate in the closed-inactivated state, from which they directly recover, bypassing the open state (Bahring et al., 2001). These features distinguish somatodendritic from other A-type channels.

Pharmacologically, this channel is blocked in a dose-dependent manner by 4-amino pyridine (4-AP) and polyunsaturated fatty acids (PUFA), such as arachidonic acid (AA). The effectiveness of PUFAs, however, is dependent on the gene subfamily that encodes the channel. For example, AA is most efficient in blocking *Shal* (Kv4*)* channels, whereas for *Shaker* (Kv1) channels there are controversial findings (Danthi et al., 2003; Villarroel and Schwarz, 1996).

Kv1.4

Channels from Kv1 (KNCA, *Shaker*) subfamily, for instance Kv1.4, also contributes to somatic transient currents in hippocampal basket interneurons (Zhang and McBain, 1995) and other neurons (Eder et al., 1996; Pardo et al., 1992). Moreover, there is evidence for heteromultimerization of Kv α-subunits from the same subfamily. It has been shown that antibodies, specific to Kv1.4 co-immunoprecipitate Kv1.2 and Kv1.1 proteins in non-denaturated brain membrane extracts (Sheng et al., 1993). The co-expression of Kv1.4 and Kv1.2 in axons and terminals of many cells suggests the native A-type K^+ current may result from Kv1.4/Kv1.2 heteromultimers within these compartments (Sheng et al., 1993; Wang et al., 1999). Such heteromultimere channels will exhibit hybrid pharmacology, for example to TEA. Therefore, there are not enough high-affinity pharmacological tools available for Kv1.4 channels.

Kv1 transient currents inactivate with time constants that change with the voltage and recover from inactivation very slowly (Po et al., 1993; Stuhmer et al., 1989). The inactivation mechanism of Kv1.4 is well understood and could be described as a 'ball-and-chain' interaction (Hoshi et al., 1990; Hoshi et al., 1991). In case of Kv1.4 channel, inactivation domain of the N-terminal of the Kv-α subunit (Zagotta et al., 1990) or of an accessory Kvβ subunit (Rettig et al., 1994) binds to a ball receptor near the inner entrance of the pore (Isacoff et al., 1991) thereby preventing ion flux through the open channel. The fast N-type inactivation of the *Shaker* channels is followed by a slower C-type inactivation, from which the channels recover slowly (Hoshi et al., 1990).

Regulatory subunits of Kv4.2 and Kv1.4

A number of proteins have been discovered recently that have been shown to interact with and modify function of Kv-α proteins, including β-subunits (Kvβs), K^+-channel Interacting Proteins (KChIPs), dipeptidyl aminopeptidase-like proteins (DPPX or DPP10), frequenin, postsynaptic density protein 95 (PSD95), filamin, etc. The physiological role of many of these proteins in native channels remains to be clarified.

β-subunits

Kvβ-subunits are proteins that are essential components of the Kv1 subfamily of voltage-gated potassium channels and are non-enzymatic homologues of aldo-keto reductases (Campomanes et al., 2002; Gulbis et al., 1999; McCormack and McCormack, 1994). Transient K^+ channels, formed by Kv1.4 proteins (and by other Kv1 α-subunits), complex with β-subunits that confer fast inactivation to otherwise non-inactivating Kv1 channels (Heinemann et al., 1996; Rettig et al., 1994). Furthermore, in this case, interaction of Kv1 with beta subunits slows down the recovery from inactivation (Heinemann et al., 1995; Heinemann et al., 1996; Serodio et al., 1996).

Another role assigned to the β-subunits is to act as chaperones during channel biosynthesis (Shi et al., 1996) and thus to increase expression levels, an effect first described for the interaction of Kvβ2 with Kv1.4 (McCormack et al., 1995).

K^+-channel Interacting Proteins (KChIPs)

Potassium channel interacting proteins (KChIPs) were found to co-immunoprecipitate and co-immunolocalize with Kv4 α-subunits in brain and heart (An et al., 2000). All KChIP subunits possess a high sequence homology region to neuronal calcium sensor-1 (NCS-1; frequenin) and calsenilin/DREAM, which belong to the superfamily of EF-hand-containing proteins. Therefore, a role for cytoplasmic calcium in the regulation of Kv4 channel function has been suggested (An et al., 2000; Weiss and Burgoyne, 2001).

It has been demonstrated that frequenin itself is responsible for a Ca^{2+}-dependent enhancement of Kv4 expression and modulation of kinetic behaviour (Nakamura et al., 2001). In agreement, KChIPs interact with NH_2 terminus of Kv4 proteins and enhance surface expression, thereby increasing I_A current densities when expressed in heterologous systems and in native tissues (An et al., 2000; Hatano et al., 2002; Liss and Roeper, 2001). For example, KChIP4a delays channel opening, but when the channel opens, it favours its open state by disrupting fast inactivation and slowing channel closing (Holmqvist et al., 2002). In contrast, KChIP1 speeds up inactivation from closed state and accelerates channel closing (Beck et al., 2002). Coexpression of KChIP1 in oocytes and mammalian cells results in increased current densities, slowed onset of inactivation, and accelerated recovery from inactivation (Nakamura et al., 2001; Hatano et al, 2002). Moreover, it has been shown that a defect in the KChIP2 gene results in complete loss of transient outward current (I_{to}) in cardiac myocytes (Kuo et al., 2001).

Postsynaptic density protein (PSD-95)

PSD-95, a scaffolding synapse-associated protein that possesses PDZ domains, associates with Kv4.2 and Kv1.4. It has been shown that PSD-95 influences Kv1.4 channel clustering (Hsueh and Sheng, 1998) and Kv4.2 channel surface expression without affecting total channel levels (Wong et al., 2002).

Dipeptidyl peptidase-like protein (DPPX)

DPPX (also known as DPP6 or BSPL) is a glycoprotein that is structurally related to the dipeptidyl aminopeptidase and cell adhesion protein CD26, but with unknown function. DPPX is co-expressed with the principal subunits of I_A-Kv4 in a somatodendritic pattern in central nervous system (CNS) neurons. DPPX associates with the pore-forming subunit Kv4 and drastically increases their intracellular trafficking and membrane targeting (Nadal et al., 2003).

Moreover, function reconstitution experiments in *Xenopus oocytes* and CHO cells demonstrated that DPPX increases the rate of inactivation of Kv4.2 currents, considerably decreases time to peak, shifts the voltage-dependence of both activation and steady-state inactivation to the left and also increases the rate of recovery from inactivation (Nadal et al., 2003).

Molecular basis of $I_{K(V)}$

Several candidate genes exist for being the molecular determinants of the delayed rectifier potassium current in pyramidal neurons. Among them are Kv2.1, Kv2.2 and Kv1.1 (Blaine and Ribera, 2001). This non-inactivating potassium current, known also as sustained potassium current, plays a major role in membrane repolarization during an action potential. Kv2 family is widespread throughout the CNS and in hippocampus, is localised on somata and dendrites of pyramidal cells and interneurones. Pharmacologically the delayed rectifier currents are sensitive to TEA and to high concentrations of 4-AP.

Structure of a Kv channel

After the cloning and expression of Kv-channel proteins it became possible to study the structure of Kv channels after cristallization and x-ray crystallography of the channel proteins. Kv potassium channels are tetramers and their monomers contain six transmembrane α-helical segments (S1-S6). An intramembrane loop between S5 and S6 (P-loop) possess specific sequence of amino acids that are responsible for potassium ions selectivity. Four subunits of voltage-gated potassium channel form the pore surrounded by integral membrane domains that can "sense" membrane voltage and open the pore in response to its change.

The "voltage sensor" (S4) features positively charged arginine residues, that enable it to move at the protein-lipid interface, within the membrane electric field, thereby allowing membrane voltage to drive the pore between closed and opened states (MacKinnon, 2003). Both, N- and C-termini are in the cytosol and play an essential role in inactivation of the channels, as well as in regulatory subunits binding.

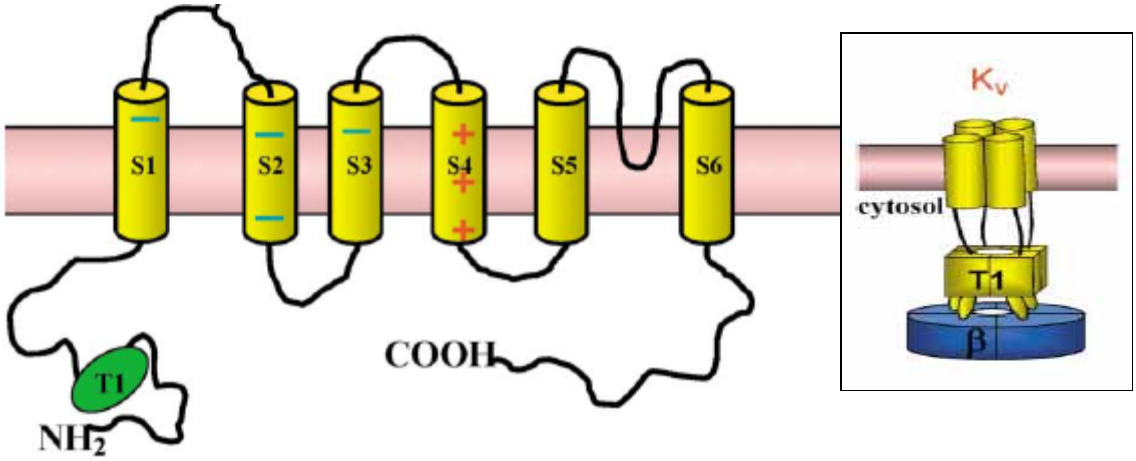

Fig. 1 Membrane topology of a voltage gated potassium channel.

Scheme of a Kv monomer. The six tansmembrane segments are shown in yellow (S1-6). A T1 recognition domain is indicated in green. Charges (+ and -) are indicated for some of the residues in the transmembrane domains of the voltage sensor (S1-4). The pore region includes S5-S6 intermembrane loop (Deutsch, 2003). **Inset:** Macrocomplex of Kv channel assemble with auxiliary subunits (dark blue). T1 domains associate with beta subunits. For simplicity the C termini are not shown. (Gulbis et al., 2000).

Arachidonic Acid

"The arachidonic acid cascade is arguably the most elaborated signaling system neurobiologists have to deal with"-D. Piomelli (Piomelli, 1993). It not only generates multiple messenger molecules (~ 20, an estimate limited to the brain), but these molecules may act both within and from the outside of neurons, aiming at intracellular as well as extracellular targets.

Arachidonic acid structure

Arachidonic acid (AA) is a polyunsaturated fatty acid (PUFA) consisting of a 20-atom-long carbon chain with 4 double bonds and a carboxylic group at one of the ends (20:4). The carbon-carbon double bonds in AA and other polyunsaturated fatty acids can lead to free-radical formation. Reactions with oxygen form unstable lipid peroxide compounds containing the same unstable oxygen-oxygen bond found in hydrogen peroxide and thus_contributes to cellular oxidative stress. ETYA is a structural analogue of AA with chemically more stable triple bonds instead of double bonds (Fig. 2B).

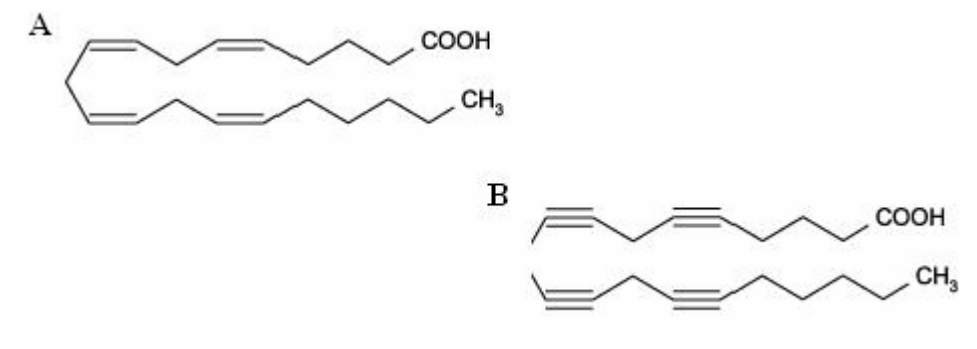

Fig. 2 Structure of arachidonic acid and ETYA

Arachidonic acid release

In neurons, a receptor-dependent event, leading to Ca^{2+}-influx or release of Ca^{2+} from intracellular stores, is required for the brain lipases to release arachidonate from the phospholipids of the cell membrane. Several neuromodulators stimulate the deacylation of membrane phospholipids, causing release of free arachidonate. These include excitatory amino acids (e.g. glutamate), biogenic amines (e.g. serotonin and histamine), and peptides (e.g. bradykinin). Even though the final effect of these various substances on arachidonate turnover is similar, they may use different mechanisms to achieve it.

At least three distinct phospholipases are thought to generate free arachidonic acid, either directly (PLA_2) or indirectly (PLC and PLD). A number of studies have shown that all phospholipases are activated by neurotransmitters. Previous reports indicate that the key enzyme responsible for agonist-induced AA release is cytosolic PLA_2 ($cPLA_2$) (Lin et al., 1992; Roshak et al., 1994). $cPLA_2$ is a cytosolic 85-kDa Ca^{2+}-dependent phospholipase and is activated by both an increase in intracellular free Ca^{2+}-concentration ($[Ca^{2+}]i$) and Ser-505 phosphorylation by mitogen-activated protein kinase (MAPK) or protein kinase C (Leslie, 1997). Hormones and growth factors also regulate PLA_2 activity (Loo et al., 1997, Leslie, 2004; Trevisi et al., 2002). In addition, H_2O_2 dose-dependently enhances cell membrane associated PLA_2 activity and stimulates AA-release (Chakraborti and Michael, 1993; Yasuda et al., 1999). It was also suggested that H_2O_2 stimulates PLA_2 through PKC (Chakraborti and Michael, 1993).

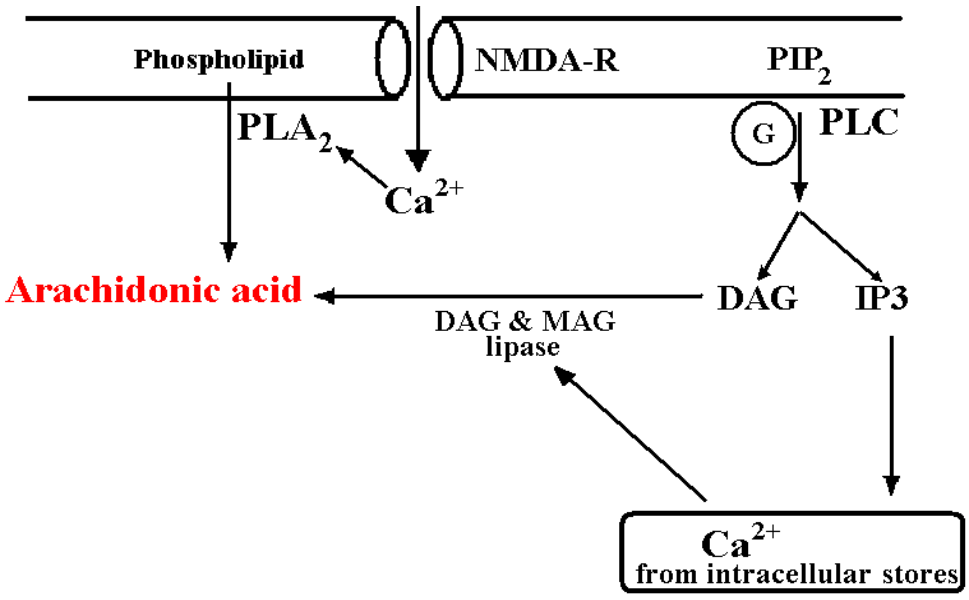

Fig. 3 Simplified scheme of arachidonic acid release events. IP3, inositol triphosphate**, PLC,** phospholipase C**, PLA2** phospholipase A2**, MAG,** monoacyl glycerol **DAG,** diacylglycerol **G,** GTP-coupled protein**, PIP2,** phosphoinositol biphosphate

Most researchers believe that a G protein ensures the coupling of receptors with PLA_2. Jelsema and Axelrod (Jelsema and Axelrod, 1987), have first to demonstrate inhibition of PLA_2 by G proteins.

Arachidonic acid metabolism

The major pathways of arachidonic acid metabolism have been discovered in most animal tissues, including brain. This pathways are controlled by lipoxygenase (LOX), cyclooxygenase (COX), and cytochrome (Cyt) P450 (Fig.4; Nishiyama et al., 1992; Nishiyama et al., 1993). AA is converted into a large number of biologically active metabolites such as *leukotrienes*, *lipoxins*, *prostaglandins*, and *thromboxanes*, termed with the common name ***eicosanoids***. These metabolites seem to play significant roles in several important processes, including vascular contraction and cell growth (Anderson et al., 1997; Gong et al., 1995).

In the brain, for example, 12-lipoxygenase products were shown to inhibit glutamate release from hippocampal mossy fiber nerve endings (Freeman et al., 1991), whereas 5-lipoxygenase metabolites were found to increase the activity of muscarine-inactivated M-K^+ channels in rat hippocampal CA1 neurons (Schweitzer et al., 1990). Some lipoxygenase metabolites of AA also activate the cardiac, muscarinic-activated K^+ channel, stimulate BK_{Ca} channels in rat pituitary tumor cells (Duerson et al., 1996), and modulate S-type K^+ channels in *Aplysia* (Piomelli et al., 1987). K^+ channel modulation by lipoxygenase products has also been reported in a number of non-neural cells, including heart myocytes (Kim and Duff, 1990). 12-Hydroxyeicosatetraenoic acid (12-HETE) is a neuromodulator that is synthesized during ischemia. Its neuronal effects include attenuation of calcium influx and glutamate release as well as inhibition of AMPA receptor (AMPA-R) activation. 12-HETE reduces ischemic injury in the heart, but it can also reduce neuronal excitotoxicity. 12-HETE could protect neurons from excitotoxicity by activating a $G_{i/o}$-protein-coupled receptor, which limits calcium influx through voltage-gated channels (Hampson and Grimaldi, 2002).

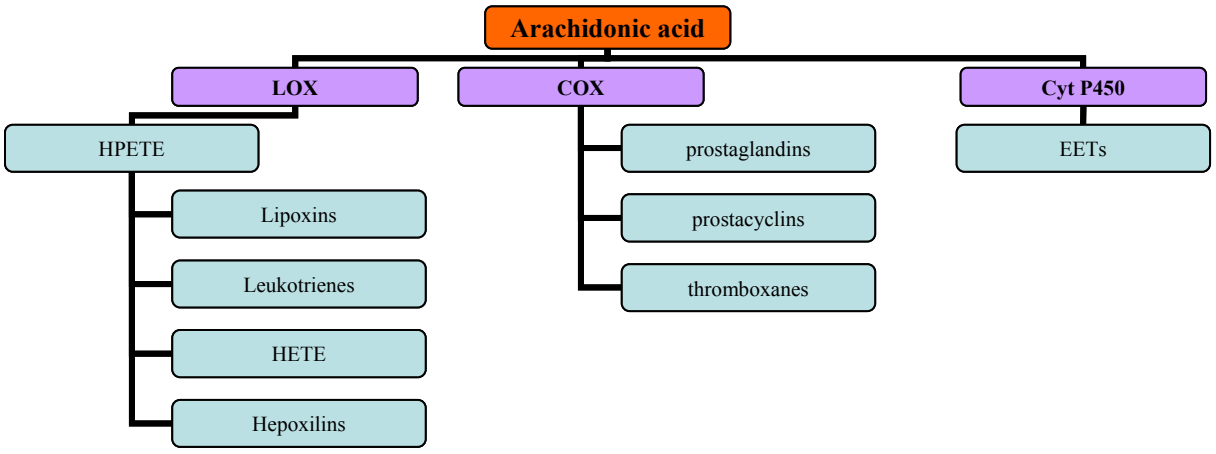

Fig. 4 Simplified scheme of arachidonic acid metabolism. LOX, lipooxigenase; **COX**, cyclo-oxigenase; **CytP450**, cytochrome; **HPETE**, hydroperoxyeicosatrienols, **HETE**, hydroxyleicosatrienols; **EETs**, epoxyeicosatrienoics

The eicosanoids produce a wide range of biological effects on inflammatory responses, on the intensity and duration of pain and fever (Samad et al., 2001; Vane, 1976), and on reproductive function (Zahradnik et al., 1992). Eicosanoids also play important roles in acid secretion (Eberhart and Dubois, 1995), regulating blood pressure through vasodilation (Pomposiello et al., 2001) or vasoconstriction (Yu et al., 2003), and inhibiting (Petroni et al., 1995) or activating (Davi et al., 1999) platelet aggregation and thrombosis.

Modulation of voltage-gated potassium channels by arachidonic acid

AA and its metabolic products have been shown to modulate a large number of ligand- and voltage-gated ion channels in a variety of systems (Bevan and Wood, 1987; Ordway et al., 1991). The potential role of arachidonic acid in mediating K^+-channel modulation and presynaptic inhibition of neurotransmitter release-one example of a second messenger role for the eicosanoids-was first suggested by J. Schwartz , based on experiments with Aplysia. AA has been shown to activate a large conductance (160 pS) K^+-channel directly in cardiac atrial muscle (Kim and Clapham, 1989) and a small conductance (23 pS) K^+-channel in smooth muscle (Ordway et al., 1991). In central neurons, AA either depresses or enhances K^+-currents through lipoxygenase or cyclooxygenase metabolites (Keyser and Alger, 1990; Schweitzer et al., 1990; Zona et al., 1993). With respect to K^+-channels in expression systems, AA has been shown to inhibit currents directly through channels formed by members of the Kv4 (*Shal*) subfamily of voltage-dependent potassium channels, whereas other members of Kv1 (*Shaker)* subfamilies were relatively insensitive to AA (Villarroel and Schwarz, 1996).

High concentrations of arachidonic acid (≥1μM) directly modulate I_A in CA1 hippocampal neurons (Colbert and Pan, 1999; Keros and McBain, 1997). Bittner and Müller showed that intracellular AA is highly potent in selectively inhibiting the A-current in cultured hippocampal neurons. Our group recently demonstrated, that extremely low concentration of AA (1 pM) attenuates I_A, but not the delayed rectifier, in CA1 pyramidal neurons from acute brain slices (Angelova and Muller, 2006).

Oxidative Stress

Cells constantly generate reactive oxygen species (ROS) during aerobic metabolism. ROS are produced as by-products of oxidative metabolism, in which energy activation and electron reduction are involved. Bearing an unpaired electron, these molecules can react with a large number of neuronal targets, beginning chain reactions that generate different radical species as intermediate products.

ROS include free radicals such as the superoxide anion (O_2^-), hydroxyl radicals (·OH), and the non-radical hydrogen peroxide (H_2O_2). They are particularly transient species due to their high chemical reactivity and can react with DNA and proteins, i.e. enzymes, ion channels and lipids. Lipid peroxidation represents a chain reaction that results in massive oxidation of membrane lipids. ROS production is enhanced severely in several disease states such as hypertension, diabetes mellitus and atherosclerosis, but also during epileptic seizures (Kovacs et al, 2002).

The high metabolic rate of neurons implies a high baseline ROS production. Correspondingly, healthy brain cells possess high concentrations of both enzymatic and small molecule antioxidant defenses.

Antioxidants

To counteract the effects of oxidative stress, cells have developed two important defense mechanisms: a thiol reducing buffer (GSH and thioredoxin), and enzymatic systems (SOD, catalase, and glutathione peroxidase). The most important thiol is the cellular redox buffer GSH, present within cells at a millimolar concentration. Thiols also exist in different cysteine-containing compounds such as amino acids (cysteine, taurine, homocysteine), peptides (GSH, Coenzyme A), and proteins (thioredoxin, glutaredoxin, albumin, glutathione peroxidase, peroxiredoxin, redox factor-1, heat shock protein, etc).

Additionally, thiol groups located on various molecules act as redox sensitive switches, thereby providing a common trigger for a variety of radical-mediated signalling events.

Glutathione (GSH)

The GSH system is probably the most important cellular defense mechanism that exists in the cell. The tripeptide GSH (Glu-Cys-Gly) not only acts as free radical scavenger but also functions in the regulation of the intracellular redox state. Recycling of the oxidized disulfide form (GSSG, Fig.5 A) maintains adequate levels of the reduced form of gluthathione (GSH, Fig.5 B). The system consists of GSH, glutathione peroxidase (GPx) and glutathione reductase. GPx catalyses the reduction of ROS and converts GSH to GSSG. GSSG is then reduced back to GSH by glutathione reductase that, in turn, is recycled by NAD^+. GSH substrates include, but are not limited to hydrogen peroxide and hydroxyl radicals:

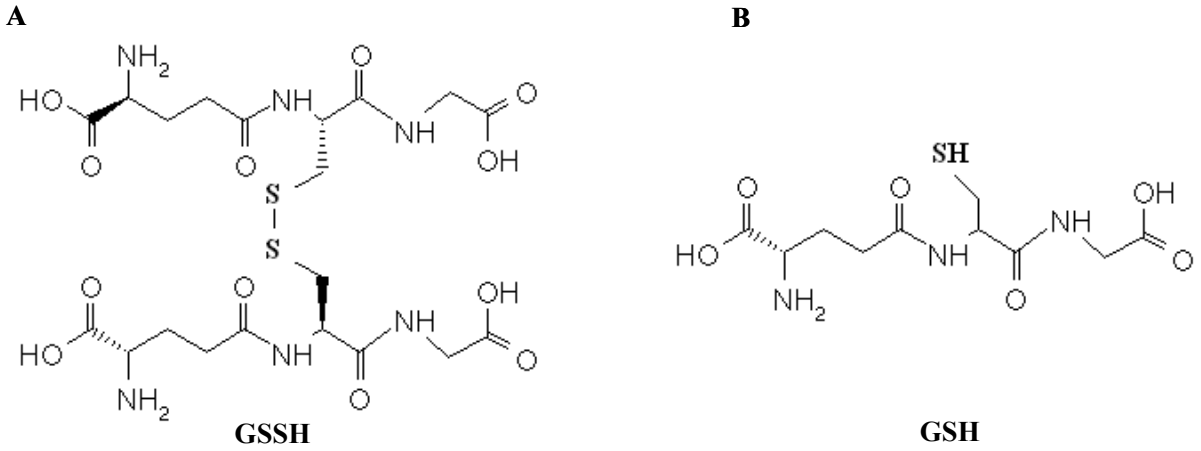

Fig. 5 Chemical structure of glutathione

The ability of the cell to regenerate GSH either by reduction of GSSG or by new synthesis of GSH is an important factor in the efficiency of that cell in managing oxidative stress. Under normal conditions, more than 95% of the GSH in a cell is reduced and so the intracellular environment is usually highly reducing (Carmody et al., 1999). In typical mammalian cells, the ratio of [GSH]/[GSSG] in the cytosol is 30:1, thereby maintaining very reduced redox potential (RP) of approximately 220 mV (Hwang et al., 1992).

Ascorbic acid

Ascorbate (Vitamin C) can not be synthesised by mammals and therefore needs to be taken up through the diet. It is playing an essential role as an easily oxidized anti-oxidant and free radical scavenger. The oxidized form of ascorbic acid is known as dehydroascorbic acid. Reactive oxygen species oxidize ascorbate to dehydroascorbate. ROS are reduced to water while the oxidized forms of ascorbate are relatively stable and unreactive, and do not cause cellular damage. Ascorbic acid is also essential for the recovery of oxidized tocopherols.

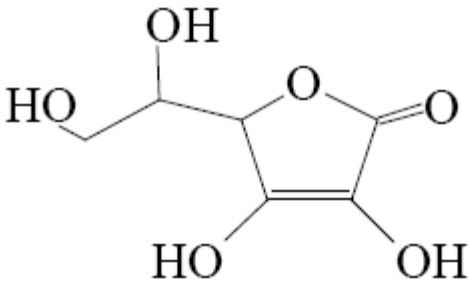

Fig. 6 Chemical structure of ascorbic acid.

α-Tocopherol and Trolox C

The term Vitamin E represents eight structurally related compounds, called also tocopherols and tocotrienols, each with their own subfamilies of α-(Fig.7 B), β-, δ- and γ-substances. They are also equipped for an antioxidant function, despite their lack of a thiol (-SH) group. In its function as a chain-breaking antioxidant, tocopherols rapidly transfers its phenolic H^+ atom to a lipid peroxyl radical, converting it into a lipid hydroperoxide and a relatively stable radical form of the vitamin (Machlin and Bendich, 1987). The tocopheryl radical can be reduced to tocopherol by ascorbic acid or reduced glutathione or alternatively to be further oxidized to quinone (Bast et al., 2002).

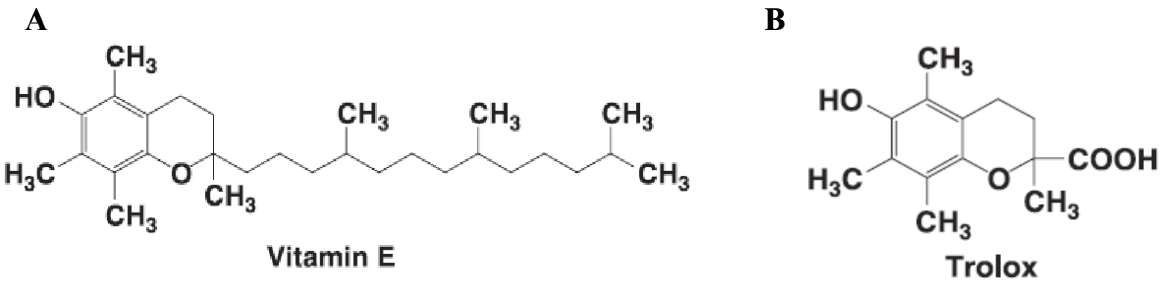

Fig. 7 Chemical structure of α-tocopherol and Trolox C

Trolox C (6-hydroxy-2,5,7,8-tetrametylchroman-2-carboxylic acid; Fig.7 B) is an α-tocopherol derivative that is lacking the phytyl tail, which enables its water-solubility. On the other hand, the aromatic structure remains unchanged implying preserved antioxidant properties.

Modulation of ion channels by ROS

Oxidative stress has met continuously growing interest for its roles in the physiology and pathophysiology of immune defense, ischemia, and neurodegenerative disease, such as Parkinson's disease, Alzheimer's dementia, and multiple sclerosis. Reactive oxygen species modify membrane lipids as well as a variety of proteins, including membrane channels, affecting cellular functions in both detrimental and protective ways (Kourie, 1998).

Ruppersberg demonstrated in 1991 that inactivation of A-type currents through Kv1.4 channels is dependent on the cellular redox state in a cysteine-dependent manner (Ruppersberg et al., 1991). Oxidation decreases the conductance of Kv1.3, Kv1.4, Kv1.5, Kv3.4 (Duprat et al., 1995) and Kv3.3 channels (Vega-Saenz de Miera and Rudy, 1992), while it enhances K^+-currents through human ether-a-gogo-related gene (HERG) K^+-channels (Taglialatela et al., 1997). Modulation of K^+-channel activity by cellular oxidative stress has emerged also as a significant determinant of vascular tone. Different kinds of ROS have been reported to modify various types of K^+-channels in vascular tissues (Liu and Gutterman,

2002; Pomposiello et al., 1999; Sobey et al., 1997). Specific oxidative modulation of voltage activated K^+-currents in cultured hippocampal neurons, as well as in slice CA1 pyramidal neurons by hydrogen peroxide and 1 pM AA has been demonstrated by the Müller lab (Bittner and Muller, 1999; Muller and Bittner, 2002, Angelova and Muller, 2006).

Hippocampal Formation

The entorhinal cortex (EC) is a part of the "limbic system" (MacLean, 1952). For a long time it was thought that the entorhinal cortex is primarily related to olfactory functions, however more recently it has been shown to also be involved in functions such as emotional and cognitive processes (Squire, 1992). The entorhinal cortex does receive major inputs from the olfactory bulb and cortex. Lately it has become clear from many studies, e.g. O'Keefe and Conway, 1978; Pouzet et al., 1999; Zola-Morgan and Squire, 1990, that the entorhinal cortex, together with the *hippocampus*, contributes importantly to learning and memory.

The entorhinal cortex functions as a gateway to the hippocampal formation, because its output via the perforant pathway is the major cortical source of input to the *hippocampus*. Furthermore, together with the *subiculum* it also provides the major output of the *hippocampus* (Witter et al., 1989).

The cells that give input to the *hippocampus* are predominantly present in layers II and III, most neurons in layer II are modified pyramidal cells, or stellate cells, whereas layer III predominantly consists of small pyramidal neurons (Fig. 8). In the rat, the layer II cells of the EC have been shown to project primarily to the dentate gyrus (Dolorfo and Amaral, 1998; Ruth et al., 1982; Ruth et al., 1988; Steward and Scoville, 1976). The entorhinal cortex layer III cells have been shown to project predominantly to CA1 and *subiculum* (Steward and Scoville, 1976).

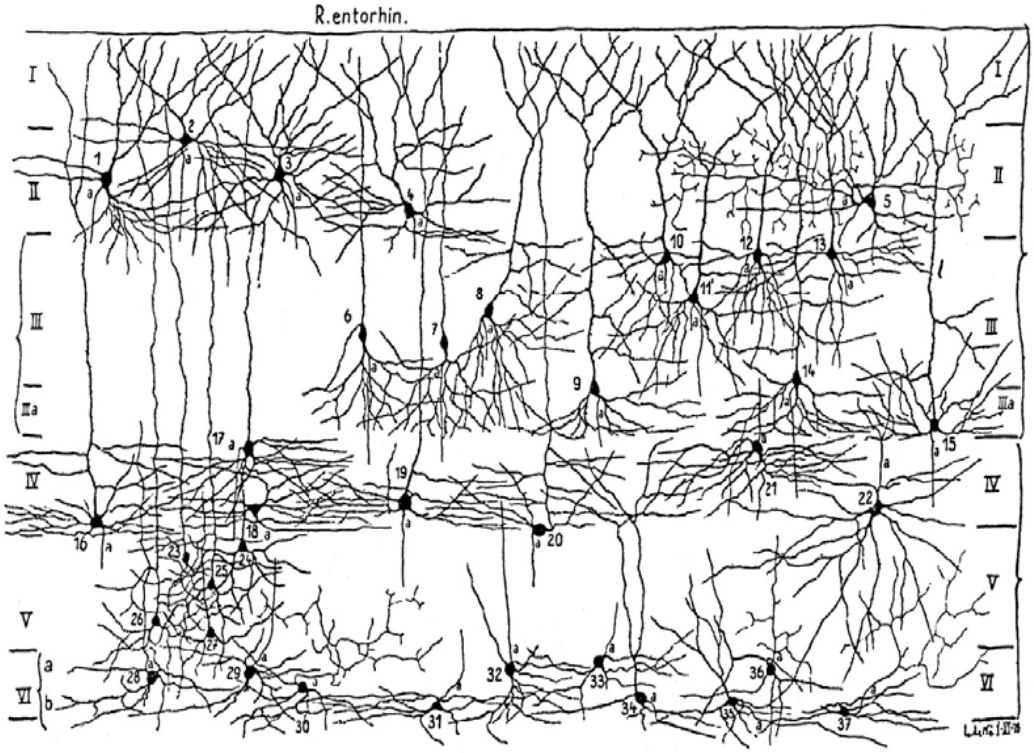

Fig. 8 Schematic drawing of a section through rodent entorhinal cortex (modified after Lorente de Nó, 1934).

Hippocampal formation damage in neurological diseases

The entorhinal cortex is damaged in various brain diseases and in degenerating disorders, such as temporal lobe epilepsy (Du et al., 1993), schizophrenia (Arnold et al., 1995), frontotemporal dementia (Frisoni et al., 1999) and Alzheimer's disease (Braak and Braak, 1992; Braak and Braak, 1995; Braak and Braak, 1996; Gomez-Isla et al., 1996). In schizophrenia, there are controversial findings regarding the damage in the entorhinal cortex (Akil and Lewis, 1997; Krimer et al., 1997).

Changes in hippocampal formation in temporal lobe epilepsy

Selective neuronal loss and active gliosis are the basic morphologic changes observed in temporal lobe epilepsy (Mathern et al., 1997). The entorhinal cortex is probably one of the primary sites in which temporal lobe seizures propagate and reverberate (Spencer and Spencer, 1994). In humans, early cell loss is most profound in the entorhinal cortex layer III (Du et al., 1993). In experimental studies of status epilepticus of rats, layer III of the medial portion of the entorhinal cortex is also suggested to be the most vulnerable (Du et al., 1995). At late stages, these changes are also prominent in CA1 region and in part of the subiculum.

Changes in hippocampal formation in Alzheimer's disease

The entorhinal cortex is one of the cortical formations that are selectively vulnerable in Alzheimer's disease. In AD, the damage in entorhinal cortex occurs very early in the disease course. Layer II shows neuronal loss and tangles formation in preclinical stages of AD and in patients with mild dementia (Braak and Braak, 1991). In later stages, amyloid accumulation and cell loss affect area CA1 and the subiculum.

AIM OF THE STUDY

Modulation of a variety of voltage-dependent potassium channels by arachidonic acid has been well documented (Meves, 1994). Despite multiple hypotheses suggested and a lot of experimental work done, there is still uncertainty which of the hypothetic mechanisms of A-type current accounts for modulation by fatty acids. Given the central importance of voltage-gated potassium channels in neuronal excitability it is not surprising that probably several mechanisms contribute to their tight control. This study was designed to investigate whether oxidative processes also contribute to AA-induced modulation of I_A. In order to test this hypothesis, some specific goals had to be defined:

- What is the effect of AA in hippocampal neurons from acute brain slices?
- Is this effect direct or an effect of one or more of its multiple metabolites?
- How does AA affect neurons in different areas of the hippocampus?
- Are there differences in A-type channels in untreated stellate cells and pyramidal neurons of the entorhinal cortex?
- Do A-type currents respond differently to 1 pM AA in neurons of the CA1 and neurons of the entorhinal cortex?
- Is oxidation involved in AA effects?
- Is it possible to identify the molecular basis of these effects, and the involved subunits?

MATERIALS AND METHODS

Brain slices

Animals

Experiments with brain slices were carried out on 14 to 21 days old male or female Wistar rats in compliance with international guiding principals for the use of animals in research. The number of animals was limited to the necessary number permitting reliable statistical analysis. According to the animal rights guidelines special procedures that minimize discomfort, pain and distress were applied. The animals were kept under standardized conditions and had access to water and dry food ad libitum. Light/darkness regime of 12:12 hours at a controlled temperature of 24 ± 1 ˚C was not inverted.

Brain slice preparation

Most of the experiments in this work were performed on horizontal hippocampus-entorhinal cortex slices (Fig.9). Prior to decapitation the animals were deeply anesthetized with ether. After decapitation the skin was cut with a scalpel from the caudal (posterior) to rostral (anterior) part, so that the calvarium could be uncovered. After careful opening of the skull with sharp scissors cutting along the still soft *sutura sagitalis* the two cranial pieces were peeled laterally. After careful removing of the *Dura mater* and disrupting the optic nerves the brain was rapidly (within half a minute) freed from the skull with spatula together with the *Cerebellum* and washed immediately with ice-cold ACSF, bubbled with 95% O_2 and 5% CO_2. Slicing was done at 4-8ºC in order to keep the tissue firm and to reduce metabolic activity. The preparation was done under submersion in ice-cold oxygenated ACSF. The Cerebellum as well as the frontal third of the brain was excised and both hemispheres were separated. The caudal third of each of the hemispheres was glued with the dorsal plane to the vibratome chamber using cyanoacrylate glue. Slice preparation was done from basal to dorsal direction. Brain pieces and slices were soaked in oxyenated ACSF (or high sucrose ACSF) during the whole process of cutting. The angle and vibration frequency of the blade were adjusted to

prevent the tissue being pushed while cutting the slices. Combined hippocampal-entorhinal cortex slices of 300 µm thickness were prepared using a vibrating microtome (Dosaka Microslicer DTK-1000, Kyoto, Japan). Slices were immediately and very carefully moved (using a brush) to an incubation chamber, containing oxygenated ACSF at room temperature (20-22˚C). There, the slices were allowed to recover for at least 1 hour before being transferred to the recording chamber.

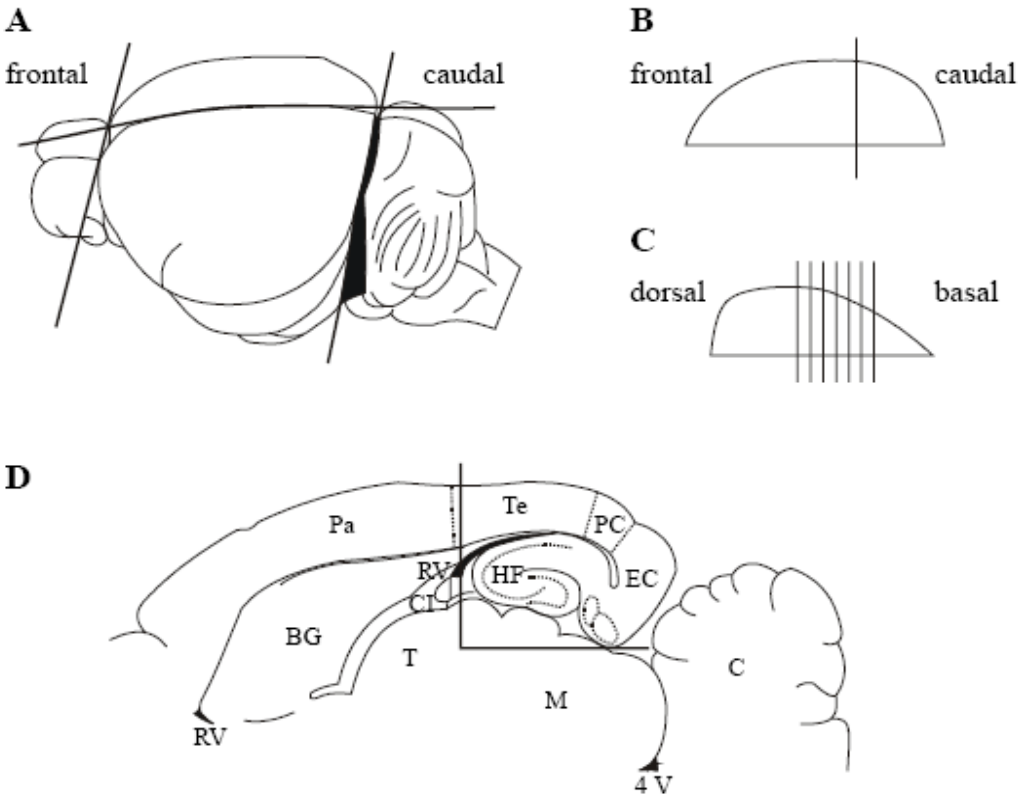

Fig. 9 Preparation of horizontal hippocampal slices (Witter et al., 2000).

Solutions

As a nutrient solution for the brain slices during preparation as well as during the experimental phase artificial cerebro-spinal fluid (ACSF) was used (Table 1). This solution was continuously bubbled with carbogen gas (5% CO_2, 95% O_2) to maintain a pH of 7.4. While recording, ACSF was superfused at 3 ml/min at room temperature (~22^oC).

Table 1 Content of acute brain slice preparation and perfusion solutions.

Compound	ACSF (Ringer) /normal/	Sucrose cutting solution	
NaCl	129 mM	87 mM	**Stock I**
$NaHPO_4$	1,25 mM	1,25 mM	
Glucose	10 mM	25 mM	
$MgSO_4$	1,8 mM	-	
$CaCl_2$	1,6 mM	0,5 mM	
KCl	3 mM	2,5 mM	
$MgCl_2$	-	7 mM	
Sucrose	-	75 mM	
$NaHCO_3$	26 mM	26 mM	**Stock II**

Both Stock I and Stock II were mixed with H_2O daily in a ratio of 1:8:1 and bubbled with carbogen minimum 1 hour before use, to adjust the pH of 7.4.

Although sucrose substitution for sodium or the use of 10 Mg^{2+}: 1 Ca^{2+} instead of 1 Mg^{2+}:1 Ca^{2+} is reported to amend the viability of slices, the modified procedure that incorporates both of these ideas did not result in significant improvement of the slice quality.

HEK 293 cells

Heterologous expression of potassium channel cDNAs was done in human embryonic kidney cells, transformed with Adenovirus Type 5, American Type Culture Collection, 12301, Parklawn Drive, Rockville, Maryland 20852, USA; code designation HEK 293 or 293 cells.

Maintaining HEK 293 cells in culture

HEK 293 cells were grown in a monolayer in plastic petri dishes of 35 or 99mm. Under optimal growth conditions (37˚C, 5% CO_2), 293 cells doubled about every 36 hours. To maintain consistency and successful transfection procedures low passage 293 cells were

employed. Untransfected HEK cells were grown on big culture plates (99 mm) in 10 ml complete growth medium (Table 2) and were split every 2 days (after reaching 80-90 % confluence). 24 hours before transfection 293 cells were harvested and replated onto small petri dishes (35 mm) in 2 ml complete medium at a density to reach around 30 % on the next day. The cultures were incubated for 24 hours at 37˚C in humidified cell-culture incubator (Heraeus, Hanau, Germany) in an atmosphere of 5% CO_2. The medium was changed 1-2 hours prior to transfection.

Transient transfection of HEK-93 cell lines

The standard calcium phosphate-mediated transfection of adherent cells (Graham and van der Eb, 1973) was used for transient transfection of HEK 293 cell lines with potassium channel cDNA. The cells were transfected with Kv1.4 and Kv4.2 potassium channel subunit cDNA.

To prevent contamination sterile media, vials, instruments and cells in a vertical laminar flow hood were used. All solutions were sterilized by filtration trough 0.22 μm-pore filtre and were brought to room temperature before use. For each transfection plate two separate 0.5 ml polystyrene tubes were prepared:

A $CaCl_2$/DNA co-precipitate **B** 100μl 2x HBS (*see* Table 3*)*

While vortexing the HBS solution, the $CaCl_2$/DNA mixture were added dropwise to the tube, incubated for 30-40 min at room temperature, during which $CaPO_4$-crystals precipitate with the adherent DNA. The solution was permitted to turn opaque, but no or only very few visible precipitates were allowed to form. After resuspending the $CaPO_4$/DNA precipitate it was quickly and gently added dropwise onto the cells and rocked back and forth few times to evenly distribute the precipitate on the cells. By observing the cells under the microscope one could see very small black particles evenly distributed over the cells. The transfected 293 cells were incubated 4-5 hours at 5% CO_2 and afterwards washed (3x) with sterile PBS (containing

no Ca^{2+} or Mg^{2+}). Thereafter PBS was replaced with pre-warmed complete medium. Incubation of 48-60 hours was usually adequate for high expression rates of the protein of interest.

The transfection efficiency drastically fell when HEK cells were of late passage or reached high confluence. Therefore it was of great importance to time the passage procedures well. Aliquots of early passages of the HEK cell line were stored in liquid nitrogen to ensure a renewable source of cells. To prepare HEK cells for freezing, cells with 80% confluence were washed once with PBS (containing no Ca^{2+} or Mg^{2+}), trypsinized and harvested. Afterwards the cells were counted, collected by centrifugation (500 x g for 10 min.) and resuspended in 4˚C Cell Freezing Medium at 1-2x10^6 cells/ml. 1ml aliquots were then dispended into labelled freezing vials and incubated at –20˚C for 1-2 hours, -80˚C overnight and subsequently transferred to liquid nitrogen (-196˚C). There the cells could be preserved for months to years. Nevertheless the viability of the frozen stocks must be confirmed two or more weeks later by starting a fresh culture. To defrost prepared aliquots, the vials were taken from liquid N_2 and placed directly into a water bath (37˚C). After short time the cells were centrifuged and the pellet was resuspended in fresh warm MEM by trituration.

Culturing media

Table 2 Content of HEK-293 cell line culturing media

	Complete medium	Freezing medium	Washing medium	Storage of compound/media	supplied by
MEM(-Glu)	88 %	10 %	-	4˚C	Gibco
FCS	10 %	80 %	-	-20˚C	Gibco
L-Glu	1 %	-	-	-20˚C	Gibco
P/S	1 %	-	-	-20˚C	Fa.Seromed/ Biochrom KG
PBS	-	-	100 %	4˚C	Gibco
DMSO	-	10 %	-	18˚C /hood/	Merck

MEM, minimum essential medium, **FCS**-fetal calf serum, **L-Glu**, L-glutamine; **PBS**-phosphate buffer saline, **DMSO**, dimethyl sulfoxide.

Transfection buffers

Table 3 Content of HEK-293 transfection solutions and buffers.

	2xHBS /HEPES buffered saline/	**$CaCl_2$**	**A**	**B**
NaCl	280 mM	-	-	100µl 2xHBS
HEPES	50 mM	-	-	
$NaHPO_4$	1,5 mM	-	-	
$CaCl_2$	-	2 mM	12,3µl	-
cDNA /Kv1.4, Kv4.2 or EGFP/	-	-	2-5µg	-
ddH_2O/sterile/	-	-	to 100µl	-
aliquots/storage	1 ml/ -20˚C	1 ml/ -20˚C	fresh	fresh

HBS, HEPES//buffered saline; **ddH_2O**, double-distilled water; **L-Glu**, L-glutamine; **$NaHPO_4$**, sodium hydrogen phosphate;

In pyramidal neurons channels responsible for transient potassium currents are known to be comprised by two distinct principal (α) subunit genes: Kv1.4 and Kv4.2. In order to investigate probable differential modulation of Kv1.4 or Kv4.2 by AA or its derivatives and by radical oxygen species, Kv α-subunit cDNAs were separately transfected into HEK 293 cells.

One part of the recorded HEK 293-Kvα-expressing cells was co-transfected with EGFP-cDNA as a reporter gene to identify transfected cells by fluorescence microscopy. However, this reduced transfection efficiency.

Superfusion solutions

In HEK 293 cells patch-clamp experiments a saline with the following composition (in mM) was used as a perfusion solution:

140 NaCl, 4 KCl, 2 $MgCl_2$, 1 $CaCl_2$, 10 HEPES, 5 glucose, pH 7.4. All solutions were always prewarmed to 37^{o}C before use in experiments to exclude a temperature shock of the HEK-293 cells.

Electrophysiological recordings

Patch pipettes

Patch pipettes were freshly pulled from borosilicate glass (GB 150F-8P, Science Products, Hofheim, Germany) using a horizontal micropipette puller (P-97 Flaming/Brown Micropipette Puller, Sutter Instrument, USA) and were then fire-polished (Microforge, Narishige, Japan). The tip of the pipette was filled with control intrapipette solution (IPS) (1-2µl) and backfilled with IPS, containing the substance of interest. It is of great importance that no air bubbles or particles block the pipette tip. Patch pipettes had initial open-pipette resistances of 3-10 MΩ. Higher resistances lead to poorer electrical access to the cell, but also less washout of interior cell contents.

Intrapipette solution (IPS)

The recording solution had the following composition in mM: 120 KCl, 1 $CaCl_2$, 10 HEPES, 11 EGTA, 2 $MgCl_2$, 20 Glucose; pH 7.3. The substances of interest were then dissolved in IPS (*see* Table 4). The filling solution was filtered with 0.22 µm filters (Nalgene 4-mm syringe filters with nylon membrane), filled into new 1 ml luer syringes and freshly–pulled plastic microtubes. For patch-clamp osmolarity and pH are critical, therefore they were adjusted for both perfusion (310 ± 10 mOsm/ kg, pH 7.4) and intrapipette (300 ± 10 mOsm/ kg, pH 7.3) solutions. All solutions were freshly prepared.

Pharmaka

Most of the substances, used in this work, were prepared in stock solutions, if possible. Prior to experiment these compounds were diluted to required concentrations in perfusion or intrapipette solutions, depending on the application site and brought to the proper osmolarity and pH values. Unstable substances demanded preparation of fresh solutions. The following table gives an overview of the substances used, their concentrations and application sites.

Table 4 Pharmaka

	Concentration	Application site	Function	Notes
Arachidonic acid /AA/	1 pM	intracellular	cellular second messenger, precursor of eicosanoids	Light- and oxygen sensitive
Eicosatetraynoic acid /ETYA/	100 pM	intracellular	non-metabolizable analogue of AA	Light-, and oxygen sensitive
Ascorbic acid /asc.acid/	20 µM 0.4 mM	intracellular bath	antioxidant	Light-, temperature and oxygen sensitive
Glutathione /GSH/	2-20 mM 20 mM	intracellular bath	antioxidant	
N-acetyl-cystein /NAC/	20 mM	incubation (extracellular)	Antioxidant, precursor of GSH	
Trolox	10 µM 100 µM	intracellular bath	antioxidant, water soluble derivative of tocopherol	
Hydrogen peroxide /H_2O_2/	80 µM	intracellular	oxidizing agent	
Tetrodotoxin /TTX/	1 µM	bath	fast sodium channel blocker	†

AA and ETYA were stored as 1M stock solutions in DMSO at –20˚C. DMSO itself, diluted to pM concentrations had no effect on I_A or $I_{K(v)}$. Ascorbic acid was used from freshly made stock, when needed and kept in dark container up to 5 days at –20˚C. GSH was stored as 20 mM stock in IPS, when used for intracellular application. During experimentation intrapipette solutions were kept on ice in darkness.

Voltage-clamp and discontinuous amplifier

The main requirement of voltage-clamp procedure is to prevent changes in cell membrane potentials. That is why in voltage-clamp is generated compensation current, which is exactly as big as the current, which flows through the membrane, but in opposite direction. This is carried out by a negative feedback mechanism, by which the membrane potential is measured and compared with a reference value – the reference voltage. Every difference of the reference value from the actual measured membrane voltage activates a controller, which injects current with reversed direction to the cell. This compensation current is measured in patch-clamp experiments. It provides direct insight into membrane conductivity and the function of ion channels and ion transporters, by which it is determined. Simplifying, one could imagine the cell membrane as an Ohm resistor. In other words, the voltage is linearly dependent on the current (Ohm's Law: U=R.I). Instead of the resistance R, one uses its reciprocal value, the conductance (1/R=g). The Ohm's Law in this case is U=I/g or I= U*g. The voltage U is in this case the offset between reference voltage U_{ref} and the reversal potential U_{rev} for a given ion species, that carry the current: with I= (U_{ref}- U_{rev}).g.

The current I is the most important measurement category for all voltage-clamp amplifiers and every current change is directly proportional to the changes of the membrane conductivity.

Recording electrode

Chlorided silver wire, connected with the probe end of the amplifier is inserted into the glass patch-pipette filled with IPS and serves as a recording electrode.

Experimental setup

In the recording chamber brain slices were superfused with carbogenated ACSF with a flow rate of 3 ml/min or HEK cells media was replaced with pre-warmed HEK perfusing saline. The electrophysiological experiments were performed at room temperature (~20°C). ECLII stellate cells and ECLIII and CA1 pyramidal neurons from acute brain slices, as well as transfected HEK 293 cells were visualized and identified under an upright microscope (Olympus BX 51WI, Germany), equipped with IR-DIC optics. In the entorhinal cortex, L III pyramidal neurons were classified by their triangular somata exhibiting one principal apical and two to three minor basal dendrites. L II stellate neurons were identified by their irregular polygonal somata. They were larger than pyramidal neurons and gave rise to four or five roughly equivalent dendrites, forming a stellate morphology. CA1 pyramidal neurons were easy to distinguish, because they are organized in clear-cut subfield within the hippocampus.

HEK cells grew in monolayer, but 2-4 days after plating there was a tendency of forming confluent cumuli. In this case the measurements were performed on the remaining single cells.

For electrophysiological recordings, only healthy cells were selected. These are cells with defined round borders, bright, with a really good contrast and a smooth appearance. Cells with rough, spotty surface or dark colour, even if they had good contrast were discarded, because those are usually seriously damaged, about to become apoptotic and do not allow formation of seals. In some cases swollen cells allowed seal formation, but no longer whole-cell recordings.

When the pipette is brought across the air-saline interface, positive pressure (0.1-0.5 psi) was applied to prevent tip contamination and to clean cell surface from tissue debris (in slices). As the HEK cells grow in monolayer high pressure would be destructive for them. After forming a bleb on the cell surface, tight seal (> 1 GΩ) was achieved by application of low negative pressure, using a 1 ml-syringe. Whole-cell break-in was accomplished by giving a very brief, sharp pulse of suction, considerably smaller in the case of HEK 293 cells. Access resistance (R_a) ranged from 10–14 MΩ, and was compensated by up to 60%; data were discarded if Ra > 15 MΩ. Input resistance was measured at a holding membrane potential level close to resting membrane potential (RMP) from the voltage response elicited by a small current pulse (-60 pA). Only cells that showed stable RMP negative to -60 mV and R_i > 120 MΩ (in current-clamp mode) were selected for study. Pharmacological tests of so selected cells were completed within 15 min. and corrected offline for eventual run down effects. Membrane potential of the cells was held at – 80 mV. All experiments were conducted at room temperature (20 - 22 ºC).

Experimental protocols

In whole-cell patch-clamp mode, total outward potassium currents were activated after 800ms hyperpolarizing prepulse at –110 mV (to remove inactivation) by subsequent depolarization of the membrane to potentials between –80 and +50 mV in increments of 10 mV (Fig.10 A1). When followed by 50 ms interval at –20 mV I_A inactivated completely (Fig.10 A2) permitting later isolation of I_A from the mixed currents.

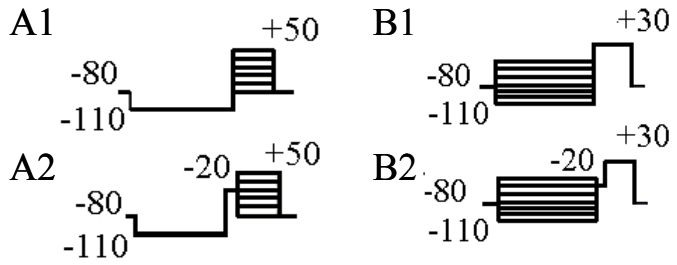

Fig. 10 Test potential protocols for activation and inactivation of total outward and delayed rectifier potassium currents.

Delayed rectifier potassium currents were also elicited from different potentials (-110 to +20mV, 10 mV increments) and recorded at +30 mV (Fig.10 B). $I_{k(v)}$ were non-inactivating in the investigated range of durations of voltage pulses. Whole-cell patch-clamp recordings were maintained in voltage-clamp mode, using an EPC-9 amplifier with built-in ITC-16 interface board, controlled by Pulse/PulseFit software (both HEKA Electronik, Lambrecht, Germany). The current signals were filtered at 3 kHz and 10 kHz and stored on a disk. The P/n method incorporated in Pulse/PulseFit software was used for leak correction (leak holding at –80 mV).

Data and statistical analysis

By depolarization of the membrane potassium permeability through a voltage-gated channel rises rapidly and then decays slower than it activates. These two processes could be described with the terms *activation* and *inactivation*. When the channels open, a mechanism is put into action to close the channel again. The special closed state in this situation is referred to as the inactivated state. The channels indeed possess two different types of gates. Closing of the inactivation gate is time dependent, whereas opening it is voltage dependent. The inactivation state can be considered time independent and is therefore termed steady-state inactivation.

On single channel level activation and inactivation corresponds to a change in probability of given channel to open or close upon depolarization. Inactivated channels could not be activated to conducting state until their inactivation is removed. Whole-cell recording makes possible to follow the changes in this probability and the duration of these states in multiple channels on the same time. The voltage-dependence of open state probability could be measured as followed: by a negative holding potential all channels of interest are brought to a state, from which activation is possible (closed state). Then the membrane potential is manipulated to more positive values (depolarization) and one part from the channels is opening. The recorded amplitude of the ionic current is a measure of the probability of the channels to open at certain test potential at the same time. The experiment is then repeated for

different test potentials and voltage-conductance relation curve is built. The conductance at each potential is normalized to the maximal conductance for the cell and plotted vs. test potentials. The resulting curve is sigmoidal and can be fitted with Boltzmann function (*see* below). Different pulse protocols and similar procedure of calculation is applied to describe steady-state inactivation of the channels. Both curves describe the voltage dependence of closed and opened states of the channels. These curves could be influenced by pharmaka, etc. If there is an overlap between the activation curve and the inactivation curve, then there will be a small, constant current in the area of overlap, called window current, that contribute to the setting of the resting membrane potential. A characteristic value that could be derived from voltage-conductance relation is the voltage (V_{50}), at which exactly the half of the channels are activated (open or closed). Another essential parameter that describes the dependence of the channel conductivity from membrane potential changes is the slope of the resulting curve *k*. Other important parameters that could be derived at each test potential are the time constants of activation and inactivation and the maximal amplitude of the current at each voltage steps.

Separation of fast and persistent K^+-currents using prepulse inactivation

Prepulse inactivation takes advantage of the differences in the inactivation properties of the fast (transient) and sustained (delayed rectifier) K^+ currents (Klee et al., 1995). TTX at 1 μM was included in the bath solution to isolate transient and persistent potassium currents from fast TTX-sensitive Na^+ currents (which are completely blocked by this TTX concentration). K^+ currents were evoked from a holding potential of -110 mV to test pulses ranging from -80 to +50 mV in 10 mV steps. Transient K^+-current (Fig.11, B) was obtained by subtracting the current obtained after a -20 mV prepulse, which elicits only the delayed rectifier K^+ current (Fig.11, C), from the current obtained after more hyperpolarized prepulse (-110 mV), which elicits both fast and persistent K^+ currents (total outward potassium current, Fig.11, A).

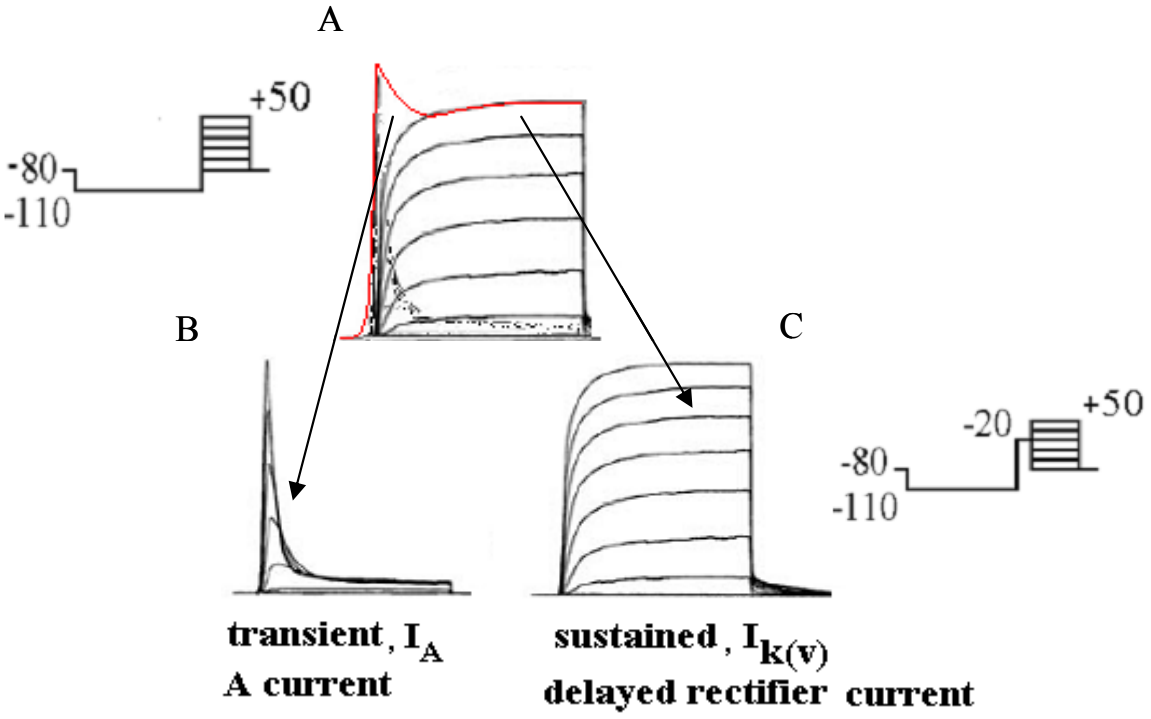

Fig. 11 Procedure for potassium current separation

The current traces were analysed "offline" using combination of Pulse/PulseFit, IgorPro and Prism software.

Data analysis

Current subtraction, rescaling and curve fitting were performed with IgorPro (WaveMetrics Inc.). Currents at each test potential were converted to conductances, using:

$g = I/(V_i - E_k)$, where I is the peak outward current, E_K is the reversal potential, and V_i is the test pulse voltage.

Voltage-conductance relations for activation and steady-state inactivation were plotted and fitted with the Boltzmann single exponential equations for

activation $g/g_{max} = 1/(1 + \exp(-(V - V_{0.5})/k))$ (1)

and inactivation $g/g_{max} = 1/(1 + \exp((V - V_{0.5})/k))$ (2),

where $V_{0.5}$ is the voltage for half-maximal activation in millivolts, V is the test pulse voltage, k is the corresponding slope factor, and g/g_{max} - the normalized conductance.

For effects on the maximum amplitude, currents at each recording time, measured at +30 mV, were normalized to the current at time=0 (immediately after obtaining whole-cell configuration, 'control') and plotted against time. Data are presented as means ± SEM (Standard Error of Means) or % of control. Statistical analyses of the data were performed with Prism (GraphPad Software Inc.) using Student's unpaired *t*-test. Probability of $p<0.05$ is considered to be significant.

RESULTS

Oxidative modulation of transient and delayed rectifier potassium currents in CA1 pyramidal neurons

In whole-cell voltage-clamp experiments of CA1 pyramidal neurons, total outward potassium currents were evoked after a 800 ms hyperpolarizing prepulse to –110 mV (to remove inactivation) during subsequent step depolarization of the membrane to potentials between –80 and +50 mV (increments of 10 mV, 200 ms duration). When the prepulse was followed by an additional 50 ms step at –20 mV, I_A inactivated completely and isolated delayed rectifier currents ($I_{K(V)}$) were recorded during subsequent voltage steps (Fig.12 A,B, pulse protocols see inset Fig.12). By subtracting delayed rectifier from mixed currents ($I_{K(V)}$)+I_A), I_A was isolated, as shown in Fig. 12 C.

Potassium currents in untreated CA1 pyramidal neurons

In control conditions, the evoked transient potassium current I_A had a maximum amplitude of 0.5-4 nA at +30 mV that was reached within 4 ms after the beginning of the voltage pulse. I_A inactivated completely with a time constant of 7.8 ± 1.5 ms (Fig. 12 C, Table 5). The maximal amplitude of I_A was stable over 15 min of whole-cell recording (-10.9 ± 4.6 %, Fig.12 C, Table 5).

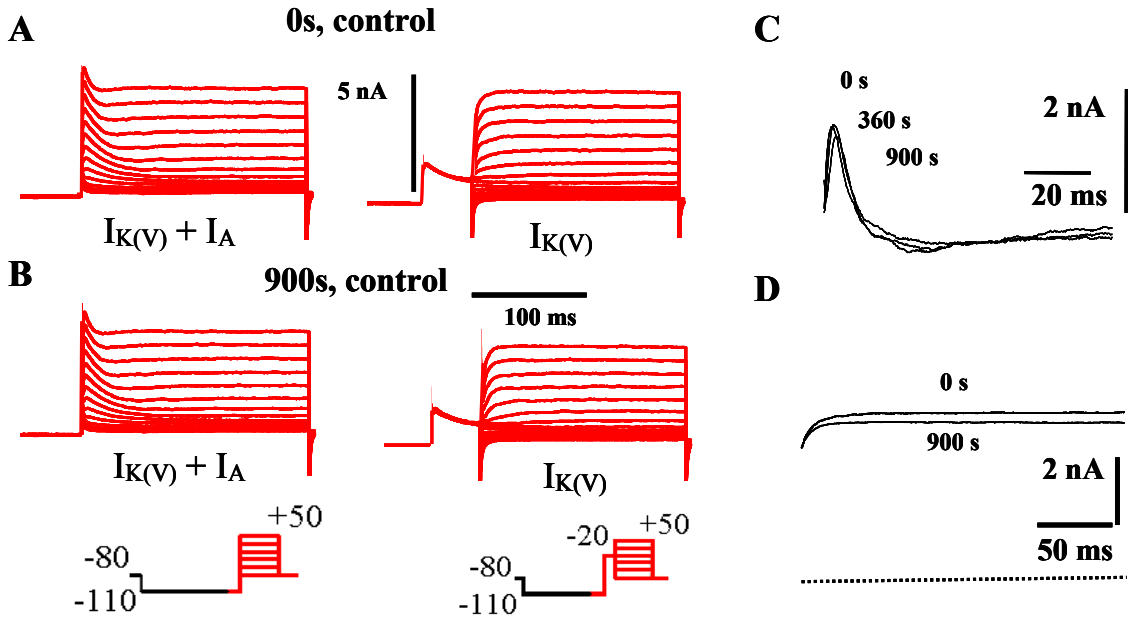

Fig. 12 Native I_A and $I_{K(V)}$ in control condition in CA1 pyramidal neurons.

A,B Original traces showing total outward potassium($I_{K(V)} + I_A$) and delayed rectifier ($I_{K(V)}$)currents at 0 s (A) and 900 s (B) after reaching whole-cell configuration. **C** Subtracted transient potassium current (I_A) recorded at +30 mV over time. **D** Delayed rectifier current at +30 mV over time.

Like I_A, $I_{K(V)}$ was stable under control conditions with a slight decrease of the current amplitude over 15 min (-12.8 ± 2.3 %, Fig.12 D, Table 6). That minimal reduction of both currents in control condition most probably could be due to a 'run-down' of these currents, suggesting that important cytoplasmic factor(s) are subject to wash-out.

Modulation of transient I_A and delayed rectifier currents $I_{K(V)}$ by arachidonic acid

When 1 pM arachidonic acid (AA) was included in the patch pipette, I_A decreased over time, starting within 6 min after obtaining the whole-cell configuration. After 15 min of intracellular AA application through the patch pipette I_A was reduced by -41.8 ± 5.5 % (n=9; $p<0.01$, Fig.13 B, C). Inclusion of AA in the patch pipette did not affect the inactivation time constant of I_A (Fig.13 D, Table 5).

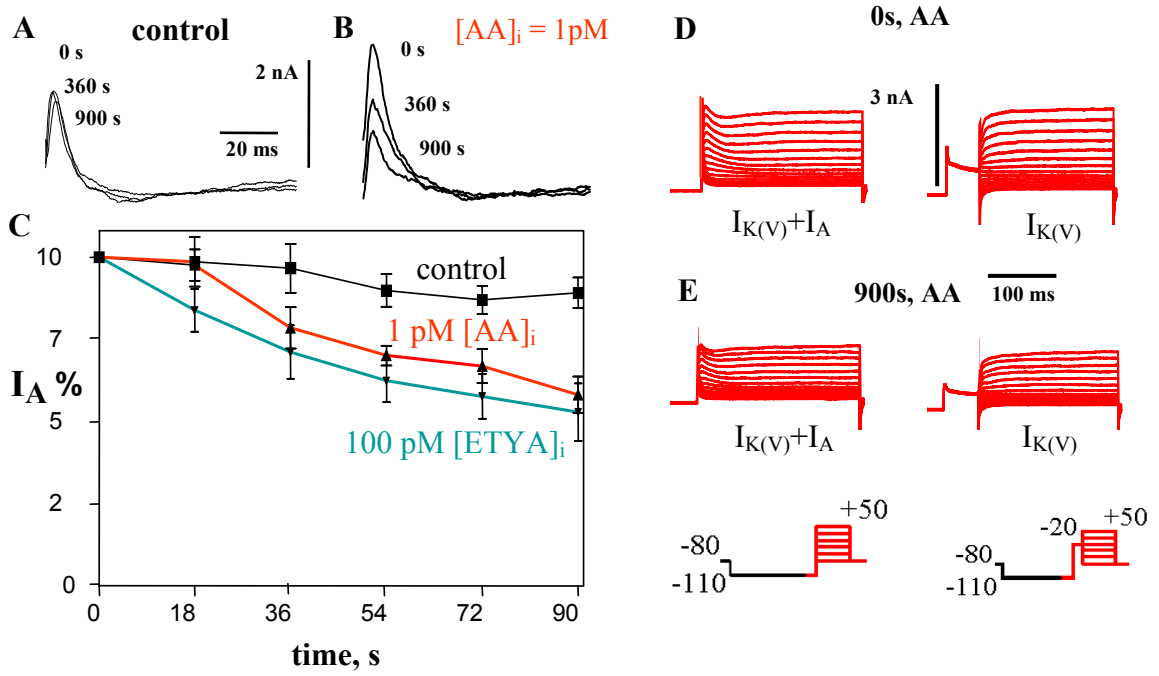

Fig. 13 Suppression of I_A by arachidonic acid (AA) in CA1 pyramidal neurons.

A: control; **B, C**: Intracellular application of 1 pM AA reduces the maximal transient potassium current (I_A) over time. The non-metabolizable AA analogue ETYA shows similar effect on I_A at 100-fold higher concentration (**C**). **D, E**: Raw current traces for combined I_A and $I_{k(v)}$ and for delayed rectifier currents (pulse protocols: inset in E).Currents are shown for control immediately after obtaining whole cell configuration (**D**, 0 s AA), after and after 900 s of recording with 1 pM of AA in the patch pipette (**E**).

In order to test whether the effects of applied AA on I_A were due to AA itself or one of its many bioactive metabolites, the non-metabolizable AA analogue eicosatetraynoic acid (ETYA) was employed. ETYA is neither hydrolyzed by cyclooxygenase, lipoxygenase, nor by cytochrome P450, but furthermore blocks the activities of these enzymes. Intracellular 1 pM ETYA was ineffective in reducing I_A. Intracellular application of a 100-fold higher concentration of ETYA (100 pM) reduced I_A to a similar extent as 1 pM AA (-47.1 ± 8.7 %, n=7, Fig.13 C). Like AA, ETYA did not affect maximum amplitude of $I_{k(v)}$ (not shown).

Fig.14 shows that $I_{K(V)}$ did not change its maximal amplitude in the presence of 1 pM intracellular arachidonic acid (-15.2 ± 1.8 %, n=9) in comparison to control (-12.8 ± 2.3 %, n=9).

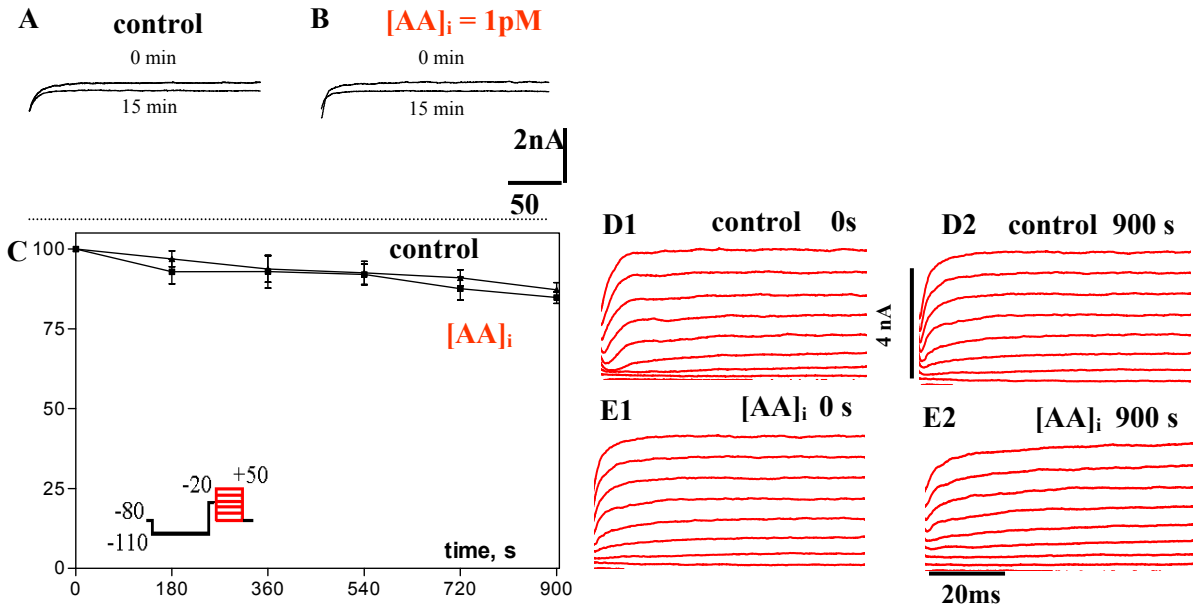

Fig. 14 The delayed rectifier current $I_{k(v)}$ is not affected by AA in CA1 pyramidal neurons.

A, B: Maximal $I_{k(v)}$ recorded at 0 s and at 900 s of whole cell recording shows a 13% decrease over time in control (**A**) as well as with 1 pM AA in the patch pipette (**B**). **C**: Plot of $I_{k(v)}$ amplitude over time of whole cell recording for control and for AA. **D, E**: Original current recordings of $I_{k(v)}$ for several voltage steps (see inset in C) for control (**D**) and for AA at 0 s (D1, E1) and 900 s (D2, E2) of whole cell recording.

The conductance–voltage plot of Fig.15 A, left curves, illustrates that AA shifted steady-state of inactivation to the left by 11 mV in CA1 pyramidal neurons in rat brain slice, in addition to the reduction of maximal conductance described above. AA did not affect the voltage dependence of activation of the transient potassium current (Fig.15 A, curves on the right side).

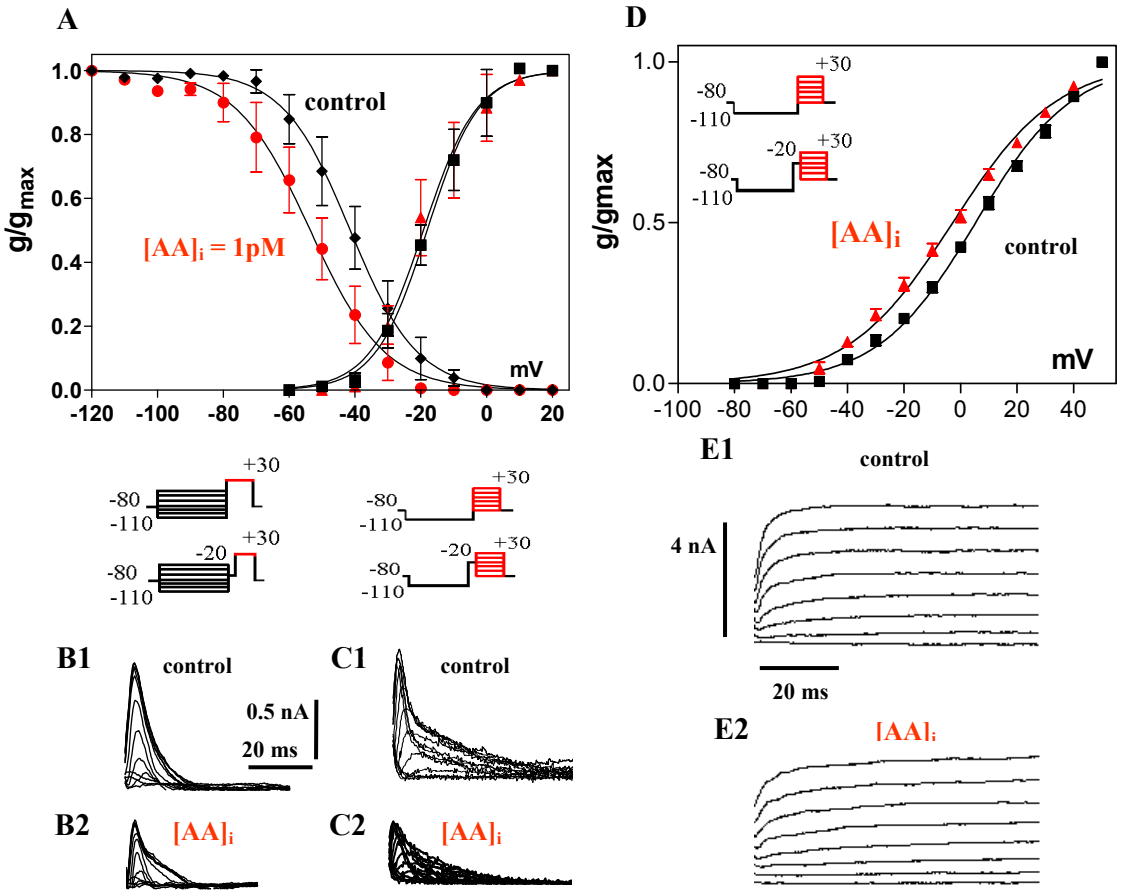

Fig.15 Intracellular AA (1pM) shifts steady-state inactivation, but not voltage dependence of activation of I_A in CA1 pyramidal neurons.

A: Conductance-voltage relations and Boltzmann fits for inactivation (left curves) and activation (right curves) of I_A. **Inset**: Pulse protocols for determining voltage dependence of steady state inactivation (left) and of activation (right). Red part shows length of the traces below. **B** and **C**: Representative recordings for inactivation (B) and activation (C).**D**: voltage-conductance dependence of $I_{K(V)}$ and pulse protocols for activation of $I_{K(V)}$ (inset). **E**: Original recordings of $I_{K(V)}$ activation in control conditions and in the presence of 1 pM AA.

Oxidative mechanism in reduction of the transient potassium current I_A by arachidonic acid

AA and ETYA may affect protein function by binding-induced conformational changes. Alternatively, both molecules are free radicals that can oxidize certain amino acids. To test for an involvement of oxidative effects of AA was used together with antioxidants, glutathione (GSH), ascorbic acid and Trolox (water-soluble analogue of α-Tocopherol) either alone or in different combinations.

Influence of glutathione on arachidonic acid-mediated effects

Figure 16 B illustrates the surprising finding that when GSH (20mM) was included in the patch pipette, the AA effect on the maximal I_A was not inhibited, but actually enhanced (-61.6 ± 5.8 % at 15min). In addition, reduction of I_A was accelerated, as visible by significant reduction of I_A after only 3 min of whole-cell recording (*, -44.1 ± 9.3 %, n=6 for AA + GSH_{in}; as compared to -2.4 ± 4.8 %, n=9 for AA alone, Fig. 16 B) and inactivation was significantly slowed ($p<0.01$, Fig. 16 C inset). GSH itself had neither effect on I_A nor on $I_{K(V)}$ maximal conductance(n=6, Tables 5 and 6; Fig.20 A, D). The augmentation of the AA effect by GSH suggests that redox reactions may be responsible for reduction of I_A by AA and by GSH.

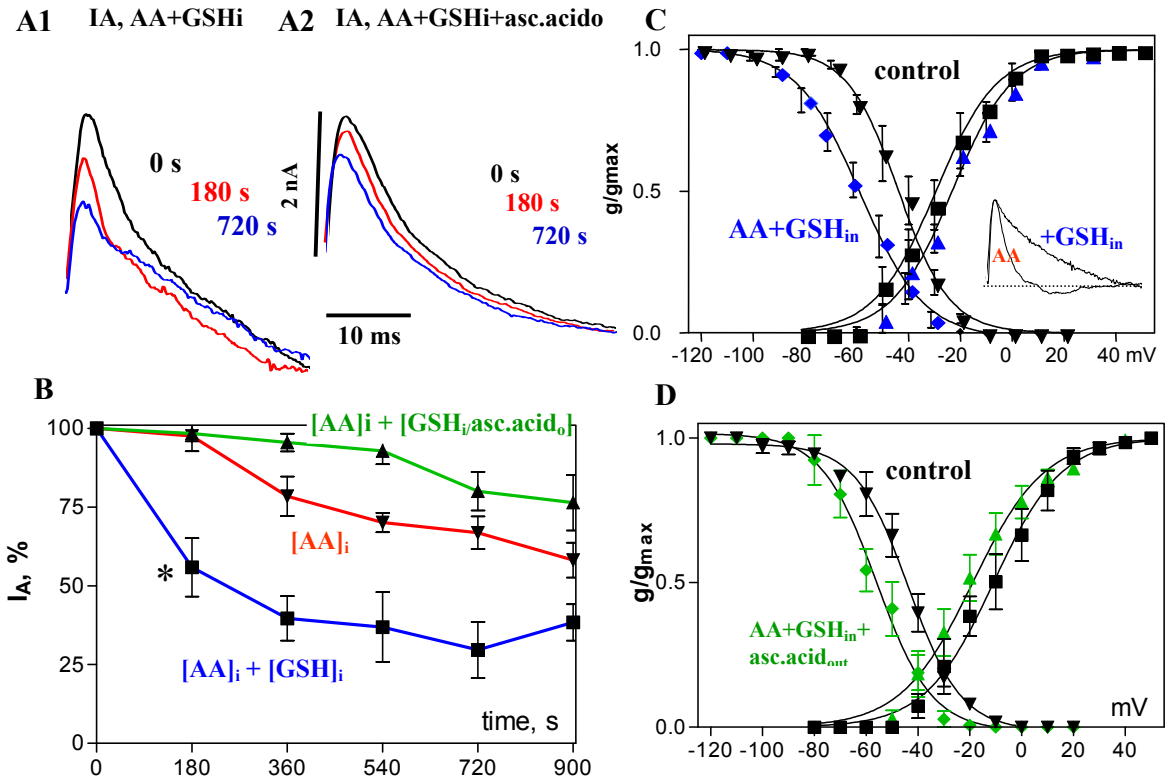

Fig. 16 Interaction of AA and antioxidants with I_A. in CA1 pyramidal neurons

A, B: GSH_i enhances the AA effect on I_A (A1, B: blue line), particularly early after begin of recording/application (*), while ascorbic acid blocks the AA effect (A2, B: green line). **C, D**: GSH_i and ascorbic $acid_o$ do not prevent the AA-mediated shift in steady-state inactivation (C, D, control=0 s vs. 900 s, left curves) but ascorbic acid slightly reduces it and shifts as well the activation curve to more negative potential (D, right curves). AA+GSH_i (but not AA, only) slow inactivation of I_A, as demonstrated by an overlay of traces after scaling to the same amplitude (C, inset, trace=40 ms).

Influence of glutathione and ascorbate on arachidonic acid–mediated effects

In contrast to GSH, ascorbic acid (0.4 mM), an antioxidant that apparently crosses cell membranes easily, blocked reduction of I_A when applied by the bath in addition to AA + GSH_{in} (Fig. 16 A2, B-green line). In slices superfused with ascorbic acid only, I_A decreased during whole cell recording over 15 min steadily to 40.9 ± 6.7 % and $I_{K(V)}$ to 60.3 ± 7.3 % of initial current amplitude (n=5). Under this conditions, tau of I_A inactivation was also significantly slowed ($p<0.01$, Table 5), further supporting that ascorbic acid can catalyze oxidative reactions with these channels, depending on the oxidative stress in the vicinity of the membrane.

Moreover, combination of GSH_{in} and ascorbic acid did not prevent the AA-mediated shift in steady-state inactivation (Fig. 16 D), further suggesting that this shift is caused by a mechanism independent of reduction of maximal conductance. GSH_{in} plus AA had, like AA alone, no effect on voltage dependence of activation. Combination of GSH and ascorbic acid plus AA caused a 6 mV shift of activation to more negative potentials that is statistically significant with 95 % confidence (Fig. 16 D, right curves).

Influence of Trolox on arachidonic acid-mediated effects

Despite its water solubility Trolox, like tocopherol, is assumed to primarily protect membrane lipids and transmembrane protein segments from oxidation. In slices superfused with Trolox (100 µM), both I_A and $I_{K(V)}$ were completely stable during 15 min whole cell recording.

The inactivation time constant of I_A was progressively slowed over 15 min during whole cell recording from 4.5 ms to 9.9 ms ($p<0.01$, Table 5). Figure 17 A shows that intracellular application of AA together with Trolox, that is applied from both sides of the cell membrane, did also enhance the early effect of AA on I_A (Fig. 17 B, *). With prolonged recording time in the presence of $Trolox_{in/out}$ I_A showed significant recovery (Fig. 17 B). Again, voltage dependent inactivation showed responses independent from modulation of maximal conductance. $Trolox_{in}$ inhibited the AA shift of steady-state inactivation (Fig. 17 C).

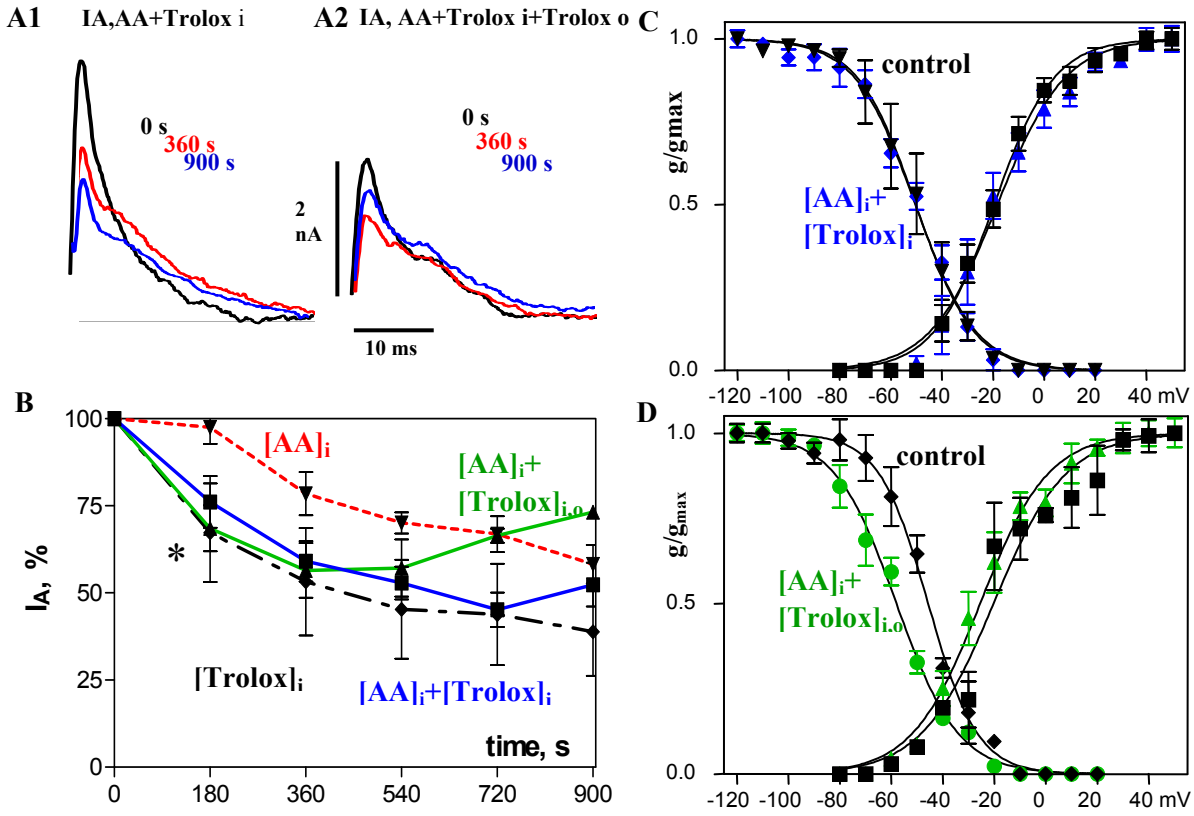

Fig. 17 Interaction of AA and antioxidants with I_A in CA1 pyramidal neurons.

A, B: Intracellular application of the vitamin E analogue Trolox (10 µM) with AA does not prevent reduction of I_A (A1, B: blue line), but Trolox, applied from both sides of the cell membrane, does significantly recover I_A with prolonged recording time (A2, B: green line). Intracellular application of 10 µM Trolox by itself reduces I_A similar to 1 pM AA (B: black line). **C**: $Trolox_i$ inhibits the AA shift of steady-state inactivation (left curves). There is no shift in voltage dependence of activation (right curves, control=0 s vs. 900 s). **D**: In the presence of Trolox on both sides of the membrane plus AA_i, steady state inactivation shifts over 900 s recording time by -12mV to more negative potential, similar to the effect of AA_i or of $Trolox_i$.

The voltage dependence of activation of I_A was unchanged. Surprisingly, AA_i in the presence of Trolox on both sides of the membrane shifted steady state inactivation by -12 mV to more negative potentials (over 15 min), similar to the effect of AA_i or of $Trolox_{in}$ alone. For the triple combination (AA_i + $Trolox_{in,out}$) there was no shift of voltage dependence of activation of the transient potassium current (Fig. 17 D, curves on right side).

Effects of H_2O_2 on outward potassium currents

To evaluate direct effects of oxidative modulation of I_A (in the absence of AA), the non-lipid oxidizing compound hydrogen peroxide (H_2O_2) was applied via the patch pipette. Generally, 80 µM H_2O_2 mimicked the effect of 1 pM AA on the maximal amplitude of I_A (-79.6 ± 1.9 %, $p<0.01$, n=6, Fig. 18A). Like AA, it also shifted the voltage dependence of inactivation to more negative potentials (-7mV, Fig. 18 B, left curves). Unlike AA, H_2O_2 in addition shifted the voltage dependence of activation to more negative potentials (-6 mV, Fig. 18 B, right curves) and slowed inactivation of I_A ($p<0.05$, Table 5). The effects of H_2O_2 further support the idea that modulation of I_A by AA is mediated primarily by oxidative reactions. Therefore it was tested for effects of antioxidants on the effects of H_2O_2, expecting complex changes as described above for AA.

Influence of glutathione on H_2O_2–mediated effects on potassium currents

The physiological antioxidant GSH_{in} (20 mM) strongly reduced inhibition of maximal I_A by H_2O_2 (-34.8 ± 7.2 %, n=4, Fig.18 A) and eliminated the H_2O_2 mediated shift of steady state inactivation (Fig. 18 C). While H_2O_2 shifted the voltage dependence of activation to the left, H_2O_2 in the presence of GSH_{in} caused a shift to the right (+7 mV, Fig. 18 C). In addition, the slope of the conductance voltage relationship was decreased (k=14.9 ± 0.8 for H_2O_2 and k=11.6 ± 0.7 for H_2O_2 plus GSH) and slowing of I_A inactivation was enhanced ($p<0.001$, Table 5).

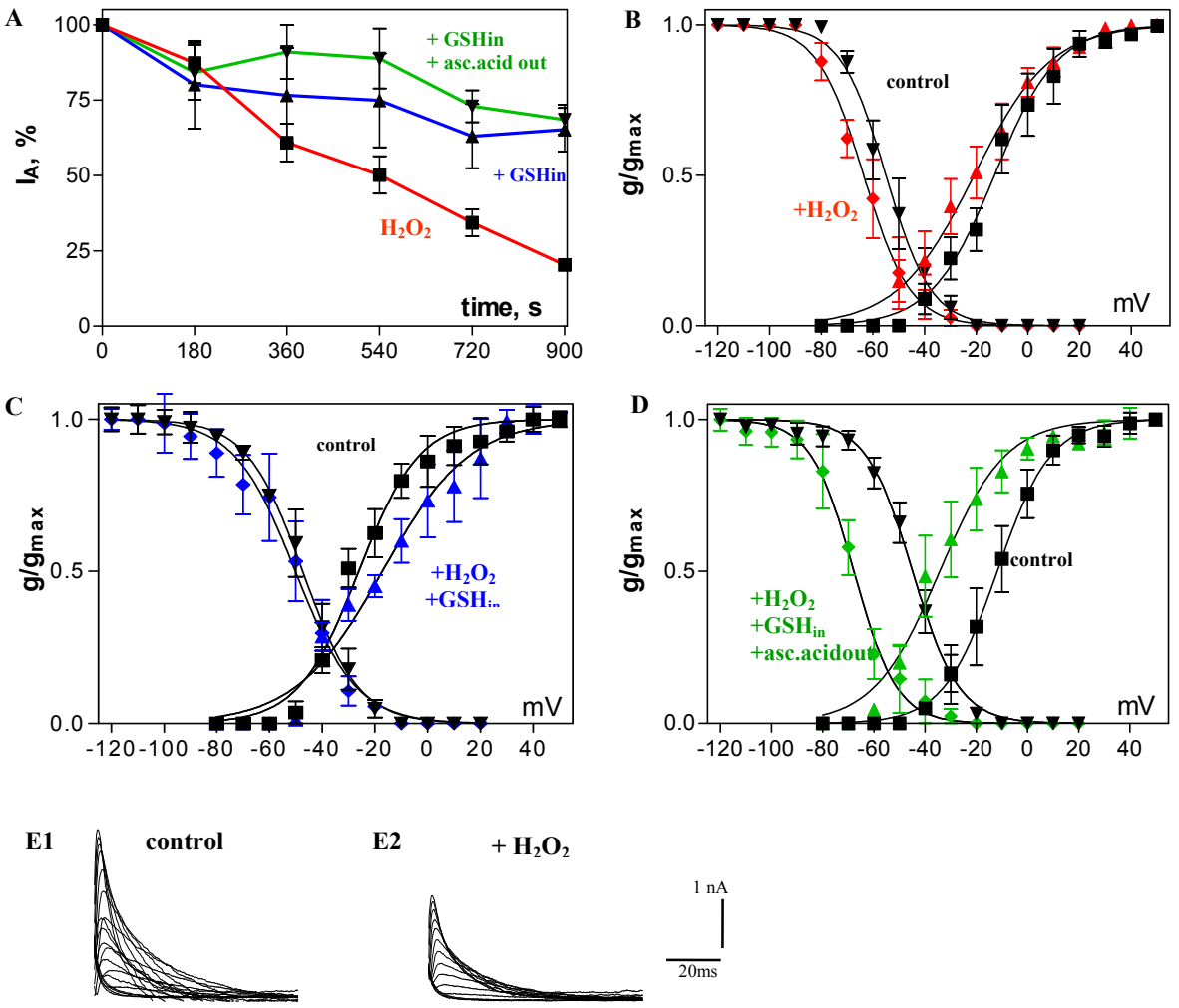

Fig. 18 Effects of intracellular H_2O_2 (80 µM) and antioxidants on I_A in CA1 pyramidal neurons.

A: H_2O_2 mimics the effect of AA on maximal I_A (red line). This effect is not enhanced but inhibited by GSH_i or GSH_i+ascorbic $acid_o$ (green and blue line, respectively). **B:** H_2O_2 shifts voltage conductance relations of inactivation (left curves) and activation (right curves) to more negative potentials. **C:** GSH_i eliminates the H_2O_2 mediated shift in inactivation (left curves), but for activation causes a shift to more positive potential and change in slope (right curve). **D:** In the presence of ascorbic $acid_o$, GSH_i + H_2O_2 shift inactivation and activation of I_A by -22 mV to more negative potentials. **E:** Representative current traces of I_A for determination of the voltage dependence of activation for control immediately after obtaining whole cell configuration (E1) and after 900 s of recording with H_2O_2 in the patch pipette (E2).

Influence of glutathione and ascorbate on H_2O_2–mediated effects on potassium currents

Addition of ascorbic acid to the ACSF (0.4 mM), appeared to strengthen inhibition of the H_2O_2 effect by GSH_{in} on maximal I_A amplitude (-31.5 ± 4.9 %, n=4, Fig. 18 A). In contrast, ascorbic acid did not support GSH_{in} inhibition of the shifts of voltage dependence of inactivation and of activation, but even enhanced shifts caused by H_2O_2 by more than 150% (Fig. 18 D, Table 5). Unlike with H_2O_2+GSH_{in} there was no significant change of slopes, neither of voltage dependence of activation, nor of inactivation (Fig. 18 D, Table 5). I_A inactivated much faster in the presence of ascorbic acid, but tau still almost doubled from 5.7 to 9.8 ms during 15 min whole cell recording with H_2O_2 + GSH_{in} ($p<0.01$, Table 5).

In agreement with results reported for neurons in primary cultures, H_2O_2 also suppressed the delayed rectifier potassium current $I_{K(V)}$ in CA1 pyramidal neurons in brain slices (-63.2 ± 5.1 %, n=6, Fig.19 A, C, Table 6). H_2O_2 shifted the voltage dependence of activation to more negative potentials (from 1.4 ± 1.5 mV to -5.7 ± 1.5 mV, n=7, Fig.19 B). GSH_{in} and also GSH_{in} plus ascorbic acid inhibited reduction of $I_{k(v)}$ by H_2O_2, (-21.0 ± 5.3 %, n= 4 and –23.0 ± 3.9 %, n=4, respectively, Fig.19 A).

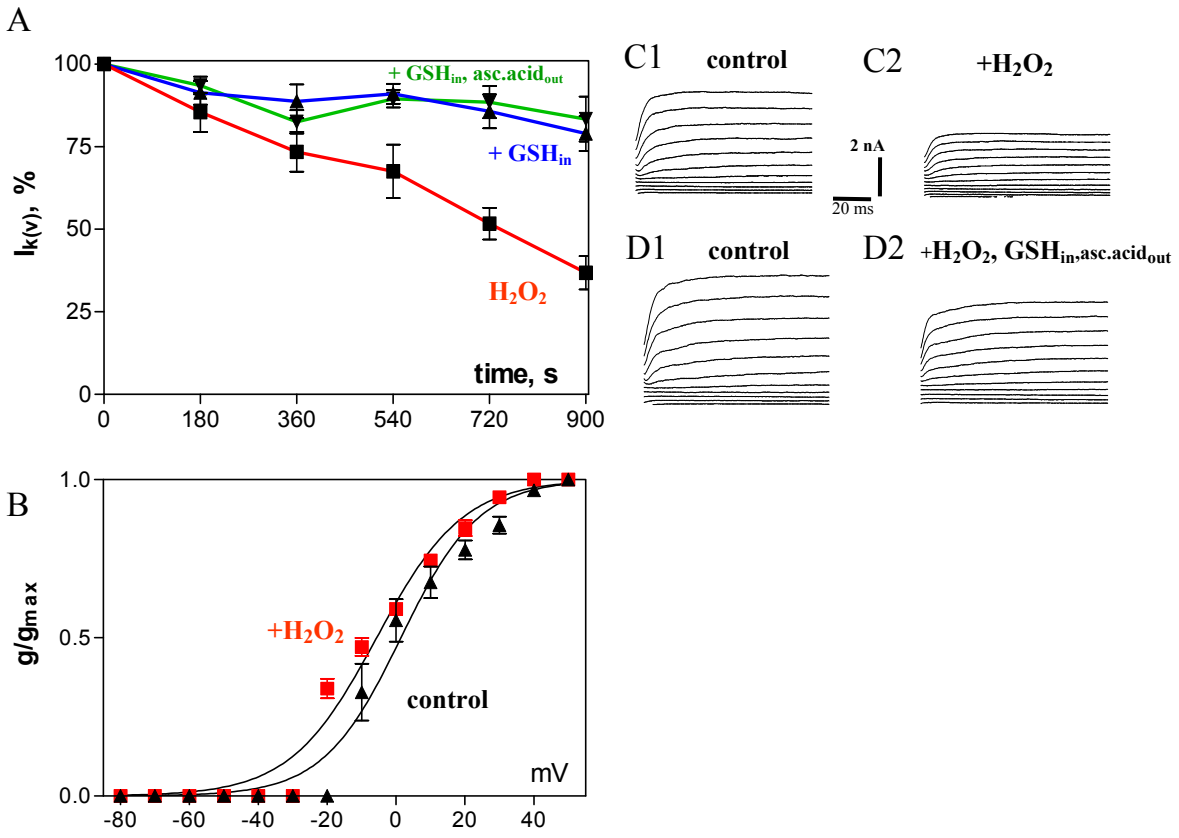

Fig. 19 Effects of intracellular H_2O_2 (80 µM) and antioxidants on $I_{K(V)}$ in CA1 pyramidal neurons.

A: H_2O_2 suppresses the delayed rectifier potassium current $I_{K(V)}$, and this effect is inhibited by GSH_i or GSH_i+ascorbic $acid_o$ (+GSH_i and +GSH_i,$asc.acid_o$, respectively). **B**: H_2O_2 shifts voltage dependence of activation of $I_{K(V)}$ to a more negative potential. **C**, **D**: Representative traces of $I_{K(V)}$ for determination of voltage dependence of activation for control immediately after obtaining whole cell configuration (C1, D1, 0 s) and after 900 s recording with H_2O_2 (C2) or H_2O_2 + GSH_i in the patch pipette (D2). Recordings of D have been obtained in the presence of ascorbic $acid_o$.

Control antioxidant studies

Due to unexpected behavior of antioxidants in this set of experiments with arachidonic acid, control (only in the presence of antioxidants) studies on I_A and $I_{K(V)}$, were performed in CA1 neurons in order to investigate potential K^+-current susceptibility to antioxidant exposure.

Intracellular GSH

Application of 20 μM GSH to the intrapipette solution for 15 min resulted in a significant leftward shift of steady-state inactivation of I_A compared to that observed in controls (-54.6 ± 0.3 mV and -65.1 ± 0.5 mV, respectively). Glutathione by itself reduced the rate of inactivation of I_A within 15 min. (τ=8.5 ± 1.3 vs. τ=12.3 ± 2.0). Under GSH_{in} conditions, the maximal conductances of I_A and $I_{K(V)}$ were reduced to ~20 % (Fig.20 A, D).

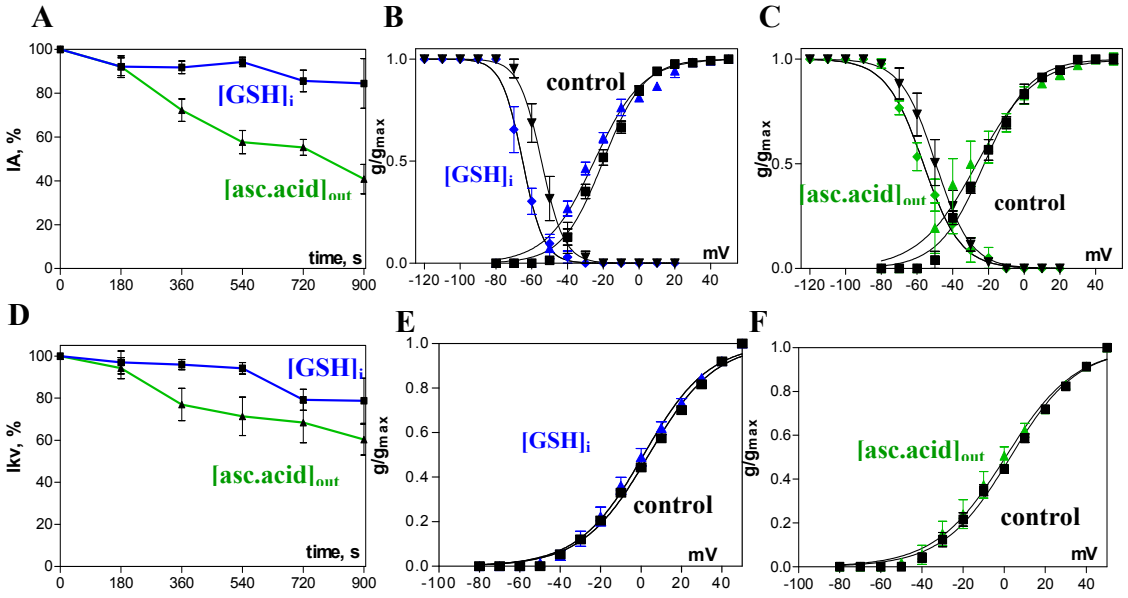

Fig. 20 Effects of GSH and ascorbate on K^+ currents behavior in CA1 pyramidal neurons.

A, D: Effects on the maximal amplitude of I_A (A) and $I_{K(V)}$ (D). **B, C:** Steady-state inactivation and activation curves for control (black line) and GSH (blue) and ascorbic acid (green) conditions. **E, F**: Kinetics of activation of $I_{K(V)}$ in the presence of GSH (E) and ascorbate (F).

Extracellular ascorbic acid

The perfusion of the slices with 0.4 mM ascorbate reduced significantly the maximal amplitude of I_A to -59.1 ± 6.7% as well as the maximal amplitude of $I_{K(V)}$ to -39.7 ± 7.3% (Fig.20, A and D). Ascorbic acid applied on the outer side of the membrane did not affect the kinetics of activation and steady-state inactivation of I_A. 0.4 mM ascorbate, applied trough the perfusion, did not influence the activation of $I_{K(V)}$ as well (Fig.20 E, F).

Intracellular Trolox

Inclusion of 10 μM Trolox to the patch pipette led to significant decrease of the peak current amplitude of I_A to -61.1 ± 2.7 % and those of $I_{K(V)}$ to -39.4 ± 10.8 % (Fig.21 A, D-blue line). Intracellular Trolox shifted voltage dependence of activation (from -21.3 ± 1.2 mV to -13.4 ± 1.0 mV) and inactivation (from -44.8± 0.4mV to -54.0 ± 0.1 mV) of I_A $Trolox_{in}$ increased the I_A time constant of inactivation (τ = 4.5 ± 0.6 at 0s and τ = 9.9 ± 1.4 at 900 s).

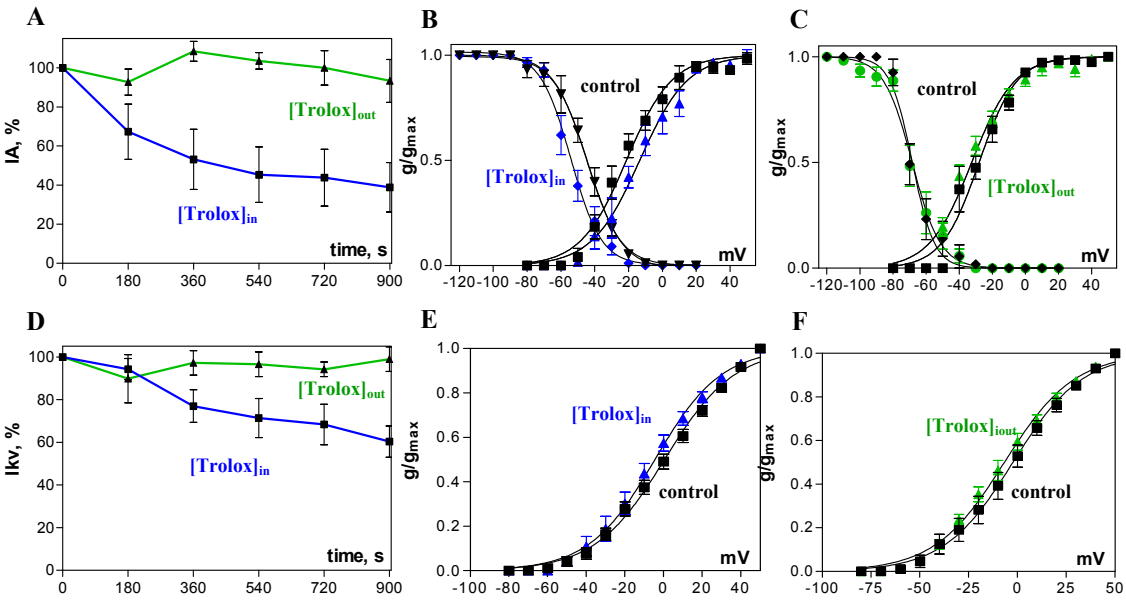

Fig. 21 Effects of Trolox on K^+ currents behavior in CA1 pyramidal neurons.

A, D: Effects on the peak amplitude of I_A (A) and $I_{K(V)}$ (D). **B, C:** Steady-state inactivation and activation curves of I_A in control (black line) and after intracellular (blue) and extracellular (green) application of Trolox. **E, F**: Activation kinetics of $I_{K(V)}$ in the presence of Trolox $_{in}$(E) and Trolox $_{out}$ (F).

On Fig.21 E, $I_{K(V)}$ voltage-conductance relation of activation in the presence of Trolox in the patch pipette showed a small shift (from 0.5 ± 0.9 mV to -4.5 ± 0.7 mV, n=5) to more hyperpolarizing values.

Extracellular Trolox

Bath application of 100 μM Trolox did not influence I_A or $I_{K(V)}$ in any way. There were neither changes in maximal amplitude nor in the kinetic of activation and steady-state inactivation of these currents (Fig.21 A, C, D, F-green line, Table 5). Trolox $_{out}$ did not affect the rate of inactivation of I_A as well.

Table 5 Overview of effects of oxidants and antioxidants on behavior parameters of I_A in CA1 pyramidal neurons.

I_A CA1	n	max amplitude, % of control	V_{50a} 0 min mV	V_{50a} 15 min mV	$k_{activation}$ 0 min	k_a 15 min	V_{50i} 0 min mV	V_{50i} 15 min mV	$k_{inactivation}$ 0 min	k_i 15 min	τ_i 0 min ms	τ_i 15 min ms
control	9	-10.9 ± 4.6	-14.3±0.3	-18.1±0.5	7.9 ± 0.3	7.8 ±0.4	-38.1±0.7	-36.7±0.6	9.2 ± 0.5	9.3 ± 0.5	7.8 ± 1.5	8.5 ± 1.4
+ 1pM AA	9	-41.8 ± 5.5	-18.1±0.4	-19.2±0.9	7.8 ± 0.4	8.1 ±0.8	-41.4±0.4	-53.6±0.6	10.2 ± 0.3	11.3±0.6	8.1 ± 1.3	10.4±1.7
control GSH_{in}	8	-15.5±7.2	-20.1±0.7	-25.0±1.2	11.5±0.7	13.5±1.1	-54.6±0.3	-65.1±0.5	6.4 ± 0.3	5.9 ± 0.4	8.5 ± 1.3	12.3±2.0
AA+GSH_{in}	6	-61.6 ± 5.8	-29.2±0.9	-21.5±1.0	13.0±0.9	12.3±0.9	-43.0±0.8	-58.7±0.7	10.1± 0.7	12.3±0.6	11.9±2.5	21.3±3.6
control asc.$acid_{out}$	5	-59.1± 6.7	-22.4±0.9	-26.6±1.6	12.9±0.8	16.3±1.5	-49.5±0.3	-56.5±0.8	9.8 ± 0.3	9.5 ± 0.7	9.9 ± 1.0	15.8±2.3
AA+GSH_{in}/ asc.$acid_{out}$	4	-23.6 ± 11.8	-10.9±0.8	-18.9±0.9	13.2±0.7	13.8±0.8	-44.7±0.6	-56.0±0.9	10.5 ± 0.5	10.7±0.8	12.9±4.9	18.3±5.1
control $Trolox_{in}$	5	-61.1±2.7	-21.3±1.2	-13.4±1.0	13.5±1.0	14.2±0.9	-44.8±0.4	-54.0±0.1	9.9 ± 0.4	9.0 ± 0.7	4.5 ± 0.6	9.9 ± 1.4
AA+$Trolox_{in}$	7	-47.6 ± 12.2	-19.5±0.8	-18.2±1.0	11.7±0.7	13.1±0.9	-50.2±0.5	-50.3±0.7	11.3 ± 0.5	11.8±0.7	8.4 ± 3.1	13.3±3.7
control $Trolox_{out}$	4	-6.6 ± 9.1	-28.1±1.4	-32.5±1.3	11.3±1.3	12.8±1.2	-68.3±0.8	-68.4±0.8	6.7 ± 0.7	8.5 ± 0.7	6.1 ± 0.8	7.5 ± 1.2
AA+$Trolox_{in,\ out}$	4	-26.8 ± 1.1	-20.3±2.1	-25.5±1.0	14.1±1.8	13.2±0.8	-45.6±0.6	-58.0±0.7	9.5 ± 0.5	12.0±0.6	8.9 ± 0.9	10.7±1.1
+80µM H_2O_2	7	-79.7 ± 1.9	-12.9±0.8	-20.8±0.9	12.2±0.7	14.9±0.8	-55.0±0.6	-63.6±0.5	8.7 ± 0.5	9.0 ± 0.5	7.9 ± 1.6	13.5±1.5
H_2O_2 +GSH_{in}	4	-34.8 ± 7.2	-26.1±1.2	-17.2±2.0	11.5±1.1	16.6±1.6	-47.4±0.4	-50.2±0.8	10.6 ± 0.4	11.6±0.7	10.0±3.3	19.5±2.6
H_2O_2 +GSH_{in}/ asc.$acid_{out}$	4	-31.5 ± 4.9	-11.8±0.4	-34.3±1.4	10.5±0.3	12.8±1.2	-44.9±0.5	-67.8±0.6	9.1 ± 0.4	8.4 ± 0.5	5.7 ± 1.0	9.8 ± 1.0

Table 6 Overview of effects of oxidants and antioxidants on behavior parameters of $I_{K(V)}$.in CA1 pyramidal neurons.

$I_{k(v)}$ CA1	n	max amplitude % of control	$V_{50activation}$ 0 min	V_{50a} 15 min	$k_{activation}$ 0 min	k_a 15 min
control (2-6.8 nA)	9	-12.8±2.3 %	6.3±1.1	0.1±1.0	18.5±1.0	18.8±0.9
+ 1pM AA	9	-15.2±1.8%	5.3±0.9	-2.8±1.0	17.3±0.8	18.6±0.9
control GSH_{in}	8	-20.8±5.7	3.8±0.8	1.2±0.7	16.4±0.7	16.2±0.6
AA+GSH_{in}	6	-13.5±4.6%	0.7±1.3	-1.9±0.9	19.1±1.1	17.3±0.8
control asc.$acid_{out}$	5	-39.7±7.3	3.0±0.8	0.7±0.7	16.4±0.8	17.0±0.8
AA+GSH_{in}/ asc.$acid_{out}$	4	-17.1±1.3%	4.4±1.1	2.8±1.0	18.4±1.0	17.8±0.9
control $Trolox_{in}$	5	-39.4±10.8	0.5±0.9	-4.5±0.7	18.0±0.8	17.1±0.6
AA+$Trolox_{in}$	7	-20.8±8.5%	-3.2±0.9	-1.2±1.0	18.2±0.8	19.4±0.9
control $Trolox_{out}$	4	-1.0±5.7	-2.3±0.7	-6.7±0.8	17.7±0.6	17.9±0.7
AA+$Trolox_{in}$/ $Trolox_{out}$	4	-18.4±10.6%	-3.3±1.1	-1.0±1.0	19.3±1.0	16.7±0.9
+80µM H_2O_2	7	-63.2±5.1%	1.4±1.5	-5.7±1.5	11.3±1.4	12.5±1.3
H_2O_2 +GSH_{in}	4	-21.1±5.3%	-3.3±1.1	-6.7±1.2	19.2±1.0	17.6±1.0
H_2O_2+GSH_{in}/ asc.$acid_{out}$	4	-23.0±3.9%	3.5±0.8	-8.2±0.9	17.7±0.7	17.7±0.8

Oxidative modulation of transient and delayed rectifier potassium currents in ECLIII pyramidal neurons

Potassium currents in untreated ECLIII pyramidal neurons

In whole-cell patch–clamp experiments with pyramidal neurons in layer III from medial entorhinal cortex the membrane potential of the cells were hyperpolarized to -110 mV for 800 ms from holding potential of -80 mV (for protocols see insets Fig.22). Depolarizing command pulses of 200 ms duration between -80 and + 50 mV (every 10 mV) elicited families of potassium outward currents, that are depicted here on Fig.22 A and B. With the above described subtracting procedure (see p. 35), the transient and delayed rectifier potassium currents were further separated. The isolated transient potassium current I_A had an amplitude of 0.5-4 nA and inactivated fast with a time constant of 13.0 ± 3.7 ms. I_A maximal amplitude showed no changes within 15 min. after opening the cells (-1.2 ± 7.2 %, n=9, Fig.22 C and Fig.23 A, black line). The time constant of inactivation of I_A was diminished after 15 min to 9.0 ± 3.5 ms (Fig.22 C, Table 7) however this difference was not statistically significant.

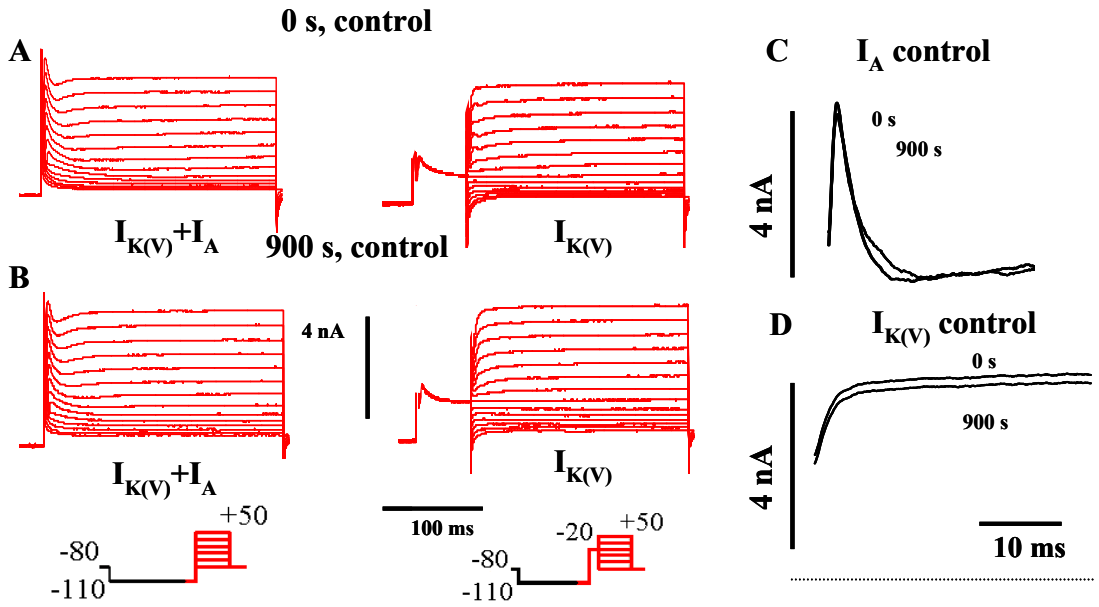

Fig. 22 Native I_A and $I_{K(V)}$ in control condition in ECLIII pyramidal neurons.

A, B Original traces showing total outward potassium ($I_{K(V)}$+IA) and delayed rectifier ($I_{K(V)}$) currents at 0 s (A) and 900 s (B) after reaching whole-cell configuration. **C** Subtracted transient potassium current (I_A) recorded at +30 mV over time. **D,** Delayed rectifier current at +30 mV over time.

As shown on Fig.23 D and Fig.24 A and C (black line) and D, $I_{K(V)}$ had maximal amplitude of 2 to 9 nA in control conditions which remained relatively stable (-10.5 ± 4.3 %, n=9) during an experiment of 15 min duration.

Modulation of transient I_A and delayed rectifier currents $I_{K(V)}$ by arachidonic acid

Application of 1 pM intracellular arachidonic acid to ECLIII pyramidal neurons strongly reduced the transient potassium current amplitude from -1.2 ± 7.2% in control to -57.9 ± 7.2 % after 15 min with AA in the pipette (Fig.23 A, red line; C). Arachidonic acid insignificantly slowed down I_A inactivation kinetics from 8.8 ± 1.6 to 12.9 ± 1.9 ms (Table 7).

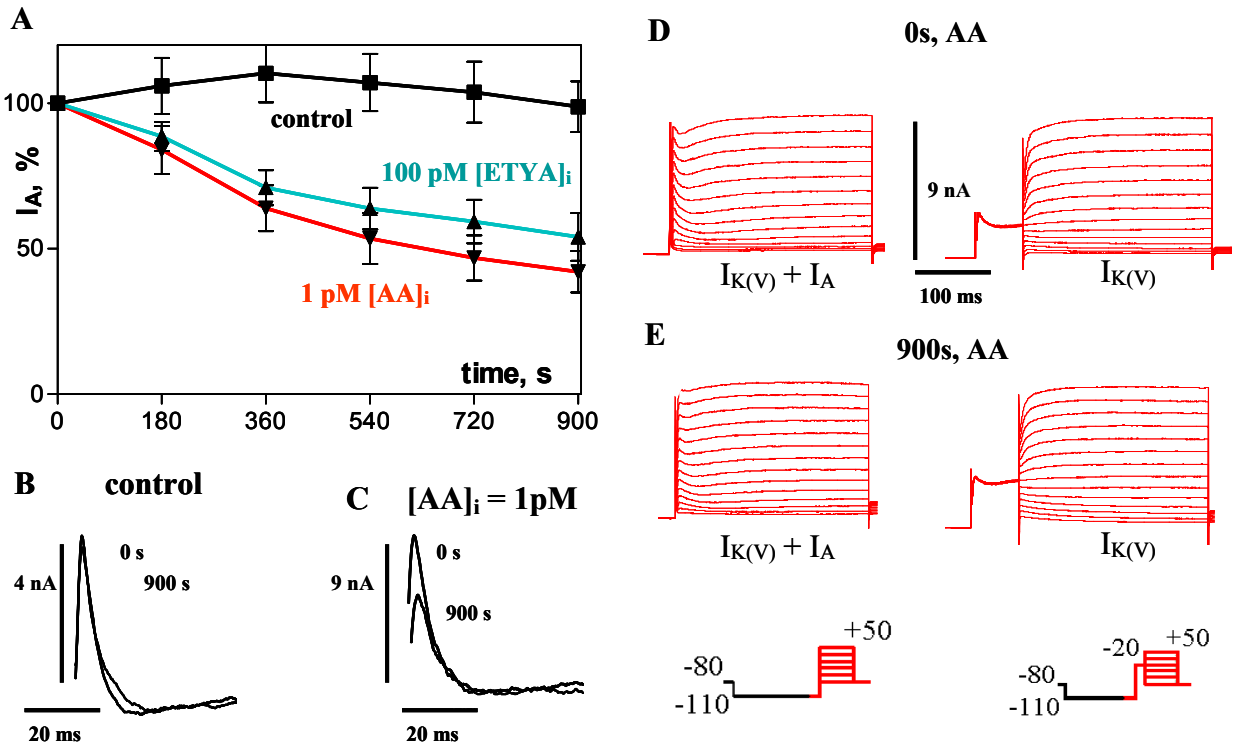

Fig. 23 Suppression of I_A by arachidonic acid (AA) in ECLIII pyramidal neurons.

A: control; **B, C**: Intracellular application of 1 pM AA reduces the maximal transient potassium current (I_A) over time. The non-metabolizable AA analogue ETYA shows similar effect on I_A at 100-fold higher concentration (**C**). **D, E**: Raw current traces for combined I_A and $I_{k(v)}$ and for delayed rectifier currents (pulse protocols: inset in E). Currents are shown for control immediately after obtaining whole cell configuration (**D**, 0 s AA), after and after 900 s of recording with 1 pM of AA in the patch pipette (**E**).

100 pM intracellularly applied ETYA mimicked the effect of 1 pM arachidonic acid, as shown on Fig.23 A, green line. This fact qualifies the effect of AA in ECLIII pyramidal neurons as direct, as ETYA blocks the enzymes from the arachidonic acid metabolitic pathway. This effect was already shown for CA1 pyramidal neurons (*see* p.40).

In contrast to I_A, $I_{K(V)}$ was found to be less sensitive to 1 pM AA (Fig.24). Its maximal amplitude in ECLIII pyramidal neurons was reduced by 19.7 ± 8.7 % (n=9).

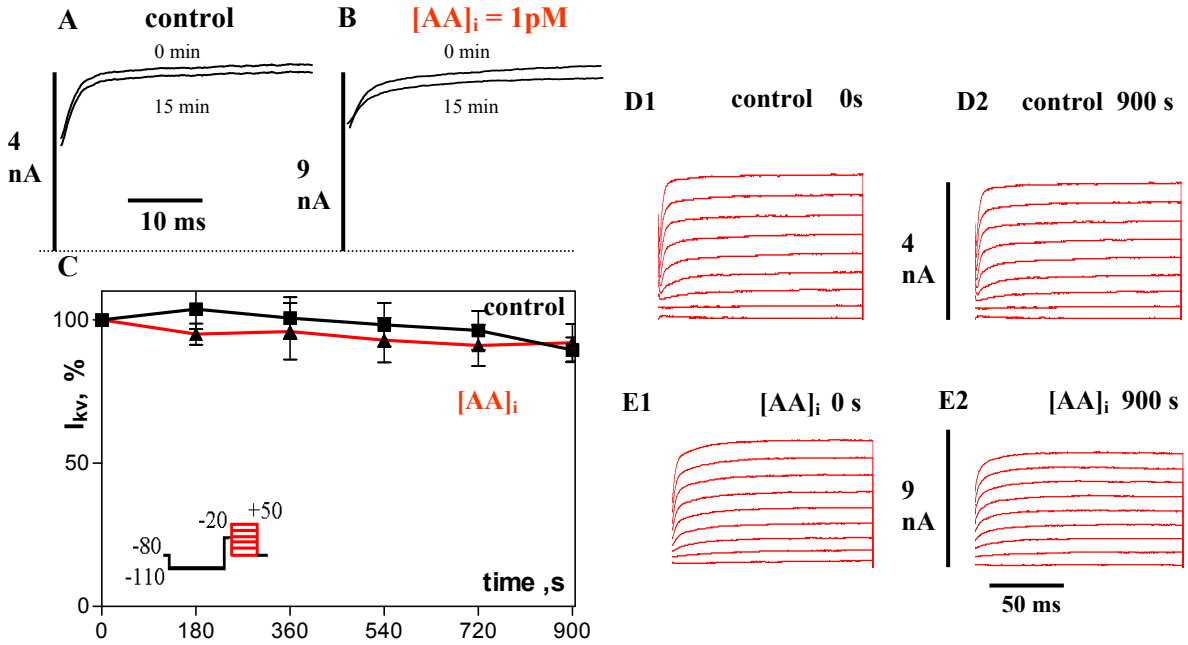

Fig. 24 The delayed rectifier current $I_{k(v)}$ is not affected by AA in ECLIII pyramidal neurons.

A, B: Maximal $I_{k(v)}$ recorded at 0 s and at 900 s of whole cell recording shows a ~ 10% decrease over time in control (**A**) and ~ 20% decrease with 1 pM AA in the patch pipette (**B**). **C**: Plot of $I_{k(v)}$ amplitude over time of whole cell recording for control and for AA. **D, E**: Original current recordings of $I_{k(v)}$ for several voltage steps (see inset in C) for control (**D**) and for AA at 0 s (D1, E1) and 900 s (D2, E2) of whole cell recording.

In ECLIII, as well as in CA1 pyramidal neurons, the activation and steady-state inactivation kinetics of the isolated I_A and $I_{K(V)}$ were best fitted with Boltzmann equations. Resulting curves revealed that I_A in control conditions is activated at ~ -60 mV and saturated at potentials more positive than +20 mV. I_A in control had a V_{50} of -18.2 ± 1.3mV and slope factor (*k*) of 16.0 ± 1.1. Inclusion of 1 pM AA to the patch pipette led to insignificant change of V_{50} and the slope factor of activation kinetic of I_A (V_{50} = -21.4 ± 1.0 mV and k= 8.6 ± 0.9). In contrast, the steady-state inactivation of I_A was shifted with ~11 mV to hyperpolarizing direction (Fig.25 A) after application of 1pM AA (Table 7). AA also significantly shifted the activation half-maximal voltage V_{50} of $I_{K(V)}$ from 5.7 ± 0.3 mV to -1.9 ± 0.5 mV (Fig.25 C).

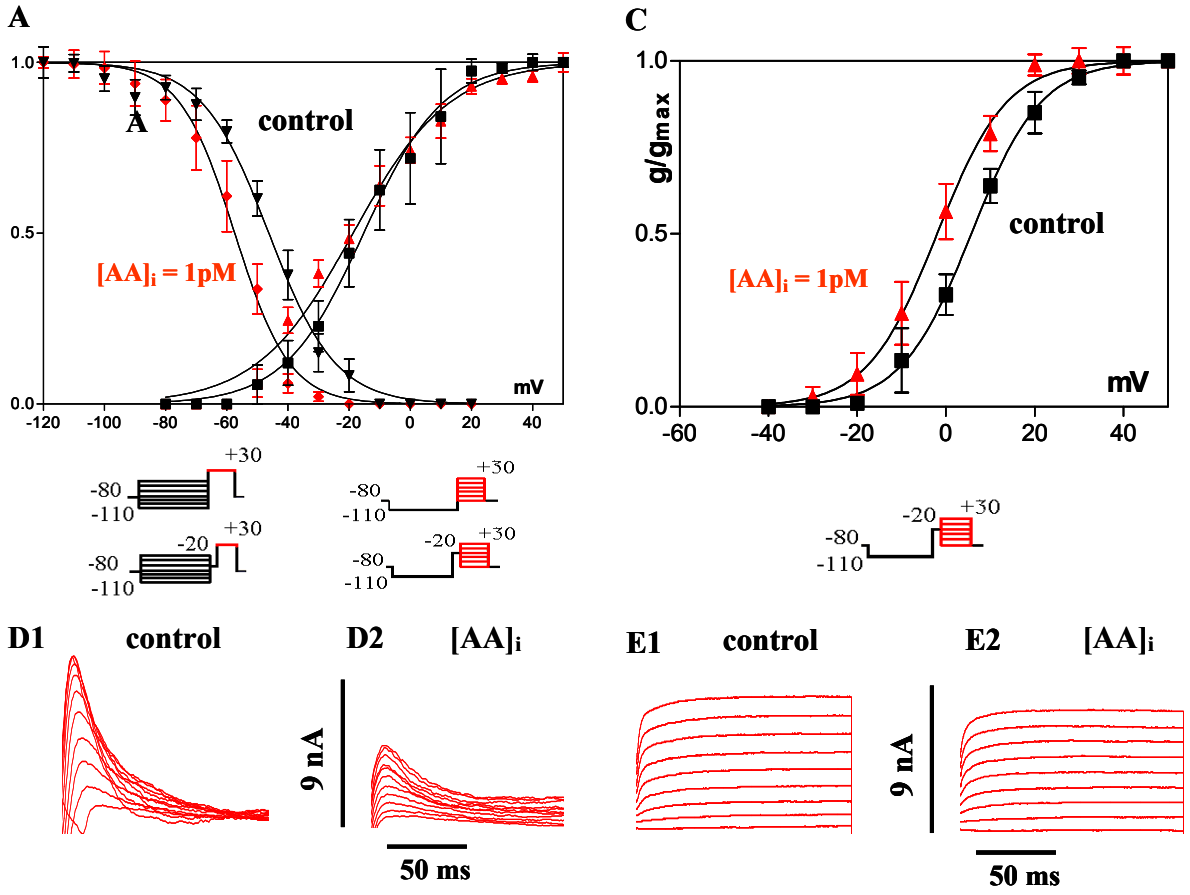

Fig. 25 Intracellular AA shifts steady-state inactivation, but does not affect voltage dependence of activation of I_A in ECLIII pyramidal neurons.

A: Conductance-voltage relations and Boltzmann fits for inactivation (left curves) and activation (right curves) of I_A. **Inset**: Pulse protocols for determining voltage dependence of steady state inactivation (left) and of activation (right). Red part shows length of the traces below. **B and C**: Representative recordings for inactivation (B) and activation (C).**D**: voltage-conductance dependence of $I_{K(V)}$ and pulse protocols for activation of $I_{K(V)}$ (inset). **E**: Original recordings of $I_{K(V)}$ activation in control conditions and in the presence of 1 pM AA.

Influence of glutathione on arachidonic acid-mediated effects

Intracellular GSH (20 mM), applied together with 1 pM AA further decreased I_A in ECLIII pyramidal neurons (Fig. 26 A, blue line), as reported for CA1 neurons. In agreement with this data, incubation of the slices for 2 hours prior to experiment with NAC (N-acetyl-L-cysteine, precursor of GSH) could not prevent the effect of arachidonic acid on I_A in ECLIII pyramidal neurons (data not shown). Additionally, GSH slowed down the inactivation of I_A from 10.3 ± 3.4 to 17.3 ± 2.8 ms, as seen on Fig.26 B1.

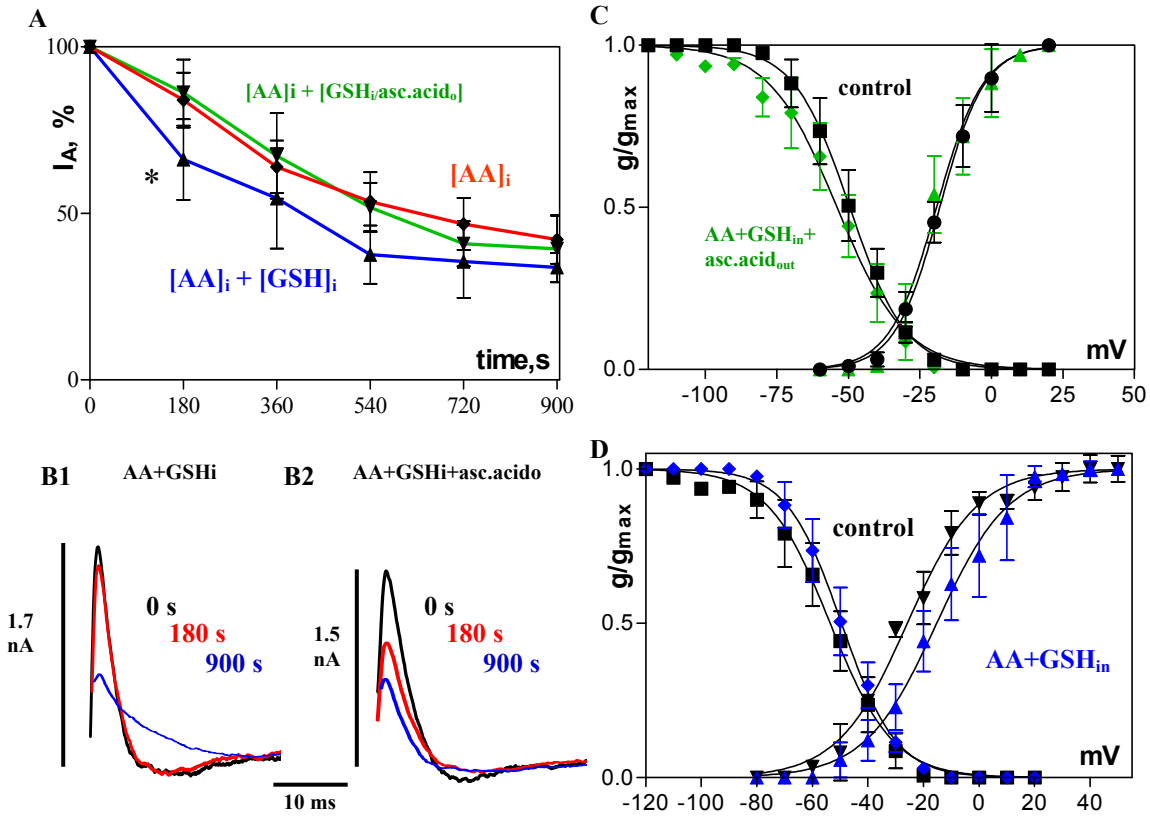

Fig. 26 Interaction of AA, GSH and ascorbic acid with I_A in ECLIII pyramidal neurons.

A, B: GSH_i enhances the AA effect on I_A (A: blue line; B1), particularly early after begin of application (*). As well, ascorbic acid could not block the AA effect (A: green line; B2). **C, D**: GSH_i and ascorbic $acid_o$ both prevent the AA-mediated shift in steady-state inactivation (C, D, control=0 s vs. 900 s, left curves) but GSH slightly shifts the activation curve to more positive potential (D, right curves).

Influence of glutathione and ascorbic acid on arachidonic acid-mediated effects

Yet, addition of ascorbic acid at concentrations up to 0.4 mM to the bath failed to remove effects of AA on the maximal I_A amplitude (Fig.26 A, green line), which is in contrast to the results obtained for CA1 pyramidal neurons, although it prevented GSH-mediated slow-down of this current (Fig.26 B2).

However, reduced glutathione, applied intracellularly, did significantly block the AA-induced shift of steady-state inactivation (Fig.26 D). Moreover, it shifted the activation V_{50} of I_A from -15.5 ± 0.7 mV to -25.8 ± 0.9 mV, as the slope factor *k* remained unaffected (Table 7). The triple combination treatment of AA and the antioxidants ascorbic acid and GSH, resulted again in blocked arachidonic acid effect on the steady-state inactivation of the transient potassium channels (Fig.26 C). $I_{K(V)}$ in the presence of AA+GSH_{in} reached 99.3 ± 9.7 % of control amplitude. Further perfusion of the slice with ascorbic acid led to $I_{K(V)}$ with maximal amplitude of 76.8 ± 6.6% and shifted $I_{K(V)}$ voltage–conductance relation of activation towards more negative potentials by ~15 mV (from -2.2 ± 0.8 mV to -17.6 ± 1.3 mV, n=6).

Influence of Trolox on arachidonic acid-mediated effects

Trolox, applied only on the inner side of the cell membrane, blocked completely the reduction of I_A by arachidonic acid (Fig.27 A, blue line). $Trolox_{in}$ did fail in preventing AA-mediated shift in inactivation and changed the activation parameters from $V_{50=}$ -27.0 ± 0.4 mV and k=9.7 ± 0.4 to $V_{50=}$ -21.8 ± 0.7 mV and k=12.2 ± 0.6 (Fig.27 C). In comparison, Trolox on both sides of the membrane accelerated the early AA effect, in GSH-like manner. It did not block the leftward shift of the steady-state inactivation curve, caused by 1pM arachidonic acid, but it shifted the activation kinetic by ~10 mV in depolarizing direction as shown on Fig.27 D. No significant changes on the time constant of inactivation of I_A in both cases with Trolox were observed (Table 7). On the other hand, Trolox, independently of the site of application, fully inhibited AA effect on the maximal amplitude of $I_{K(V)}$ (Table 8).

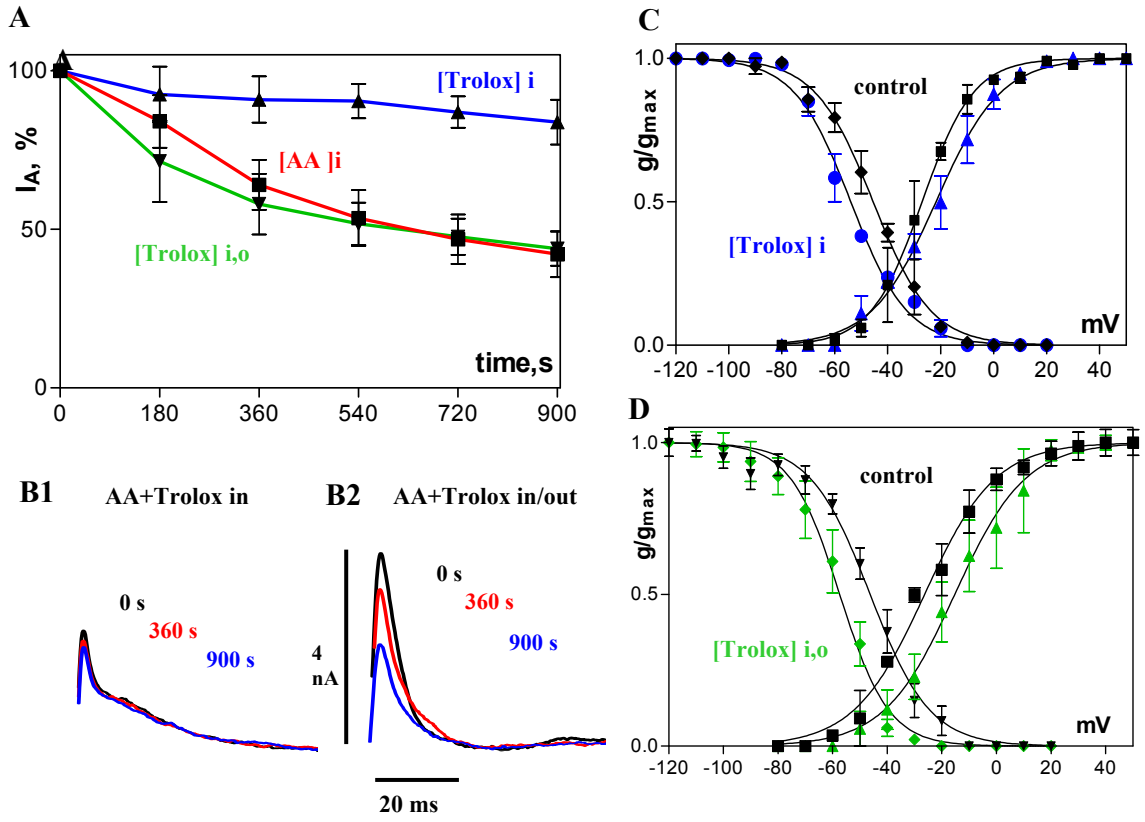

Fig. 27 Interaction of AA and Trolox with I_A in ECLIII pyramidal neurons.

A, B: Intracellular application of the vitamin E analogue Trolox (10 µM) with AA (A1, B: blue line) did significantly recover I_A, but Trolox, applied from both sides of the cell membrane, did not prevent reduction of I_A (A2, B: green line). **C**: $Trolox_i$ did not inhibit the AA shift of steady-state inactivation (left curves). There is shift in voltage dependence of activation (right curves, control=0 s vs. 900 s). **D**: In the presence of Trolox on both sides of the membrane plus AA_i, steady state inactivation shifts over 900 s recording time by -12mV to more negative potential, as well as activation mV to more positive potential, similar to the effect of $Trolox_i$.

Effects of H_2O_2 on outward potassium currents

As observed for CA1 pyramidal neurons, H_2O_2 mimics the effect of AA on maximal I_A in ECLIII pyramidal neurons (Fig.28 A, red line).

H_2O_2 did shift voltage conductance relations of inactivation to more negative and activation to more positive potentials (Fig.28 B). Mean parameters were: for activation, V_{50}= -24.9 ± 1.7 mV; *k*=14.2 ± 1.5 and for inactivation, V_{50}= -53.6 ± 0.6 mV; *k*=11.3 ± 0.5 (n=7).

Influence of glutathione and ascorbate on H_2O_2–mediated effects on potassium currents

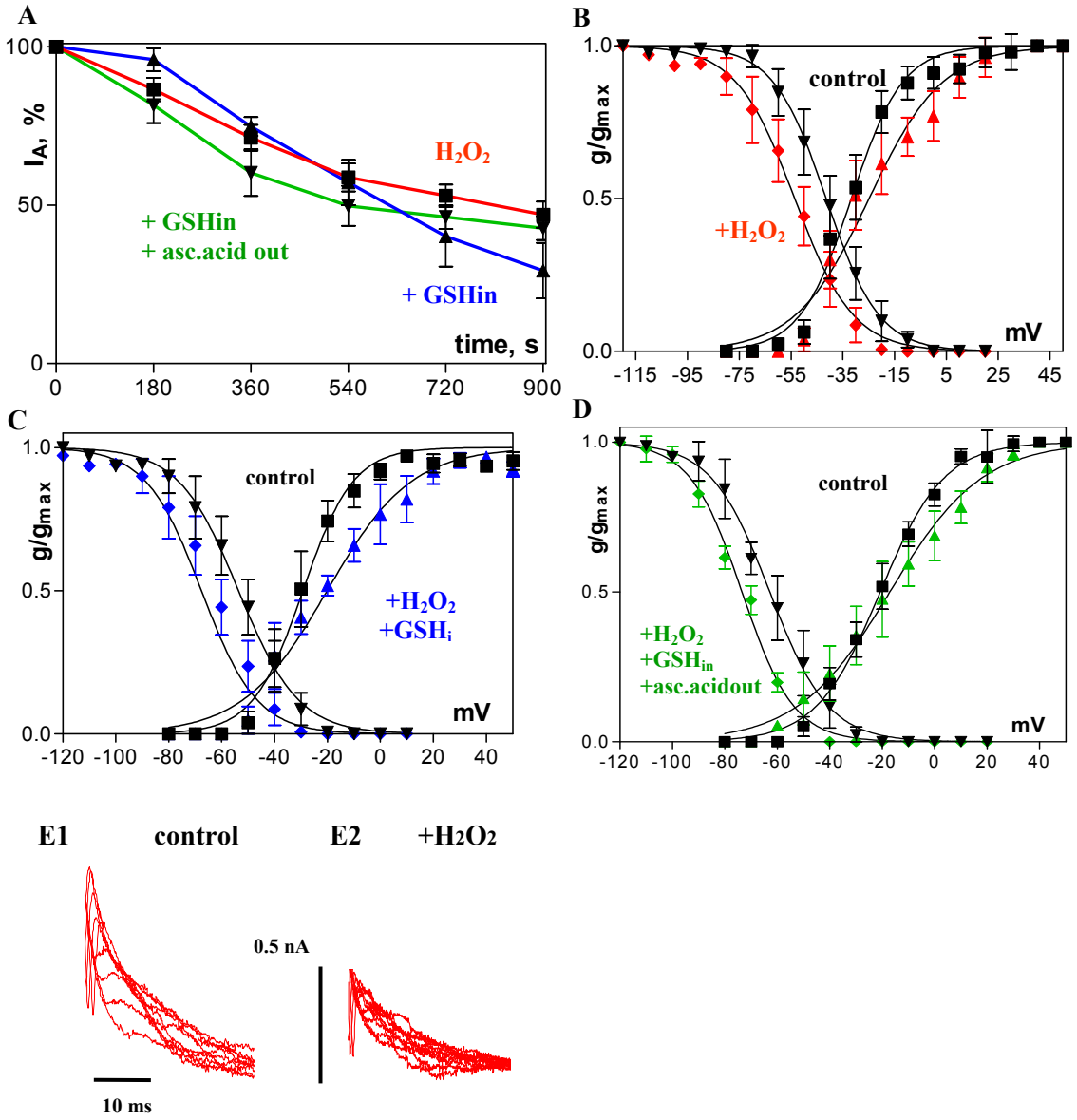

Fig. 28 Effects of intracellular H_2O_2 (80 µM) and antioxidants on I_A in ECLIII pyramidal neurons.

A: H_2O_2 mimics the effect of AA on maximal I_A. This effect is not inhibited by GSH_i or by GSH_i+ascorbic $acid_o$. **B**: Voltage conductance relations of inactivation (left curves) and activation (right curves) in the presence of H_2O_2. **C**: GSH_i does not eliminate the H_2O_2 mediated shift in inactivation (left curves), but leads to further shift of activation (right curve). **D**: Steady-state inactivation (left curves) and activation (right curves) kinetics of I_A in the presence of ascorbic $acid_o$, GSH_i and H_2O_2. **E**: Representative current traces of I_A for determination of the voltage dependence of activation for control immediately after obtaining whole cell configuration (E1) and after 900 s of recording with H_2O_2 in the patch pipette (E2).

As seen on Fig.28 C, GSH_i does not eliminate the H_2O_2 mediated shift in inactivation, but augments the rightward shift of the steady state activation curve. In the presence of H_2O_2, GSH_i and ascorbic $acid_o$, the steady-state inactivation and activation kinetics of I_A were not significantly different from those for H_2O_2 alone (Fig.28 D).

The delayed rectifier current from ECLIII pyramidal neurons is sensitive to H_2O_2, as already shown for CA1 pyramidal neurons. H_2O_2 reduced $I_{K(V)}$ by 26.3 ± 5.5 %, n=7 (Fig.29 A, red line). Intracellular GSH as well as GSH in combination with ascorbic acid, reduced the effect of H_2O_2 on the maximal amplitude to -3.7 ± 8.6 %, n=8 and -12.7 ± 7.7 %, n=6 (Fig.29 A, blue and green lines), respectively. Although a change in the activation voltage dependence of $I_{K(V)}$ in the presence of H_2O_2 was not observed (Fig.29 B), application of antioxidants on one or both sides of the membrane shifted it to more negative values. GSH_{in} caused a small, but significant shift from -5.7 ± 0.7 mV to -11.3 ± 1.5 mV, and moreover, changed the slope factor *k* from 17.8 ± 0.6 to 22.8 ± 1.4, n=8. In the case of GSH_{in} and ascorbic $acid_{out}$ the shift of the steady state activation curve was large, with V_{50} of about ~20 mV (from -0.1 ± 0.9 mV to -22.0 ± 1.5 mV, n=6), while the slope of the steady-state activation curve remained unaltered (Table 8).

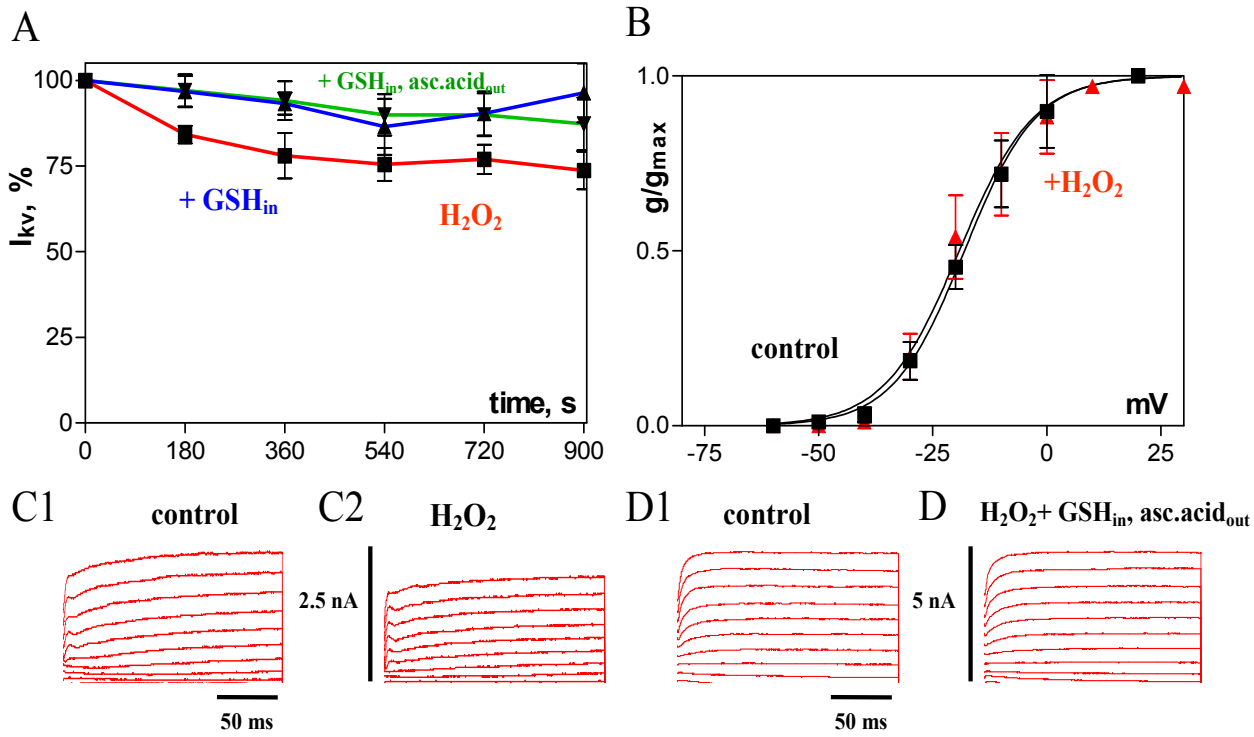

Fig. 29 Effects of intracellular H_2O_2 (80 µM) and antioxidants on $I_{K(V)}$ in ECLIII pyramidal neurons.

A: H_2O_2 suppresses the delayed rectifier potassium current $I_{K(V)}$ (red line), and this effect is inhibited by GSH_i or GSH_i+ascorbic $acid_o$ (blue and green lines, respectively). **B**: H_2O_2 does not shift voltage dependence of activation of $I_{K(V)}$. **C**, **D**: Representative traces of $I_{K(V)}$ for determination of voltage dependence of activation for control immediately after obtaining whole cell configuration (C1, D1, 0 s) and after 900 s recording with H_2O_2 (C2) or H_2O_2 + GSH_i in the patch pipette (D2). Recordings of D have been obtained in the presence of ascorbic $acid_o$.

Table 7 Overview of effects of oxidants and antioxidants on behavior parameters of I_A in ECLIII pyramidal neurons.

I_A ECLIIIpn	n	max amplitude, % of control	V_{50a} 0 min mV	V_{50a} 15 min mV	$k_{activation}$ 0 min	k_a 15 min	V_{50i} 0 min mV	V_{50i} 15 min mV	$k_{inactivation}$ 0 min	k_i 15 min	τ_i 0 min ms	τ_i 15 min ms
control	9	-1.2±7.2%	-21.0±1.5	-18.2±1.3	15.6±1.3	16.0±1.1	-52.2±0.9	-50.8±1.0	15.2±0.8	15.8±1.1	13.0±3.7	9.0±3.5
+ 1pM AA	9	-57.9±7.2%	-18.7±0.7	-21.4±1.0	8.9 ±0.7	8.6 ±0.9	-44.4±0.8	-53.3±1.6	9.8 ±0.7	10.7±1.5	8.8 ±1.6	12.9 ±1.9
AA+GSH_{in}	6	-66.3±4.4%	-15.5±0.7	-25.8±0.9	12.9±0.8	12.6±0.8	-49.5±0.3	-53.6±0.6	9.8±0.3	11.2±0.5	10.3±3.4	17.3±2.8
control asc.$acid_{in}$	6	-41.9±9.5%	-18.7±1.3	-18.3±1.9	15.9±1.1	16.4±1.7	no data	no data	no data	no data	17.4±6.4	17.7±7.1
AA+GSH_{in}/ asc.$acid_{out}$	6	-60.7±10.0%	-18.1±0.4	-19.2±0.9	7.8±0.4	8.1±0.8	-49.5±0.3	-54.0±0.8	9.8±0.3	11.9±0.7	6.4±1.4	7.1±1.9
AA+$Trolox_{in}$	7	-16.2±3.9%	-27.0±0.4	-21.8±0.7	9.7±0.4	12.2±0.6	-45.5±0.5	-54.0±0.8	11.0±0.4	10.7±0.7	7.0±2.5	9.5±2.1
AA+$Trolox_{in}$, $_{out}$	6	-56.1±5.4%	-26.3±0.9	-15.3±0.7	12.9±0.8	12.9±0.6	-46.3±0.8	-57.4±0.7	11.0±0.7	9.0±0.6	3.6±0.4	4.6±0.5
+80µM H_2O_2	7	-53.0±4.1%	-31.7±1.0	-24.9±1.7	9.9±0.8	14.2±1.5	-41.4±0.3	-53.6±0.6	10.2±0.3	11.3±0.5	3.3±0.5	3.2±0.5
H_2O_2 +GSH_{in}	8	-70.7±8.7 %	-29.3±1.0	-20.1±1.5	9.5±0.9	15.9±1.3	-53.1±0.7	-63.6±0.6	11.3±0.6	11.3±0.6	9.9±2.7	5.2±1.2
H_2O_2+GSH_{in}/ asc.$acid_{out}$	6	-57.3±3.7 %	-20.8±0.6	-17.1±1.0	12.2±0.5	17.6±0.9	-62.9±0.5	-73.5±0.6	11.2±0.4	9.9±0.6	4.9±1.5	9.8±2.8

Table 8 Overview of effects of oxidants and antioxidants on behavior parameters of $I_{K(V)}$ in ECLIII pyramidal neurons.

$I_{k(v)}$ ECLIIIpn	n	max amplitude % of control	$V_{50activation}$ 0 min	V_{50a} 15 min	$k_{activation}$ 0 min	k_a 15 min
control	9	-10.5±4.3 %	-10.7±1.3	-12.8±1.3	19.5±1.5	19.4±1.1
+ 1pM AA	9	-19.7±8.7 %	5.7±0.3	-1.9±0.5	18.1±1.1	19.9±0.7
AA+GSH_{in}	6	-0.7±9.7 %	1.5±1.2	-0.9±0.6	18.5±0.9	17.2±0.6
control asc.$acid_{in}$	6	-36.3±6.5 %	-8.8±1.3	-10.4±1.3	19.7±1.1	19.3±1.0
AA+GSH_{in}/ asc.$acid_{out}$	6	-23.2±6.6 %	-2.2±0.8	-17.6±1.3	18.9±0.7	22.1±1.2
AA+$Trolox_{in}$	7	-4.1±10.2 %	1.1±0.8	2.4±0.8	14.3±0.7	15.8±0.7
AA+$Trolox_{in}$/ $Trolox_{out}$	6	-7.9±6.5 %	-7.5±1.1	-2.7±0.8	21.1±1.0	17.1±0.7
+80µM H_2O_2	7	-26.3±5.5 %	-18.1±0.4	-19.2±0.9	16.1±0.6	17.9±0.8
H_2O_2 +GSH_{in}	8	-3.7±8.6 %	-5.7±0.7	-11.3±1.5	17.8±0.6	22.8±1.4
H_2O_2+GSH_{in}/ asc.$acid_{out}$	6	-12.7±7.7 %	-0.1±0.9	-22.0±1.5	16.3±0.8	19.1±1.3

Oxidative modulation of transient and delayed rectifier potassium currents in ECLII stellate neurons

Potassium currents in untreated ECLII stellate cells

Step depolarization of the membrane potential (protocols: inset Fig.30 B) of LII stellate neurons from the entorhinal cortex activated large outward potassium currents (0.5-13 nA) that are illustrated in Fig. 30 A. Digital subtraction of the sustain component ($I_{K(V)}$) revealed robust transient potassium current I_A that was stable during the course (15 min.) of the experiment (-11.8 ± 4.7 % from control, n=9, Fig.29 C). Analysis of the delayed rectifier current also showed stability of $I_{K(V)}$ over 15 min. (-12.7 ± 7.6 %, n=9, Fig.30 D).

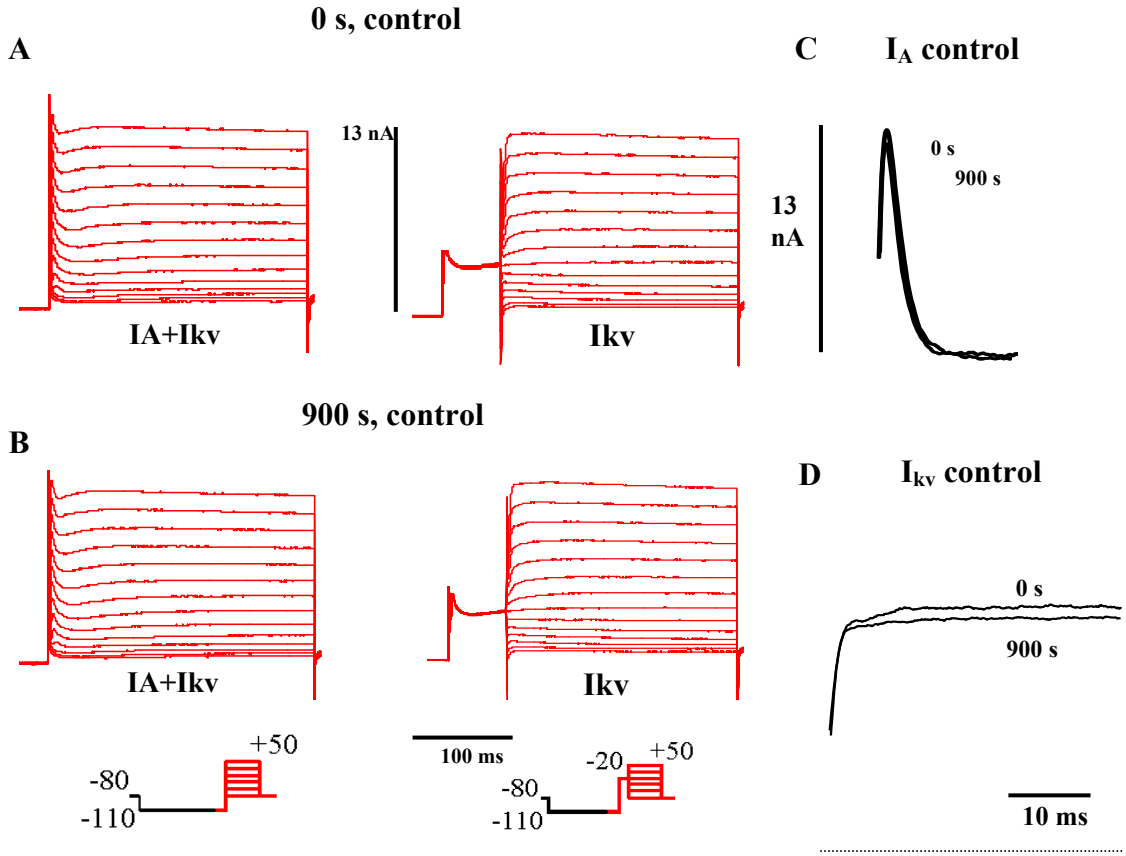

Fig. 30 Native I_A and $I_{K(V)}$ in control condition in ECLII stellate neurons.

A, B Original traces showing total outward potassium ($I_{K(V)}$ + I_A) and delayed rectifier ($I_{K(V)}$) currents at 0 s (A) and 900 s (B) after reaching whole-cell configuration. **C** Subtracted transient potassium current (I_A) recorded at +30 mV over time. **D** Delayed rectifier current at +30 mV over time.

Modulation of transient I_A and delayed rectifier currents $I_{K(V)}$ by arachidonic acid

1pM intracellular arachidonic acid reduced the subtracted I_A current by -66.3 ± 9.6 %, n=10 within 15 min. (Fig.31 A, red line). ETYA, inhibitor of the enzymes that metabolize AA and triple-bond analogue of arachidonic acid, required higher concentration (100 pM) to mimic the effect of 1 pM AA (Fig.31 A, green line). However, this effect tended to develop faster (in the first 3 min.) which is probably the result of the higher concentration of ETYA.

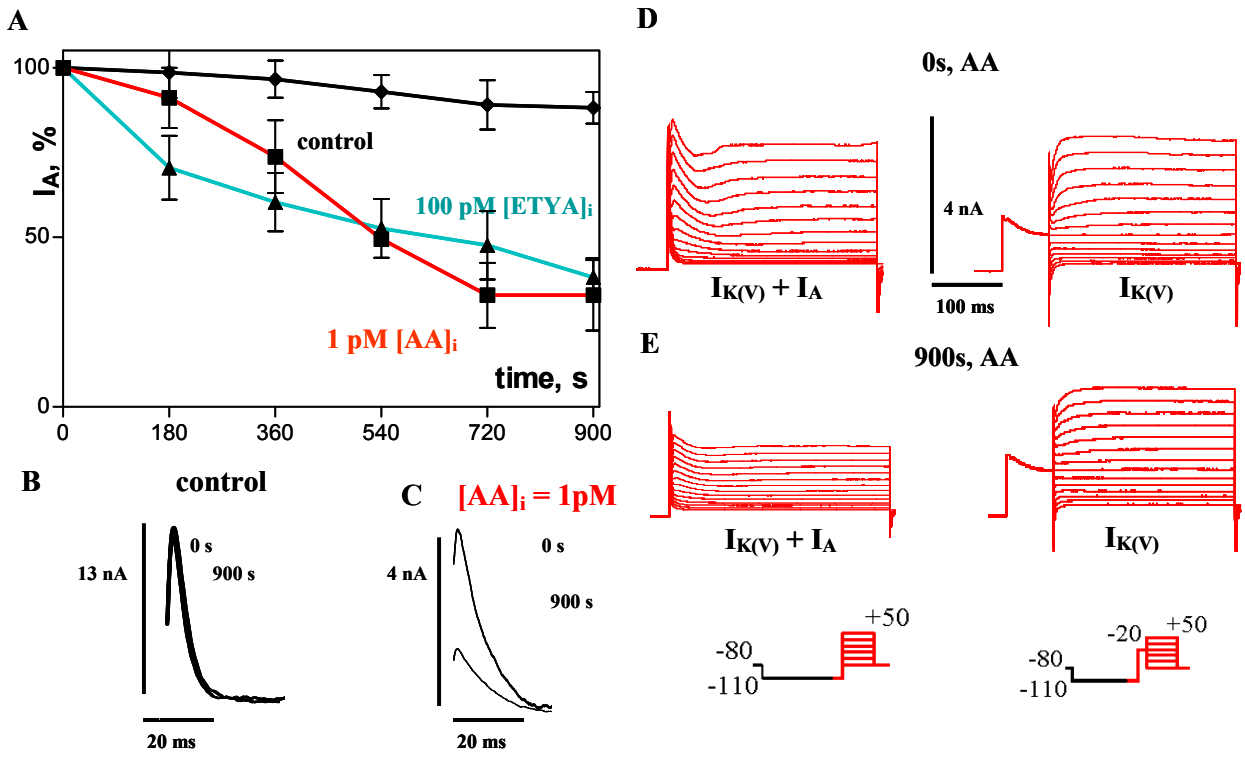

Fig. 31 Suppression of I_A by arachidonic acid (AA) in ECLII stellate cells.

A (black line), **B**: control; **A, C**: Intracellular application of 1 pM AA reduces the maximal transient potassium current (I_A) over time. The non-metabolizable AA analogue ETYA shows similar effect on I_A at 100-fold higher concentration. **D, E**: Raw current traces for combined I_A and $I_{k(v)}$ and for pure delayed rectifier currents (pulse protocols: inset in E).Currents are shown for control immediately after obtaining whole cell configuration (**D**, 0 s AA) and after 900 s of recording with 1 pM of AA in the patch pipette (**E**).

An additional effect of 1 pM AA was an 11 mV leftward shift of the steady-state inactivation curve with a slight change of the slope factor (from V_{50}= -42.8 ± 0.4 mV; k= 9.2 ± 0.6 to V_{50}= -55.1 ± 0.7 mV; k= 12.4 ± 0.6, n=10; Fig.32 A, left curves). AA did not affect the time constant of I_A inactivation. The steady state activation curve of I_A was also shifted to the left by ~6mV and the slope factor changed from 9.1 ± 0.5 to 13.7 ± 0.7 (Fig.32 A, right curves).

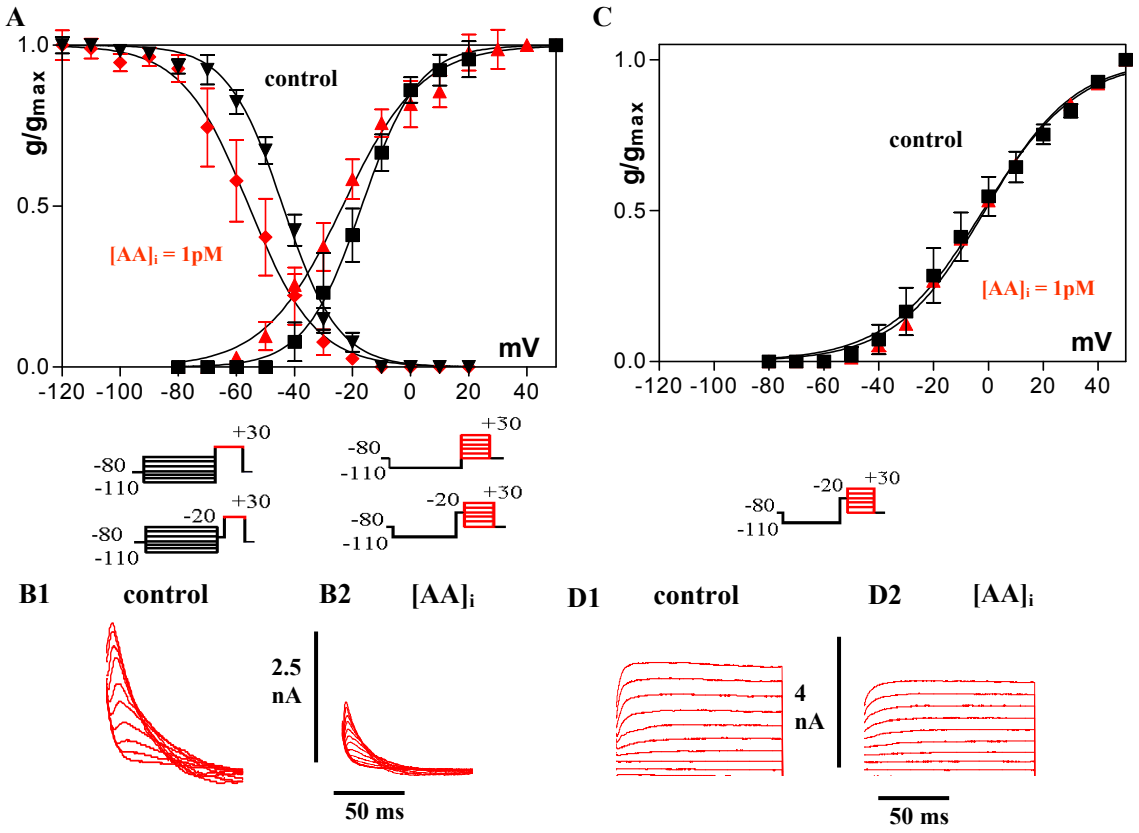

Fig. 32 Intracellular AA shifts steady-state inactivation, but does not affect voltage dependence of activation of I_A in ECLII stellate neurons.

A: Conductance-voltage relations and Boltzmann fits for inactivation (left curves) and activation (right curves) of I_A. **Inset**: Pulse protocols for determining voltage dependence of steady state inactivation (left) and of activation (right). Red part shows length of the traces below. **B**: Representative recordings of transient potassium current for control (B1) and in the presence of 1 pM AA (B2). **C**: Voltage-conductance dependence of $I_{K(V)}$ and pulse protocols for activation of $I_{K(V)}$ (inset). **D**: Original recordings of $I_{K(V)}$ activation in control conditions (D1) and in the presence of 1 pM AA (D2).

Like in ECLIII pyramidal neurons, arachidonic acid had a modest, but significant effect on the delayed rectifier current in ECLII stellate cells (Fig.33 B, E). As in ECLIII pyramidal neurons, 1 pM AA suppressed $I_{K(V)}$ by -29.1 ± 6.7 %, n=10 (Fig.33 C). This suggests that this effect is probably specific to the delayed rectifier current in the entorhinal cortex.

However, 1 pM arachidonic acid did not alter the voltage dependence of activation of the delayed rectifier current in ECLII stellate neurons (Fig.33 C).

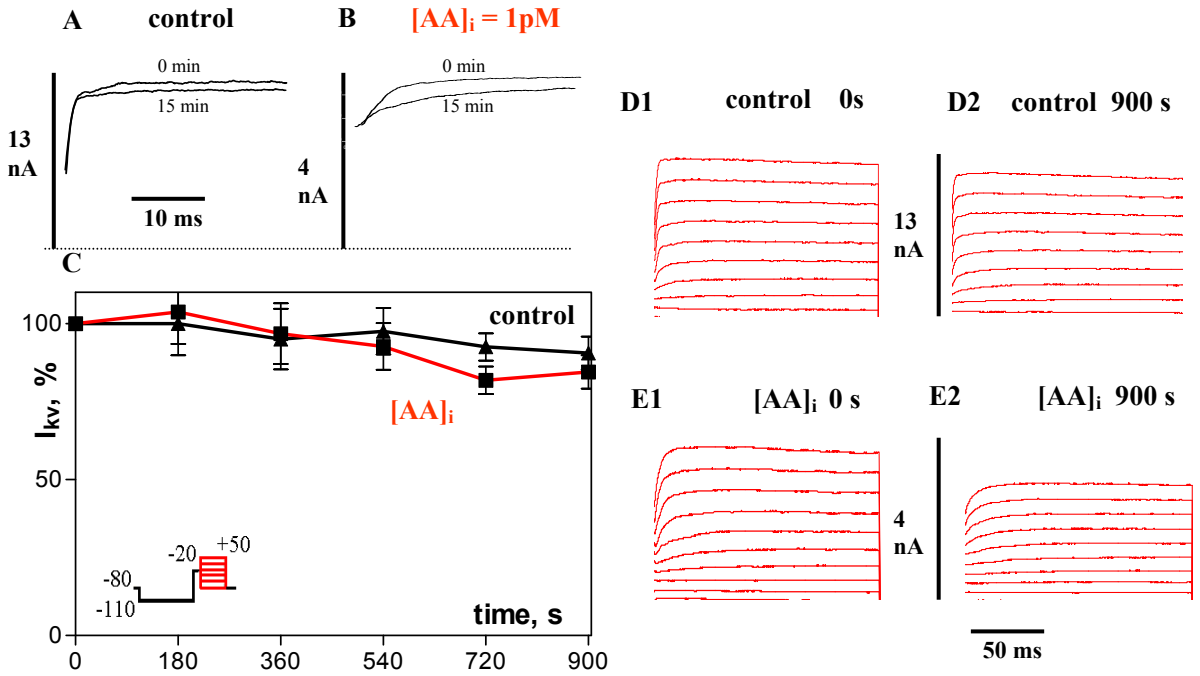

Fig. 33 The delayed rectifier current $I_{k(v)}$ is not affected by AA in ECLII stellate neurons.

A, B: Maximal $I_{k(v)}$ recorded at 0 s and at 900 s of whole cell recording shows a 13% decrease over time in control (**A**) and 30 % decrease with 1 pM AA in the patch pipette (**B**). **C**: Plot of $I_{k(v)}$ amplitude over time of whole cell recording for control and for AA. **D, E**: Original current recordings of $I_{k(v)}$ for several voltage steps (see inset in C) for control (**D**) and for AA at 0 s (D1, E1) and 900 s (D2, E2) of whole cell recording.

Influence of glutathione on arachidonic acid-mediated effects

Glutathione (20 mM), added to AA in the patch pipette failed to block the AA-mediated decrease of the maximal amplitude of the transient current (-75.6 ± 9.3 %, n=6 compared to -66.3 ± 9.6 %, n=10). Moreover, GSH_{in}+AA significantly reduced the I_A current within first 3 min. of the experiment (Fig.34 A, blue line, *). GSH_{in} did not prevent the leftward shift of voltage dependence of inactivation, caused by 1pM AA (Fig.34 D, left curves), but slowed the kinetic of inactivation of the transient potassium current (Table 9).

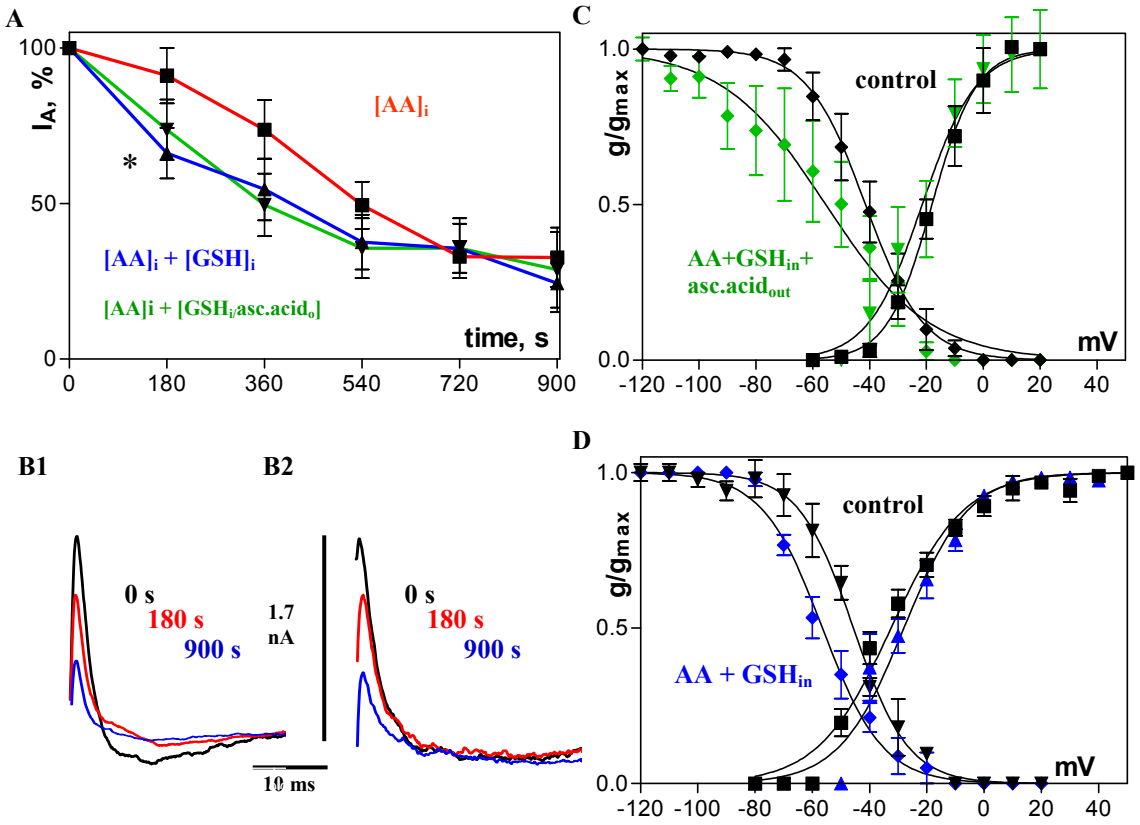

Fig. 34 Interaction of AA, GSH and ascorbic acid with I_A in ECLII stellate neurons.

A, B: GSH_i (A: blue line, B1), as well as ascorbic acid (A: green line, B2) enhanced the AA effect on I_A, particularly early after begin of recording/application (*). **C, D**: GSH_i and ascorbic $acid_o$ do not prevent the AA-mediated shift in steady-state inactivation (C, D, control=0 s vs. 900 s, left curves). Ascorbic acid further shifts the inactivation curve to more negative potential and changes its slope (C, left curves).

Influence of glutathione and ascorbic acid on arachidonic acid-mediated effects

Addition of 4 mM ascorbic acid to the perfusion solution (AA and GSH in the patch pipette) resulted in effects similar to those of GSH_{in} and AA: slowed inactivation (Fig.34 B2), acceleration of the AA effect on the maximal conductance, no change of the voltage dependence of activation, large (V_{50}= -41.4 ± 0.4 mV vs. -55.4 ± 1.9 mV, n=6) shift of the steady-state inactivation to more negative potentials (Fig.34 A: green line, C).

On one hand, GSH on the inner side of the cell membrane did not result in significant attenuation of the AA effect on the maximal amplitude of the delayed rectifier current (-19.8 ± 8.9 % , n=6 vs. -29.1 ± 6.7 %, n=10). On the other hand, in addition to GSH, ascorbic acid on the outer side of the membrane did reduce the maximal amplitude of $I_{K(V)}$ to -10.0 ± 11.6 %, n=6 and also changed V_{50} (from -7.9 ± 0.8 mV to -16.4 ± 1.4 mV) and the slope factor (from 16.8 ± 0.7 to 22.0 ± 1.3) of the voltage dependence activation of $I_{K(V)}$ (Table 10).

Influence of Trolox on arachidonic acid-mediated effects

The vitamin E-based antioxidant Trolox C, on the inner membrane of the ECLII stellate neurons, failed to block the arachidonic acid effect on the maximal amplitude of the transient potassium current, -74.3 ± 0.7 % vs. -66.3 ± 9.6 %, n=6 (Fig.35 A: blue line), but it was successful in blocking the effect of AA on the voltage dependence of steady-state inactivation and activation and their slopes (Fig.35 C). Trolox, applied through the pipette and through the bath, tended to slightly reduce the effect of AA (-60.4 ± 3.5 % vs. -66.3 ± 9.6 %, n=8) at late recording time, however this result is not statistically significant (Fig.35 A: green line). It also blocked the effect of 1 pM AA on the steady-state inactivation kinetic and further shifted it by ~10 mV to more positive potentials (Fig.34 D). Trolox, applied on the both sides of the membrane, block the effect of AA on the voltage-conductance relation of the I_A activation, but not the effect on its slope (Fig.35 D). Moreover, it did accelerate the kinetic of inactivation of I_A (Fig.35 B2). Interestingly, Trolox, applied both through pipette and

perfusion or only through the patch pipette accelerated the effect of 1 pM arachidonic acid on the maximal conductance of I_A (Fig.35 A).

$Trolox_{in}$ reduced the effect of 1pM AA on the maximal amplitude of the delayed rectifier current from -29.1 ± 6.7 % to -18.9 ± 4.9 % and shifted it activation voltage dependence by ~6 mV more negative potentials (Table 10). No changes of the slope of the voltage dependence of activation were observed. Trolox $_{in/out}$, did not block the reducing effect of AA on the $I_{K(V)}$ maximal amplitude (-33.7 ± 6.8 % vs. -29.1 ± 6.7 %, n=8). It shifted the voltage dependence of $I_{K(V)}$ activation by ~5 mV to the left, without affecting its slope (Table 10).

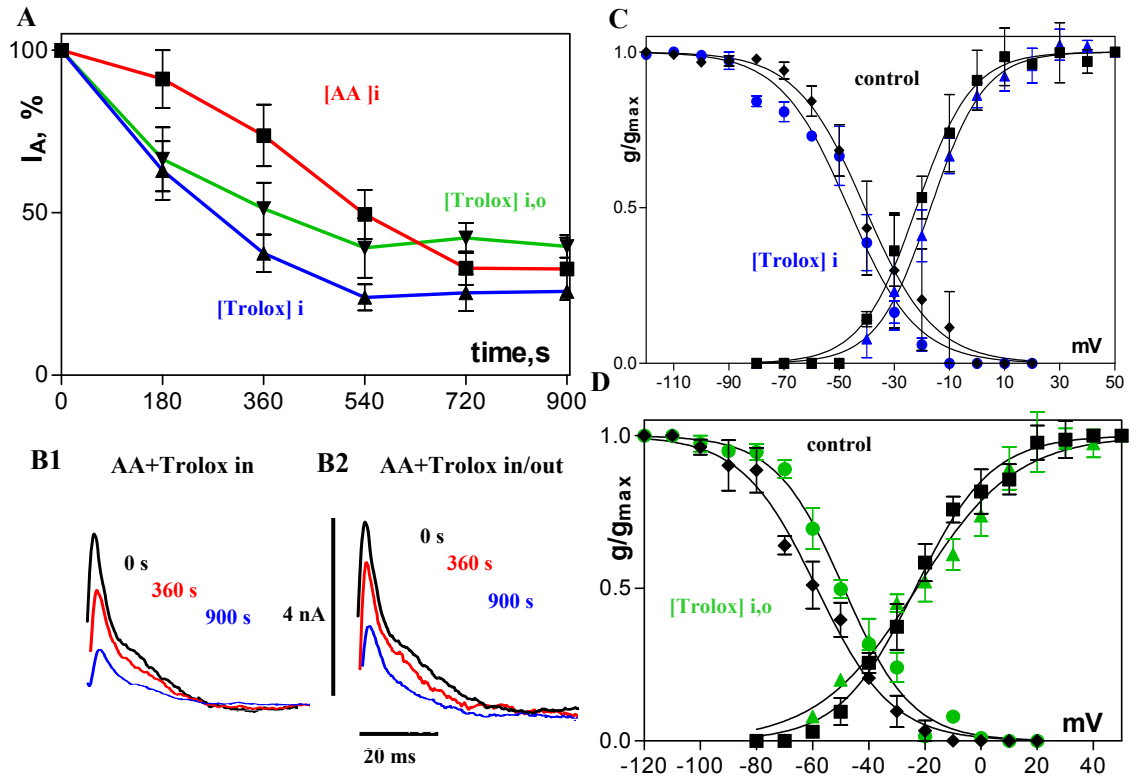

Fig. 35 Interaction of AA and Trolox with I_A in ECLII stellate neurons.

A, B: Intracellular application of the vitamin E analogue Trolox (10 µM) with AA does not prevent reduction of I_A (A: blue line, B1). Trolox, applied from both sides of the cell membrane, does unsignificantly recover I_A with prolonged recording time (A: green line, B2). **C**: $Trolox_i$ inhibits the AA shift of steady-state inactivation (left curves). There is no shift in voltage dependence of activation (right curves, control=0 s vs. 900 s). **D**: In the presence of Trolox on both sides of the membrane plus AA_i, steady state inactivation shifts over 900 s recording time by -10 mV to more positive potential.

Effects of H_2O_2 on outward potassium currents

As an oxidative damage model system to compare the effects of AA, the effect of H_2O_2 on the transient potassium and delayed rectifier channels was used. To obtain an effect, similar to that of 1 pM AA on the maximal amplitude of I_A and $I_{K(V)}$, 80 µM H_2O_2 was required (Fig.36 A: red line).

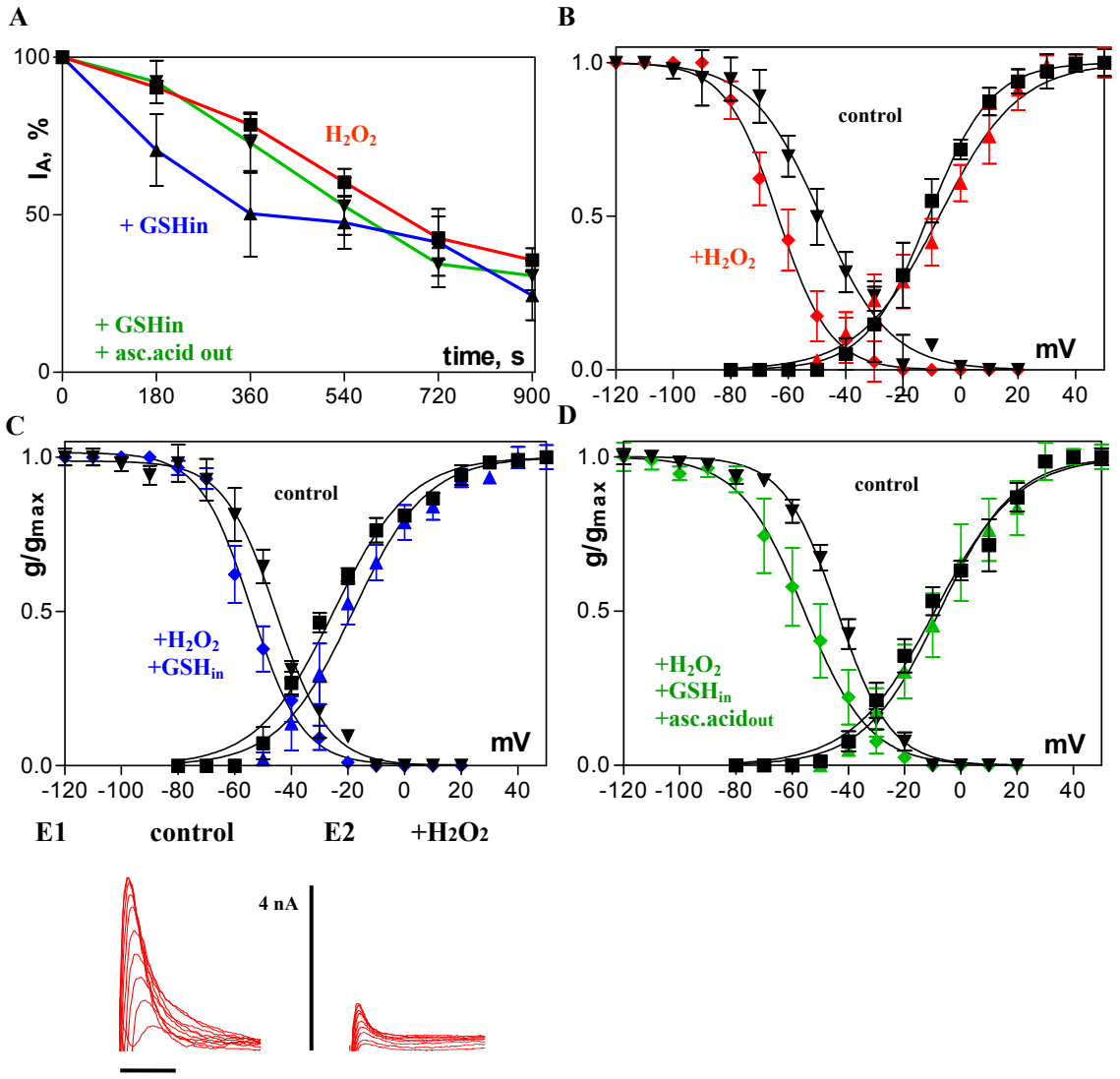

Fig. 36 Effects of intracellular H_2O_2 (80 µM) and antioxidants on I_A in ECLII stellate neurons.

A: H_2O_2 mimics the effect of AA on maximal I_A (red line). This effect is enhanced early by GSH_i and in the presence of ascorbic $acid_o$ does not differ from those for H_2O_2 (blue and green line, respectively). **B:** H_2O_2 shifts voltage conductance relations of inactivation (left curves) to more negative potentials as well as changes the slope of activation and inactivation curves. **C:** GSH_i diminishes the H_2O_2 mediated shift in inactivation (left curves), but for activation causes a slight shift to more positive potential. **D:** In the presence of ascorbic $acid_o$, GSH_i + H_2O_2 shift inactivation and activation of I_A back by -12 mV to more negative potentials. **E:** Representative current traces of I_A for determination of the voltage dependence of activation for control immediately after obtaining whole cell configuration (E1) and after 900 s of recording with H_2O_2 in the patch pipette (E2).

H_2O_2 reduced the maximal amplitude of I_A by -64.4 ± 3.8 %, shifted leftwards the the steady-state inactivation curve leftward by ~12mV, but did not affect significantly the rate of I_A inactivation (Fig.36 A, B). Those effects are consistent with the effects of 1 pM arachidonic acid on the transient potassium current characteristics in ECLII stellate neurons (Table 9). In the presence of H_2O_2, the voltage dependence of activation of I_A was did not change, but slope factor was altered from 10.9 ± 0.3 to 13.9 ± 0.9, n=8 (Fig.36 B).

Influence of glutathione and ascorbic acid on H_2O_2-mediated effects

Application of GSH through the patch pipette resulted in stronger attenuation of the I_A current during the first 6 min. of the experiment (Fig.36 A: blue line), an effect previously observed in other types of neurons (*see* p.43 and p. 59). In general, the effect of H_2O_2 on the maximal amplitude of the transient potassium current could be blocked neither by GSH, nor by addition of ascorbic acid to the bath (Fig.36 A). Intracellular GSH decreased the leftward shift in voltage dependence of inactivation from ~12 mV to ~7 mV (Fig.36 C). GSH_{in} did not block the right shift of voltage dependence of activation, but abolished the slope effect. With GSH_{in} and AA, the time constant of inactivation of I_A in ECLII stellate cells was reduced from τ_i=7.8 ± 1.1 ms to τ_i=4.8 ± 1.3 ms (n=4). Addition of ascorbic acid to the perfusion solution did not block H_2O_2-induced ~12mV left shift of the voltage dependence of inactivation of I_A (-44.0 ± 0.5 mV vs. -55.7 ± 0.6 mV, n=8), did not alter the voltage-conductance relation for activation and accelerated the rate of I_A inactivation kinetics (Fig.36 D, Table 9).

As seen on Fig.37 A, H_2O_2 suppressed the delayed rectifier current to an extent, which was similar to that of 1 pM arachidonic acid (-22.2 ± 9.1 % and -29.1 ± 6.7 %, respectively). However, 80 μM H_2O_2 caused a small (~6mV), albeit significant shift of $I_{K(V)}$ voltage dependence of steady-state inactivation to more negative potentials (Fig.37 B). Intracellular GSH blocked the effect of H_2O_2 on the maximal conductance of $I_{K(V)}$ (-12.3 ± 9.6 %, n=4), as did GSH_{in}, combined with $asc.acid_{out}$ (-14.1 ± 5.1 %, n=8), but these effects seemed not to be

statistically significant. Glutathione, applied on the inner side of the neuronal membrane led to a ~3 mV shift to hyperpolarizing direction of the voltage dependence of activation of $I_{K(V)}$ with small change of the slope (from 17.4 ± 0.7 to 19.5 ± 1.0, n=8). Ascorbic acid, in the presence of GSH and AA shifted the voltage dependence of activation of $I_{K(V)}$ from V_{50}= -5.9 ± 1.0 mV to V_{50}= -14.2 ± 1.1 mV, without affecting its slope (Table 10).

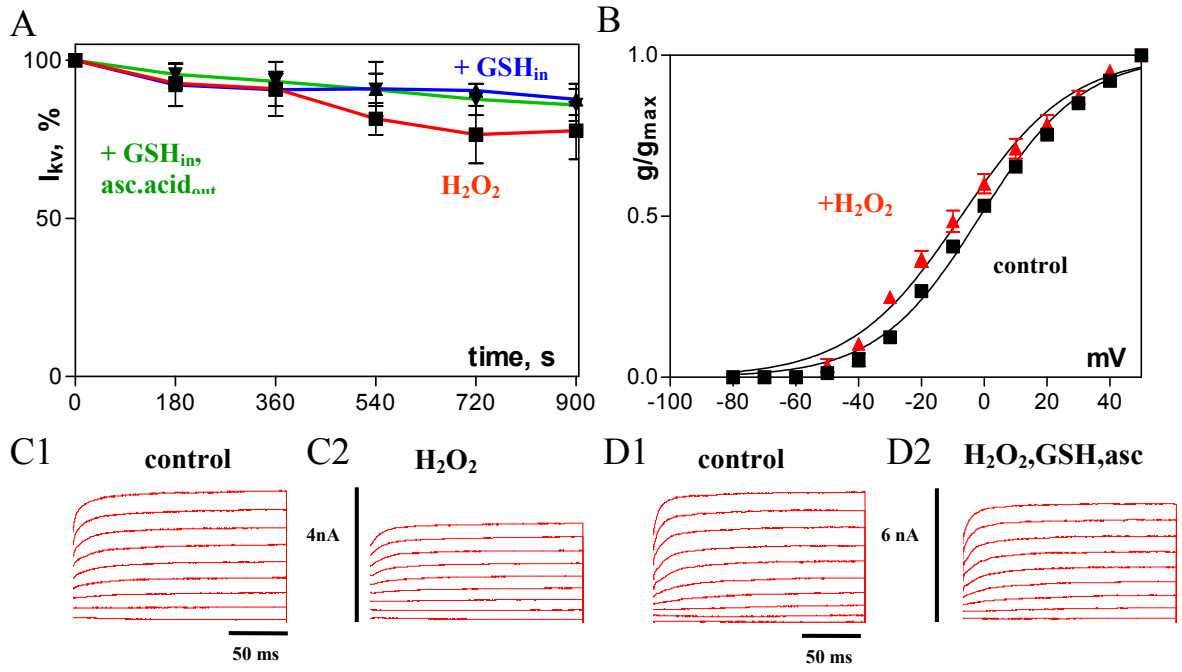

Fig. 37 Effects of intracellular H_2O_2 (80 µM) and antioxidants on $I_{K(V)}$ in ECLII stellate neurons.

A: H_2O_2 suppresses the delayed rectifier potassium current $I_{K(V)}$, and this effect is fully inhibited by GSH_i or GSH_i+ascorbic $acid_o$ (blue and green line, respectively). **B:** H_2O_2 insignificantly shifts voltage dependence of activation of $I_{K(V)}$ to a more negative potential. **C, D:** Representative traces of $I_{K(V)}$ for determination of voltage dependence of activation for control immediately after obtaining whole cell configuration (C1, D1, 0 s) and after 900 s recording with H_2O_2 (C2) or H_2O_2 + GSH_i in the patch pipette (D2). Recordings of D have been obtained in the presence of ascorbic $acid_o$.

Table 9 Overview of effects of oxidants and antioxidants on behavior parameters of I_A in ECLII stellate neurons.

I_A ECLIIst	n	max amplitude, % of control	V_{50a} 0 min mV	V_{50a} 15 min mV	$k_{activation}$ 0 min	k_a 15 min	V_{50i} 0 min mV	V_{50i} 15 min mV	$k_{inactivation}$ 0 min	k_i 15 min	τ_i 0 min ms	τ_i 15 min ms
control	9	-11.8±4.7%	-12.2±1.0	-14.3±0.3	9.0±0.9	7.9±0.3	-45.3±0.8	-48.8±0.5	9.5±0.7	7.7±0.4	8.6±2.3	9.2±2.1
+ 1pM AA	10	-66.3±9.6%	-17.8±0.5	-23.7±1.8	9.1±0.5	13.7±0.7	-42.8±0.4	-55.1±0.7	9.2±0.6	12.4±0.6	6.6±2.7	7.4±2.9
AA+GSH_{in}	6	-75.6±9.3%	-32.1±0.7	-28.5±0.9	12.8±1.6	11.3±1.3	-45.8±0.8	-56.2±0.8	9.7±0.5	10.5±0.7	12.0±2.3	18.6±2.5
AA+GSH_{in}/ asc.$acid_{out}$	6	-71.3±12.1%	-18.1±0.4	-21.5±1.2	7.8±0.4	9.5±1.0	-41.4±0.4	-55.4±1.9	10.2±0.5	18.3±1.7	3.6±0.6	6.2±0.5
AA+$Trolox_{in}$	6	-74.3±0.7%	-22.0±0.7	-16.9±0.5	10.1±0.6	9.6±0.4	-40.7±0.8	-46.7±1.3	12.5±0.7	12.4±1.1	9.1±5.9	8.4±3.0
AA+$Trolox_{in}$, $_{out}$	8	-60.4±3.5%	-23.4±0.9	-22.9±1.5	13.5±0.8	17.7±1.3	-58.6±0.9	-48.9±0.9	13.4±0.8	12.1±0.8	3.2±0.4	5.3±0.9
+80µM H_2O_2	4	-64.4±3.8%	-11.2±0.4	-7.4±1.0	10.9±0.3	13.9±0.9	-48.8±0.8	-60.1±0.9	9.4±0.9	11.1±0.8	5.6±1.7	5.3±1.4
H_2O_2 +GSH_{in}	4	-72.6±7.6%	-25.5±1.0	-18.4±1.3	10.3±0.8	10.5±0.7	-45.2±0.9	-53.8±0.9	10.8±0.5	11.2±0.4	7.8±1.1	4.8±1.3
H_2O_2 +GSH_{in}/ asc.$acid_{out}$	8	-69.3±4.6%	-9.2±1.1	-7.6±0.8	14.7±1.0	13.3±0.7	-44.0±0.5	-55.7±0.6	10.5±0.5	11.6±0.5	7.5±0.9	5.3±0.7

Table 10 Overview of effects of oxidants and antioxidants on behavior parameters of in ECLII stellate neurons $I_{K(V)}$.

$I_{k(v)}$ ECLIIst	n	max amplitude % of control	$V_{50activation}$ 0 min	V_{50a} 15 min	$k_{activation}$ 0 min	k_a 15 min
control	9	-12.7±7.6 %	-7.1±1.2	-8.2±1.5	18.3±0.7	18.7±0.6
+ 1pM AA	10	-29.1±6.7 %	-1.7±1.1	-1.5±1.1	17.3±1.0	16.9±1.0
AA+GSH_{in}	6	-19.8±8.9 %	-18.1±0.4	-21.5±1.2	8.7±0.4	9.5±1.0
AA+GSH_{in}/asc.$acid_{out}$	6	-10.0±11.6 %	-7.9±0.8	-16.4±1.4	16.8±0.7	22.0±1.3
AA+$Trolox_{in}$	6	-18.9±4.9 %	-10.6±1.2	-16.7±1.4	17.4±1.0	17.3±1.2
AA+$Trolox_{in}$/$Trolox_{out}$	8	-33.7±6.8 %	-22.9±1.3	-30.5±1.2	21.1±1.2	24.8±1.1
+80µM H_2O_2	4	-22.2±9.1 %	-1.3±0.9	-7.4±1.1	16.3±0.8	17.6±1.0
H_2O_2 +GSH_{in}	4	-12.3±9.6 %	-6.6±0.8	-10.0±0.9	17.4±0.7	19.5±1.0
H_2O_2+GSH_{in}/asc.$acid_{out}$	8	-14.1±5.1%	-5.9±1.0	-14.2±1.1	20.3±0.9	20.0±1.0

Functional expression of Kv1 and Kv4 α-subunit-induced K^+-currents in HEK-293 cell line

Whole-cell voltage-clamp recordings from untransfected or mock-transfected HEK-293 cells revealed endogenous voltage-gated outward potassium currents in response to depolarization to potentials positive to 0 mV. The amplitudes of these currents, however, were very small: (~50 pA), a similar current amplitude was measured at +30 mV in mock-transfected (EGFP) cells further revealing that expression of EGFP alone does not influence functional potassium current densities (Fig.38 A, B). Cell input resistances were in the range of 1-20 GΩ. Leak currents were always ≤ 50 pA at -80 mV and were therefore not corrected.

Large outward potassium currents, however, were seen routinely after transfection of HEK-293 cells with Kv1.4 or Kv4.2, alone or in combination with EGFP (Fig.38 C, D).

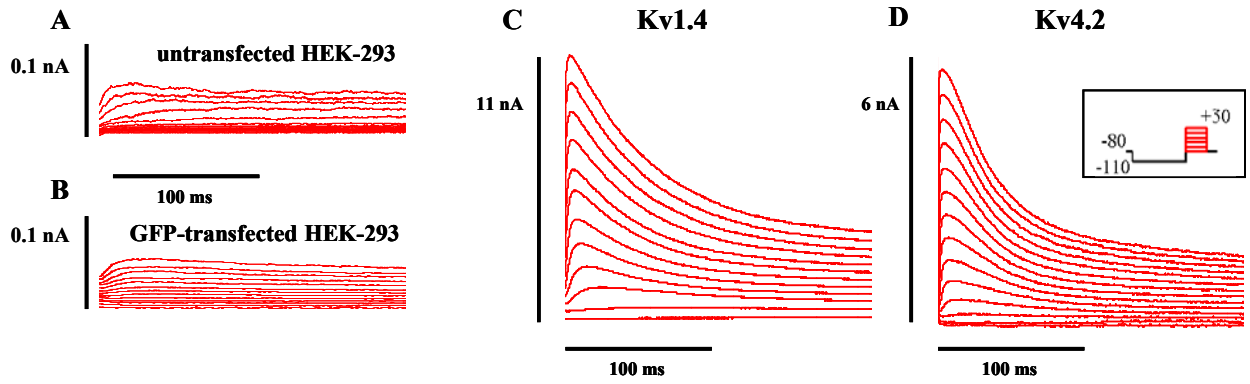

Fig. 38 Outward K^+-currents in untransfected (A) or mock-transfected (EGFP alone, B), Kv1.4-transfected (C) and Kv4.2-transfected HEK-293 cells (D).

Voltage-gated potassium channel pore-forming (α) subunits of the Kv1 and Kv4 subfamilies are thought to be the molecular determinants of A-currents in the brain. Heterologous expression of these subunits in human embryonal kidney cell line, however, resulted in transient K^+-currents that show quantitatively distinct time- and voltage-dependent properties to those recorded from brain neurons.

Part of the experiments with Kv-transfected HEK-293 cells was performed in cells that were co-transfected with EGFP, and recordings were obtained only from EGFP-positive cells. The transfection efficiency was low (1-5%) and approximately 50% of EGFP-positive cells also expressed Kv1.4 or Kv4.2, as revealed by electrophysiological experiments with those cells.

Modulation of transient potassium current by arachidonic acid and Trolox in heterologously expressed Kv1.4-α in HEK-293 cell line

Transient potassium current in untreated Kv1.4-transfected HEK-293 cells

Whole-cell outward potassium currents were activated during 200 ms-long depolarization steps to test potentials between -80 and +50 mV from a holding potential of -80 mV (pulse protocols: inset Fig.38). An 800 ms-long prepulse at -110 mV was performed in order to remove inactivation of I_A. The mean ± SEM peak outward K^+-current amplitudes in Kv-transfected HEK cells at +30 mV were significantly ($p<0.001$) higher than those in untransfected or mock-transfected HEK-293 cells (Fig.38). For inactivating HEK A-currents, the maximal amplitude of the currents were recorded during the +30 mV steps following each conditioning prepulse from -120 mV to +20 mV (pulse protocols: see inset Fig.39, B2).

As seen on Fig.39 A, B, in HEK-293 cells, transfected with Kv1.4 (and EGFP) large (5.5-11 nA) outward potassium currents were evident. The amplitude of the peak current at +30 mV (maximal amplitude for each cell) was followed over 15 min and evolvement over time was plotted as shown on Fig. 39 C. The maximal amplitude of the transient potassium current in Kv1.4-transfected HEK cells did not change significantly under control conditions during the

course of a 15 min-recording (-12.1 ± 6.1 %, n=7). The A-currents from Kv1.4-transfected HEK-293 cells activated and inactivated fast (τ_i=51.7 ± 2.9 ms), but significantly slower as native I_A currents from brain slice neurons (CA1 τ_i=7.8 ± 1.5 ms; ECLIII τ_i=13.0 ± 3.7 ms; ECLII τ_i=8.6 ± 2.3 ms). On Fig.39, A2 and B2, one can clearly see the atypical voltage–conductance dependence for the steady-state inactivation curve of Kv1.4-potassium current in comparison to the native neuronal I_A currents (for example Fig. 39 B1). Distorted voltage dependence of inactivation is probably due to lack of supplementary β-subunit and/or other auxiliary Kv-channel subunits and factors in HEK cells that could stabilize inactivation of I_A channels.

The amplitude of the peak currents at each test potential were measured and peak outward conductances were then calculated (using the K^+ equilibrium potential of -92 mV) and normalized to the peak conductance at +30 mV in the same cell. Mean (± SEM) normalized peak conductances for control conditions were plotted as a function of test potentials in Fig 39 D and best fitted with Boltzman monoexponential equation (*see* Materials and Methods, *p*.36). Kv1.4-currents activated at ~ -60 mV and reached steady-state at potentials positive to +30 mV. Although the mean (± SEM) voltages at which half of the channels are activated (V_{50a}) derived from this fits at time=0s (-24.7 ± 2.4 mV) differ from V_{50a} for time = 900 s (-4.8 ± 1.8 mV), those differences are not statistically significant. Voltage-dependence of inactivation and the maximum amplitude in control conditions remain unchanged over recording time of 15 min (Fig.39 C, D; Table 11).

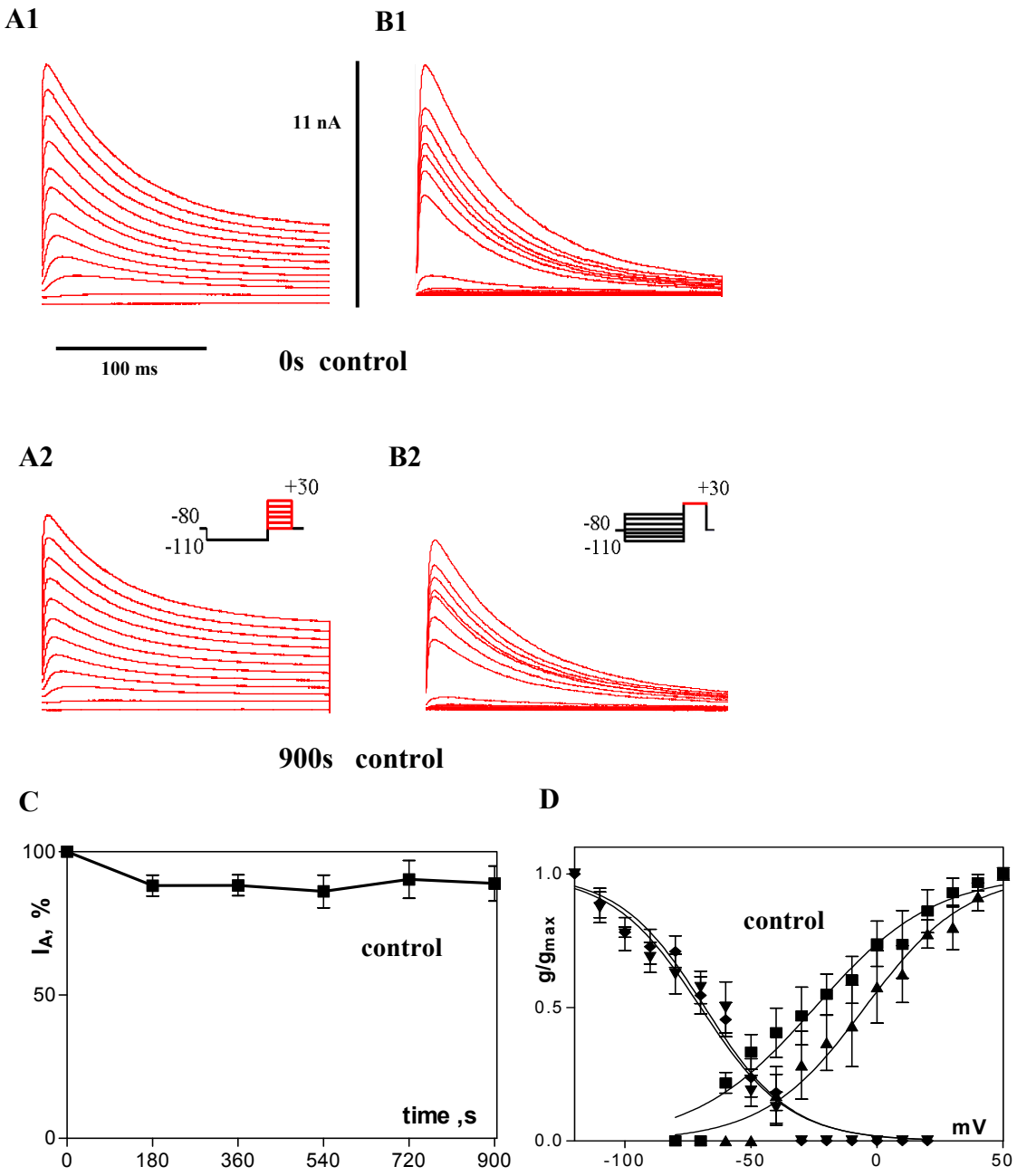

Fig. 39 Transient potassium current in Kv1.4-transfected HEK-293 cells.

A, B: Original traces showing I_A activation (A) and inactivation (B) at 0 s and 900 s (pulse protocols: inset A2, B2). **C**: Transient potassium current (I_A) recorded at +30 mV over time in control condition. **D**: Voltage-conductance dependence of activation (right curves) and steady-state inactivation (left curves) of I_A.

Modulation of I_A by arachidonic acid in Kv1.4-transfected HEK-293 cells

Application of 1 pM arachidonic acid through the patch-pipette decreased the Kv1.4-mediated A-currents, expressed in HEK293 cells by 71.4 ± 6.3 % (n=9; p<0.001). This robust response of Kv1.4 channels to 1pM AA was contradictory with the findings of Villarroel and Schwarz (*see* Villaroel and Schwarz, 1996).

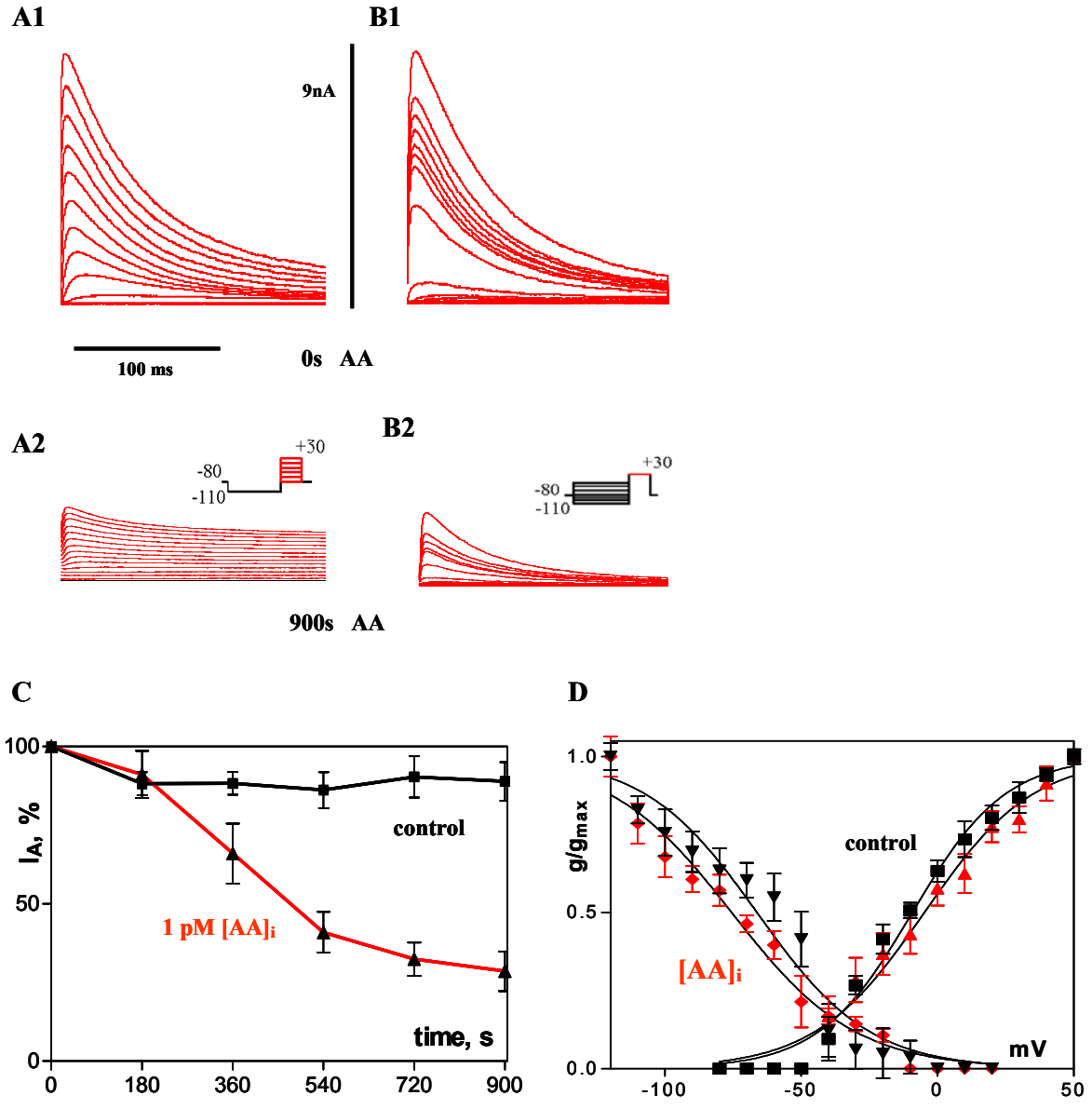

Fig. 40 Suppression of Kv1.4- I_A by arachidonic acid.

A, B: Control activation (A1) and inactivation (B1) of I_A (pulse protocols: inset A2, B2). Raw current traces of I_A are shown for control immediately after obtaining whole cell configuration (A1, B1, 0 s AA) and after 900 s of recording with 1 pM of AA in the patch pipette (A2, B2, 900 s AA). **C**: Intracellular application of 1 pM AA (red line) reduces the maximal transient potassium current (I_A) over time. **D**: Activation (left curves) and steady-state inactivation (right curves) kinetics in control condition (black symbols) and after application of 1 pM arachidonic acid through the pipette (red symbols).

As seen on Fig. 40 C, AA difused to the cytoplasm within 3 min. and reached full effect on the maximal amplitude of I_A within 10 min.

AA did not significantly alter the voltage-dependence of activation (V_{50a} from -9.2 ± 1.4 mV to -5.2 ± 1.6 mV and *k* from 17.1 ± 1.3 to 19.4 ± 1.5, n=9; Fig.40 D, right curves). AA shifted the voltage dependence of steady-state inactivation of Kv1.4-encoded channels from -66.2 ± 2.6 mV to -75.5 ± 2.1 mV (k from 19.6 ± 2.2 to 22.6 ± 1.9, n=9; Fig.40 D, right curves), but did not affected I_A -inactivation kinetic (τ_i =52.8 ± 2.8ms to 49.4 ± 2.4ms).

Influence of Trolox on arachidonic acid-mediated effects

To examine possible involvement of free radicals in the AA effect on Kv1.4 α-current, the water-soluble analogue of Vit.E, Trolox C was applied. Co-application of 10 μM Trolox with AA to the pipette solution did not significantly block the effect of 1pM AA on the maximal amplitude of Kv1.4 currents (-64.8 ± 7.9 % vs. -71.4 ± 6.3 %; Fig.41 C). $Trolox_{in}$+AA caused a large leftward shift of the voltage-dependence of I_A activation (V_{50a} from -5.6 ± 1.3 mV to -37.1 ± 1.8 mV, n=9), as well as slope factor change from 18.1 ± 1.2 to 12.8 ± 1.6 (Fig.41 D, right curves). Under these conditions (AA+$Trolox_{in}$) voltage dependence of the steady-state inactivation remained unchanged (Fig.41 D, left curves). Trolox C, applied intracellularly, slowed down the rate of inactivation of Kv1.4 channels (from τ_i=34.3 ± 2.9 ms to τ_i =47.9 ± 3.2 ms).

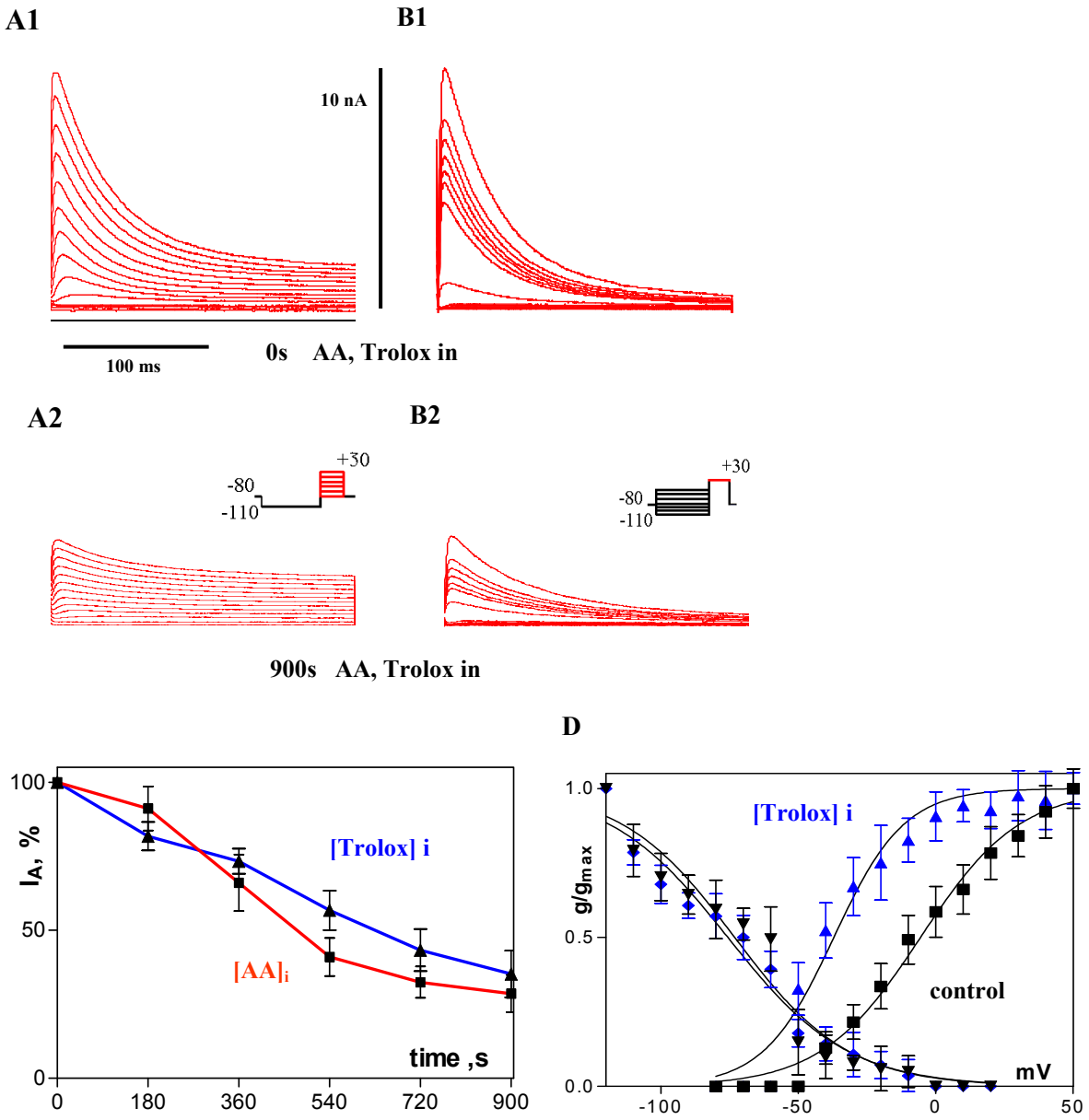

Fig. 41 Interaction of AA and Trolox$_{in}$ with I_A in Kv1.4-transfected HEK-293 cells.

A, B: Intracellular application of the vitamin E analogue Trolox (10 µM) does not prevent reduction of I_A by arachidonic acid. **C:** Intracellular application of Trolox and AA reduces I_A similar to 1 pM AA (blue line**). D:** In the presence of Trolox on the inner side of the cell membrane, AA shifts activation kinetic of I_A by 30 mV to more negative potential over 900 s recording time (right curves). There was no shift in voltage dependence of steady-state inactivation (left curves).

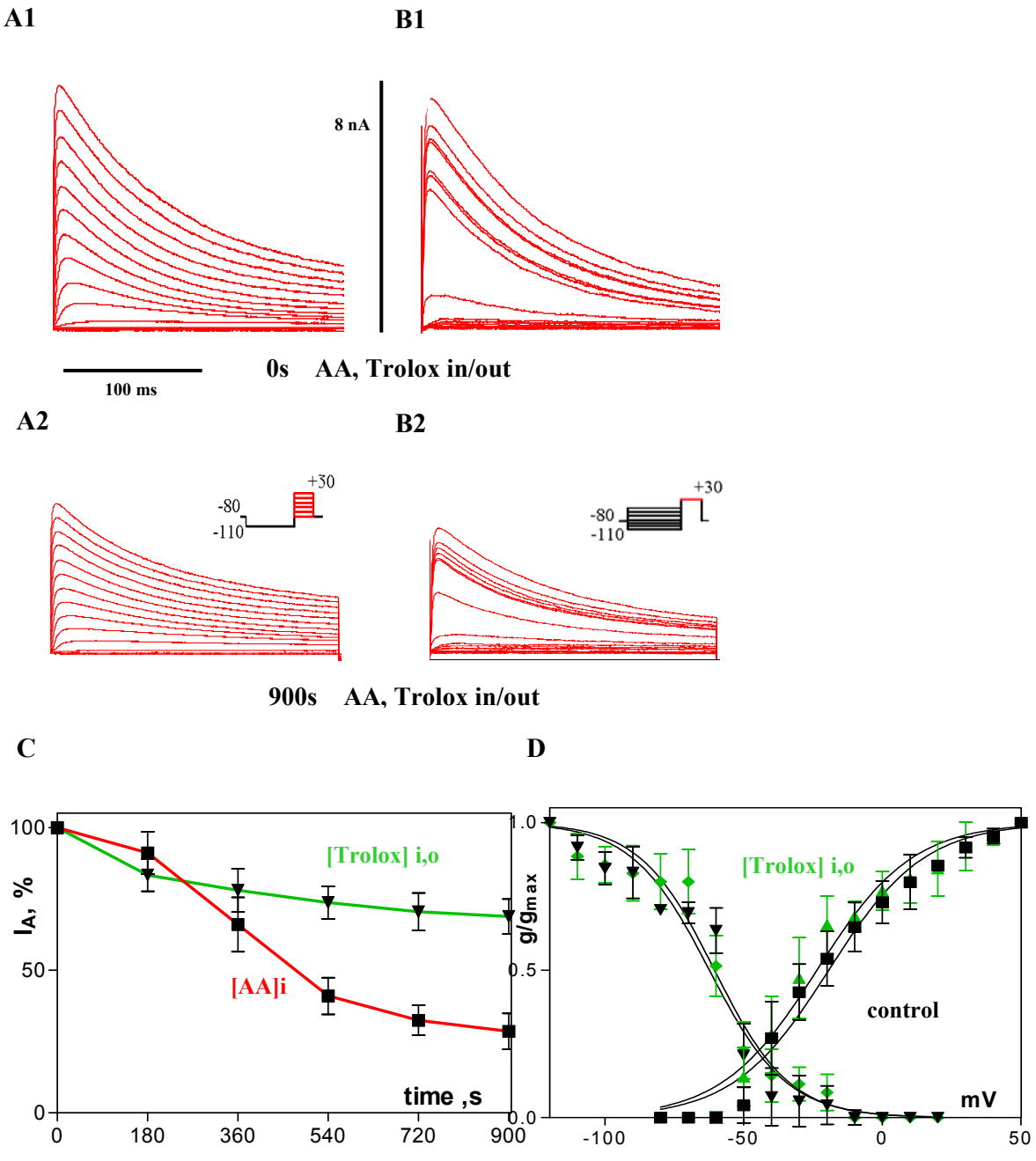

Fig. 42 Interaction of AA and Trolox$_{out}$ with I_A in Kv1.4-transfected HEK-293 cells.

A, B: Original traces for activation (A) and inactivation (B) of transient potassium current prior to (0 s) and after (900 s) application of AA+Trolox$_{in/out}$. Protocols: inset in A2, B2. **C:** Trolox, applied from both sides of the cell membrane (green line), did significantly recover I_A from 1 pM AA (red line). **D:** No shift of activation or steady-state inactivation occurs after intra- and extracellular application of Trolox and AA.

When applied on the both sides of the HEK cell membrane, Trolox reduced significantly (-31.2 ± 6.1 %, n=6) the effect of 1 pM arachidonic acid (-71.4 ± 6.3 %, n=9) on the maximal amplitude of the Kv1.4-induced currents (Fig.42 C). Trolox, applied simultaneously through the pipette and the bath solutions, did not alter Kv1.4 channel characteristics as voltage dependences of activation and steady-state inactivation, slope factors or rate of inactivation (Fig.42 D).

Modulation of transient potassium current by arachidonic acid and Trolox in heterologously expressed Kv4.2-α in HEK-293 cell line

Transient potassium current in untreated Kv4.2-transfected HEK-293 cells

Transfection of Kv4.2 α-subunit in HEK-293 cells resulted in expression of robust outward current with amplitude at +30 mV of 2 to 8 nA (Fig.42 A, B). Kv4.2 current characteristics as maximal amplitude voltage dependences of activation and inactivation did not change significantly over the recording time of 15 min. (Fig.43 C, D, Table 11).

Modulation of transient potassium current by AA in Kv4.2-transfected HEK-293 cells

Fig.44 shows the effect of 1pM arachidonic acid observed as 54.7 ± 6.9 % (n=12) reduction of the maximum amplitude of the Kv4.2-encoded current, measured at +30 mV. The inhibition of the Kv4.2 currents by AA was accompanied by a modest (~3 mV) shift in depolarizing direction of the voltage-conductance relation of Kv4.2 channel inactivation (Fig.44 D, left curves). No changes in voltage dependence of activation or time course of inactivation of Kv4.2 channels were observed after intracellular application of 1 pM AA (Fig.44 A, D; Table 11).

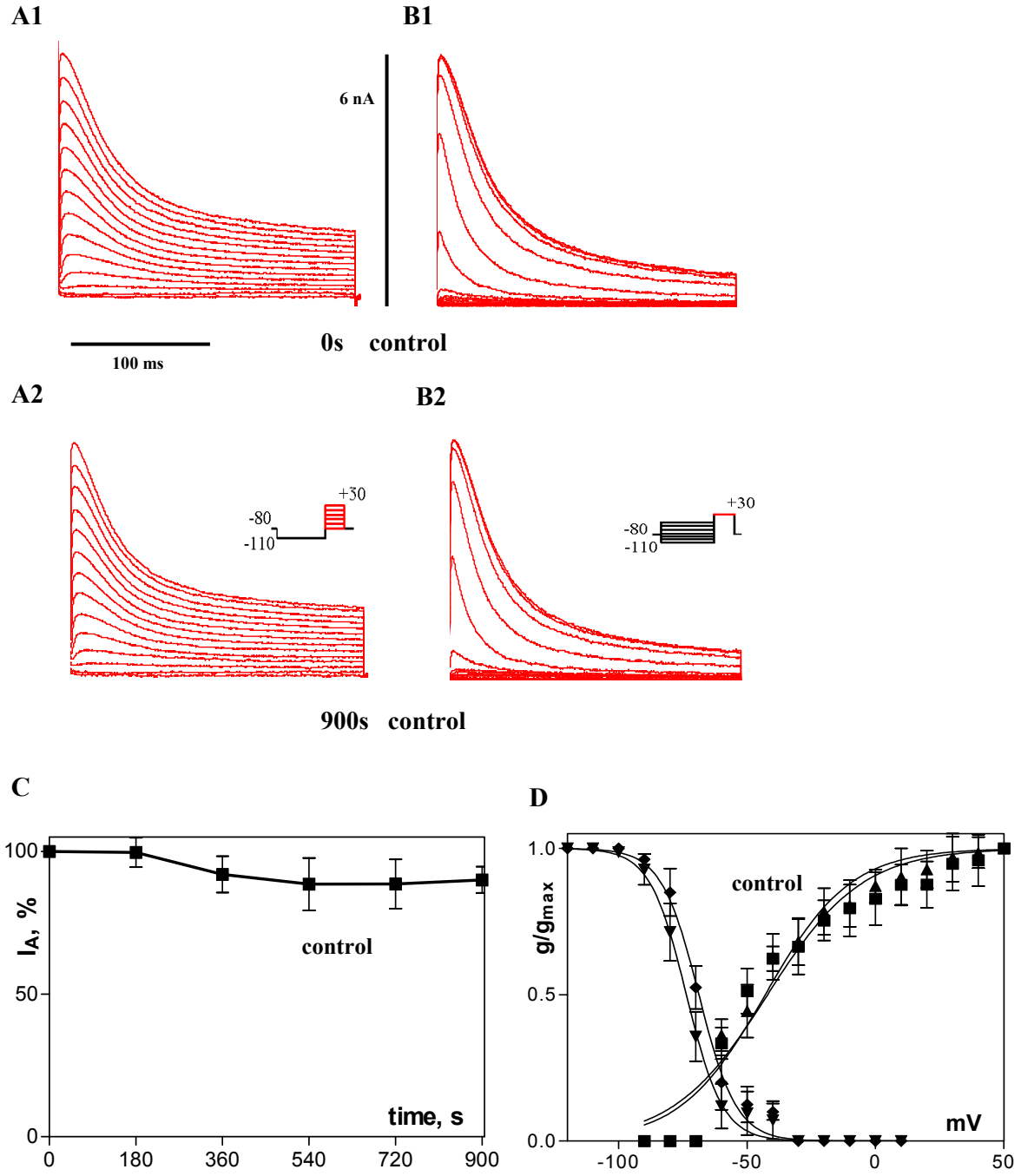

Fig. 43 Transient potassium current in Kv4.2-transfected HEK-293 cells.

A, B: Original traces showing I_A activation (A) and inactivation (B) at 0 s (1) and 900 s (2) of recording. Pulse protocols: inset A2, B2. **C:** Transient potassium current (I_A) recorded at +30 mV over time in control condition. **D:** Voltage-conductance dependence of activation (right curves) and steady-state inactivation (left curves) of I_A at 0 s and 900 s after opening the cell.

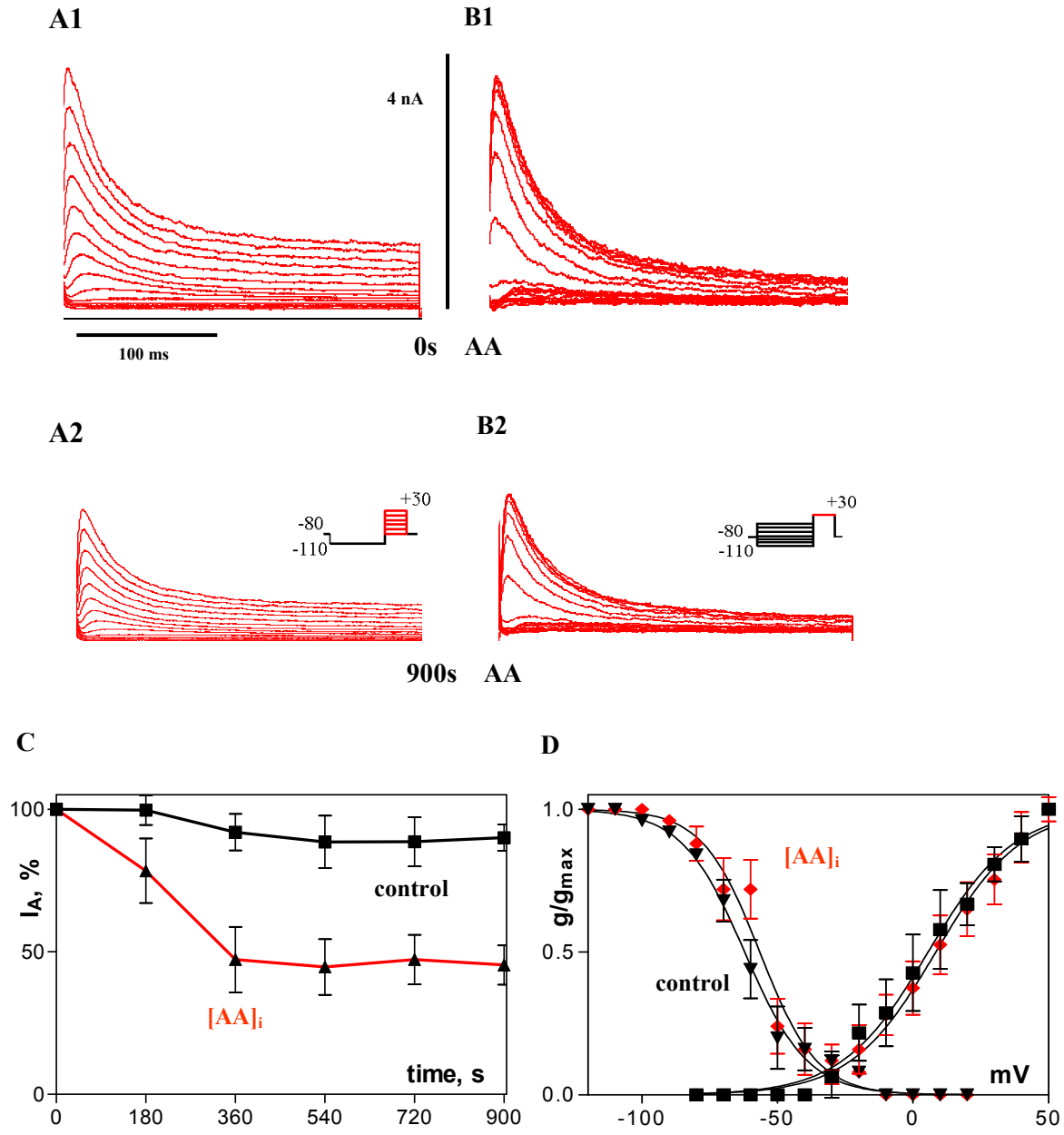

Fig. 44 Suppression of Kv4.2- I_A by arachidonic acid (AA).

A, B: Control activation (A1) and inactivation (B1) of I_A. Raw current traces of I_A are shown for control immediately after obtaining whole cell configuration (A1, B1, 0 s AA) and after 900 s of recording with 1 pM of AA in the patch pipette (A2, B2, 900 s AA). Pulse protocols: inset A2, B2. **C:** Intracellular application of 1 pM AA (red line) reduces the maximal transient potassium current (I_A) over time. **D:** Activation (left curves) and steady-state inactivation (right curves) kinetics in control condition (black symbols) and after application of 1 pM arachidonic acid through the pipette (red symbols).

Influence of Trolox on arachidonic acid-mediated effects

Again, Trolox C that showed the greatest potency as antioxidant in experiments with CA1, ECLII and III neurons, was used in Kv4.2–transfected HEK-293 cells to test the hypothesis that AA modulates the A-current through an oxidative mechanism.

Trolox failed to block the effect of 1 pM arachidonic acid on the maximal Kv4.2 current when applied to the pipette solution (-63.3 ± 7.1 %, vs. -54.4 ± 6.9 %; Fig.45 C). Intracellular Trolox had effect neither on the voltage dependence, nor on the time course of Kv4.2-current inactivation (Fig.45 B; D, left curves). In the presence of Trolox inside the cell V_{50} of Kv4.2-current inactivation was shifted from -82.5 ± 1.7 mV to -87.6 ± 1.0 mV and the slope factor changed from 17.5 ± 1.6 to 12.8 ± 0.9 (Fig.45 D, left curves).

As observed in Kv1.4-transfected HEK-293 cells, Trolox applied both through the pipette and the bath significantly attenuated the effect of 1 pM AA on the maximal conductance of Kv4.2 channels (-24.8 ± 7.4 % vs. -54.7 ± 6.9 %; Fig.46 C).

Trolox, applied to the both sides of the cell membrane dramatically affected Kv4.2 activation by shifting its voltage dependence to depolarizing direction from -25.7 ± 1.8 mV to 7.2 ± 0.6 mV (n=7) and altering its slope factor from 17.8 ± 1.7 to 13.1 ± 0.5 (Fig.46 D, right curves).

On the other hand, no effects of Trolox in/out +AA on Kv4.2-current time constant or voltage dependence of steady-state inactivation were observed (Fig.46 B, D, left curves, Table 11).

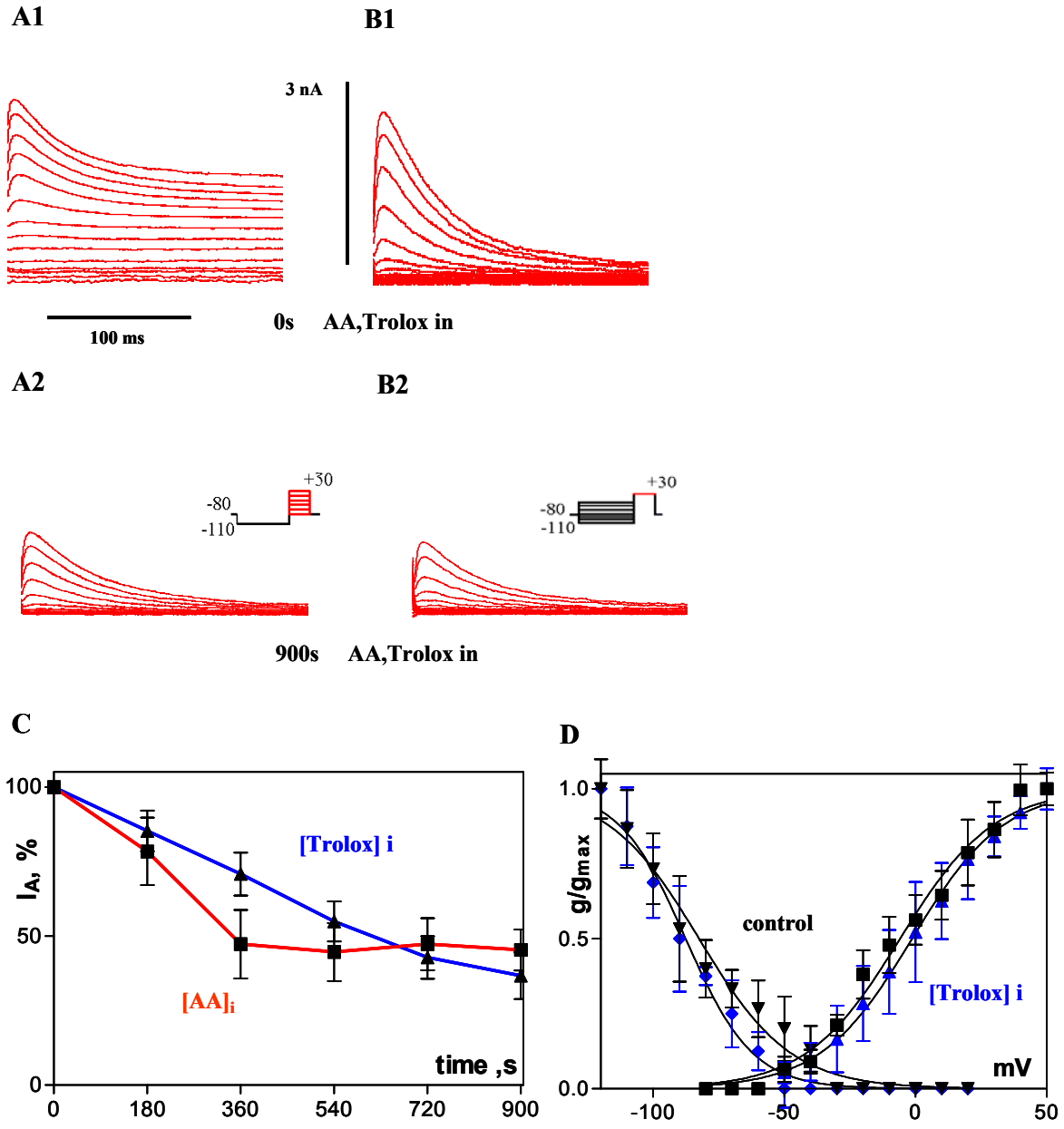

Fig. 45 Interaction of AA and Trolox$_{in}$ with I_A in Kv4.2-transfected HEK-293 cells.

A, B: Intracellular application of the vitamin E analogue Trolox (10 µM) with AA has similar effect on I_A as AA only (red line). Original traces for activation (A1, A2) and inactivation (B1, B2), immediately after obtaining whole-cell configuration (0 s, A1, B1) and after 900 s of recording (A2, B2). Protocols: inset A2 and B2. **C:** Intracellular Trolox (blue line) did not inhibit the AA-induced reduction of the maximal I_A amplitude (red line) over time. **D:** In the presence of Trolox on the inner side of the membrane plus AA_i (blue symbols), no significant changes in activation (right curves) and inactivation (left curves) kinetics occur in comparison to control activation and inactivation kinetics (black symbols).

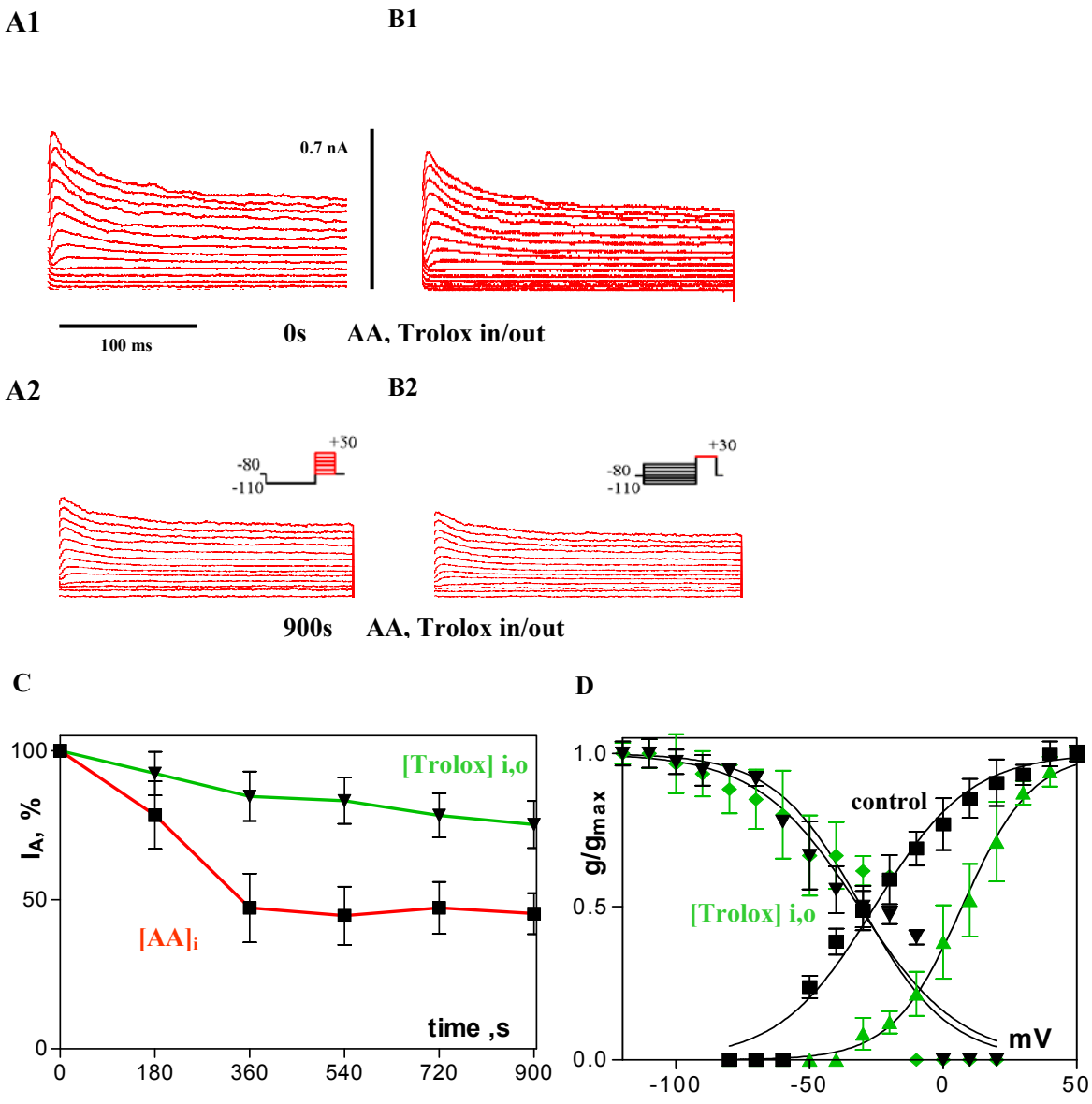

Fig. 46 Interaction of AA and Trolox$_{out}$ with I_A in Kv4.2-transfected HEK-293 cells.

A, B: Raw current traces for activation (A) and inactivation (B) of transient potassium current prior to (0 s) and after (900 s) application of AA+Trolox$_{in/out}$. Protocols: inset in A2, B2. **C**: Trolox, applied from both sides of the cell membrane (green line), did significantly recover I_A from 1 pM AA (red line). **D**: Intra- and extracellular application of Trolox (green symbols), together with AAi, causes a 30 mV shift to more positive direction of I_A activation (right curves), but does not affect its steady-state inactivation (left curves).

Table 11 Overview of effects of oxidants and antioxidants on behavior parameters of I_A in HEK-293 cells, transfected with Kv1.4 and Kv4.2.

I_A Kv1.4	n	max amplitude, % of control	V_{50a} 0 min mV	V_{50a} 15 min mV	$k_{activation}$ 0 min	k_a 15 min	V_{50i} 0 min mV	V_{50i} 15 min mV	$k_{inactivation}$ 0 min	k_i 15 min	τ_i 0 min ms	τ_i 15 min ms
Control	7	-12.1±6.1%	-24.7±2.4	-4.8±1.8	23.8±2.3	20.0±1.6	-70.0±2.1	-68.3±1.7	17.6±1.9	17.0±1.5	51.7±2.9	52.9±2.8
+ 1pM AA	9	-71.4±6.3%	-9.2±1.4	-5.2±1.6	17.1±1.3	19.4±1.5	-66.2±2.6	-75.5±2.1	19.6±2.2	22.6±1.9	52.8±2.8	49.4±2.4
AA+$Trolox_{in}$	9	-64.8±7.9%	-5.6±1.3	-37.1±1.8	18.1±1.2	12.8±1.6	-73.1±2.6	-75.6±2.0	20.6±2.4	21.7±1.9	34.3±2.9	47.9±3.2
AA+$Trolox_{in, out}$	6	-31.2±6.1%	-19.4±1.8	-23.6±2.0	17.2±1.6	17.2±1.8	-62.4±2.2	-60.6±1.8	14.0±1.9	13.5±1.6	67.4±4.8	75.9±3.9
I_A Kv4.2												
Control	6	-9.9±7.6%	-42.0±2.9	-42.9±2.4	18.4±2.7	16.6±2.2	-73.6±0.6	-68.8±0.7	7.1±0.5	7.3±0.6	35.6±3.9	32.5±3.6
+ 1pM AA	12	-54.7±6.9%	5.5±1.1	8.4±1.0	15.9±1.0	15.8±0.9	-62.2±0.8	-56.6±1.4	11.6±0.7	10.5±1.2	27.2±4.1	25.2±3.9
AA+$Trolox_{in}$	4	-63.3±7.1%	-5.9±1.4	-1.3±0.8	17.9±1.3	17.5±0.7	-82.5±1.7	-87.6±1.0	17.5±1.6	12.8±0.9	41.3±3.4	37.4±3.7
AA+$Trolox_{in, out}$	7	-24.8±7.4%	-25.7±1.8	7.2±0.6	17.8±1.7	13.1±0.5	-31.5±2.8	-30.6±3.7	19.0±2.5	16.3±3.3	24.5±4.8	25.6±4.6

DISCUSSION

Effect of arachidonic acid on the transient potassium current

In the present study, an ultra low patch pipette concentration of AA (1 pM) consistently inhibited the maximal conductance of the transient K^+ current I_A in all studied preparations.

In CA1 pyramidal neurons intracellular arachidonic acid reduced the maximal conductance of the transient potassium current I_A by about 45 %, while not affecting the delayed rectifier current $I_{k(v)}$. The effect of arachidonic acid develops over 15 min of dialysis in agreement with diffusional exchange between the patch pipette and soma / proximal dendrites of a CA1 pyramidal neuron (Pusch and Neher, 1988). ETYA, a non-metabolizable analogue of AA requires higher concentration (100 pM) to mimic the effect of 1 pM arachidonic acid. This may probably be due to substitution of the four highly reactive double carbon bonds of AA with the much more stable triple bonds of ETYA. Higher concentration is also probably the reason for the effect of ETYA to develop faster in comparison to those of AA. As ETYA inhibits the AA-metabolizing enzymes cyclooxygenase, lipoxygenase and cytochrome P450, these results suggest a direct specific effect of AA (1 pM) or ETYA (100 pM) on I_A. “Direct” should be understood as effect that is not exerted by AA metabolites and should not exclude the possibility that AA effects could be mediated by other processes or intermediate compounds, e.g. ROS production, altered redox potential or membrane fluidity.

The effect of 1 pM AA on the maximal conductance of IA is stronger in neurons from the entorhinal cortex, where IA was suppressed by 60-70 %.

1 pM AA affects clearly the inactivation of the A-channels. In addition to the reduction of the maximal conduction of I_A, AA causes a significant shift (~12 mV) of steady-state inactivation to more negative potentials in hippocampal, as well as entorhinal cortex neurons. This will correspond to a decrease in the probability of the channels to be found in open state at certain test voltage.

Thus, AA shift will cause further reduction of I_A by 10–40% when I_A is activated from a membrane potential of -60 to -50 mV. Actually, in neurons the transient potassium current I_A is comprised by Kv1.4 and Kv4.2 that belong to different gene subfamilies and the channels they form exhibit different types of inactivation. HEK-293 cell lines were transfected separately with cDNAs, coding only the pore-forming subunits of those channels. Interestingly, the effect of 1 pM AA on the maximal conductance was still present. I_A was reduced by ~ 70% in Kv1.4- and by ~ 55 % in Kv4.2-transfected HEK cells. There is, at first sight, a contradiction of the findings that Kv1.4 (*Shal* family) channel shows insensibility to 25 µM AA in *Xenopus oocytes* (Villarroel and Schwarz, 1996) and above presented results. In fact, it is already known, that the same channels in different expression systems may exhibit different values for time- and voltage-dependence or drug effects. It has been shown, for example, that kinetic properties of Kv 4.2- and Kv1.4-evoked currents depend strongly on the expression environment in experiment comparing ventricular myocytes, oocytes and HEK-293 cell lines (Petersen and Nerbonne, 1999). Additionally, some members of Shaw family also encode A-type currents albeit with lower 4-AP sensitivity. Products of Kv3.1 and Kv3.2 genes express delayed-rectifier type currents in heterologous expression systems, while Kv 3.3 and Kv3.4 proteins express A-type currents. However, Kv3.3 currents, which are also transient when expressed in *oocytes*, resemble Kv3.1 and Kv3.2 currents when expressed in CHO or HEK-293 cells (Rudy et al., 1999).

It must be noted that Kv1.4- and Kv4.2-elicited currents have some similarities with native currents, but in general possess quantitatively distinct properties, concerning time- and voltage-dependence. As observed by the present and other studies (Villarroel and Schwarz, 1996; Holmqvist et al., 2001), in different non-neuronal expression systems the reduction of the Kv-α-currents maximal amplitude by arachidonic acid isn’t accompanied by kinetic changes.

One can assume that this is due to absence of important auxiliary subunits and/or cytosol factors in the expression model system. In agreement, Kv1.4-transfetced HEK-293 cells exhibited A-type current with distorted inactivation in control conditions.

In addition, both Kv1.4 and Kv4.2 current inactivation is significantly slower compared to neuronal A-current. Moreover, in my study, the Kv-α-evoked currents inactivation in HEK 293 cells is in general insensitive to arachidonic acid. Taken together with the strong reduction of the maximal conductance of Kv-α-currents by 1 pM AA, one can hypothesize that there are at least two action sites for arachidonic acid to modulate A-channels and at least one of them is situated on or in the vicinity of the α-subunits. It can be also concluded that neuronal regulatory subunits are necessary for AA effect. Holmqvist et al, 2001, found out that KChIP1 is required for Kv4 current modulation by 10 μM arachidonic acid in Chinese hamster ovary (CHO) cells and *Xenopus oocytes*.

Oxidation is involved in arachidonic acid-mediated modulation of the A-current

Rationale for studying the oxidation as a mediating process for arachidonic acid modulation of potassium channels was its photo- and air-sensitivity. Unsaturated fatty acids are highly susceptible to oxidative breakdown (Frankel, 1984). PUFAs can autooxidize to form hydroperoxide, carbon or cyclic peroxy radicals. Therefore some researchers add ascorbic acid to protect arachidonic acid in solution from autooxidation. Further motivation was the fact that the concentration of arachidonic acid in effectively suppressing transient potassium current in my experiments is 1 pM. This extremely low concentration supposes very specific arachidonic acid-channel protein interaction or alternatively, an amplifying reaction, which would be in this case a radical chain reaction.

Moreover, oxidative stress is emerging as a cause and consequence of several neurodegenerative diseases, including Alzheimer's disease, temporal lobe epilepsy, Parkinson's disease, etc. Entorhinal cortex shows neuronal loss early in AD (layer II) and TLE (layer III). CA1 neurons from the hippocampus are damaged late in both diseases. Therefore, in this study the susceptibility of A-type potassium current to oxidative modulation in ECLII stellate cells, ECLIII and CA1 pyramidal neurons was compared. A-currents from the entorhinal cortex neurons are more sensitive to 1 pM AA.

Moreover, studies with antioxidants conclude involvement of oxidation in arachidonic acid effects. Both of the described AA effects, reduction of maximal conductance and shift of steady-state inactivation, are independently affected by GSH, ascorbic acid, Trolox and H_2O_2. These results further support the hypothesis that the effects of AA are mediated by at least two oxidation sites of the channel protein. The oxidation sites are most likely intracellular; as intracellular AA and membrane-impermeable antioxidants (Trolox, GSH) applied from the inside have strong effects. Surprisingly, intracellular application of 20 mM GSH did not block the effect of AA in CA1, ECLIII and ECLII neurons from brain slice, as reported for hippocampal neurons in primary culture (Bittner and Muller, 1999; Muller and Bittner, 2002), but strongly enhanced it, particularly at 3 min of whole-cell recording. In contrast, combination of GSHi with extracellular application of ascorbic acid (0.4 mM) significantly inhibited the reduction of I_A by AA in CA1 pyramidal neurons, but not in neurons from the entorhinal cortex. Shift of steady-state inactivation to more negative potentials was not affected by GSHi or by the combination of GSHi and ascorbic acid in CA1 or ECLII neurons, but was blocked in ECLIII pyramidal neurons. Additionally, GSH and ascorbic acid affected voltage dependence of activation in neurons from acute slice. Enhancement of the AA effect by some antioxidants may be mediated by catalysing the underlying reactions between AA and other radicals in the slice tissue and channel protein.

Antioxidants have some capacity to buffer oxidants but in this process they themselves become oxidants that may, in turn, more effectively oxidize certain targets. For example, GSH reductase becomes oxidized by the reduction of GSSG to GSH and, in turn, is reduced by oxidizing $NADP^+$ to NADPH, thereby acting as a catalyst of the reaction between $NADP^+$ and GSSG.

Very interesting and important finding of this study is the reduction of the transient and the delayed rectifier currents by antioxidants. In CA1 pyramidal neurons, GSH_{in} did not affected the maximal amplitudes of these currents, but shifted the voltage-conductance dependence in AA-similar way. Ascorbic $acid_{out}$ in turn dramatically suppressed I_A and $I_{K(V)}$ amplitudes, without affecting their voltage dependences of activation and inactivation. This suggests that potassium channels can sense redox changes.

Trolox applied from the inside blocks the reduction of the maximal amplitude of I_A by AA only in ECLIII pyramidal neurons, but abolishes AA effect on the voltage-conductance dependence inactivation in CA1 and ECLII neurons. In these two types of neurons $Trolox_{in}$ had the same enhancing influence on AA effect as GSH. Interestingly, intracellular Trolox by itself reduced I_A in CA1 pyramidal neurons and produced AA-similar shift of inactivation voltage-dependence. On the other hand, Trolox applied both inside and outside of the membrane significantly recover the AA-mediated reduction of I_A with prolonged recording time only in CA1 pyramidal neurons. Additionally, $Trolox_{in/out}$ completely block the effect of arachidonic acid on the maximal conductance of Kv1.4 and Kv4.2 channels. This further supports the reduction of maximal I_A conductance and shift of steady-state inactivation being independent modifications of the channel protein. Reduction of superoxide anions to H_2O_2 by superoxide dismutase gives an electroneutral molecule that much better permeates into lipid membranes (Nelson and Cox, 2005). Oxidation of channel proteins may be facilitated by antioxidants in a similar way. Such a view is further supported by the effects of H_2O_2 on I_A.

H_2O_2 as a model oxidative modulation of ion channels

Intracellular application of H_2O_2 reduced I_A more effectively than AA in CA1 pyramidal neurons, but to the same extent as AA in neurons from the entorhinal cortex.

Furthermore, H_2O_2 strongly reduced $I_{K(V)}$ in CA1 neurons. It has been shown that H_2O_2 dose-dependently enhances the cell membrane associated PLA_2 activity and stimulates AA-release (Chakraborti and Michael, 1993; Yasuda et al., 1999). Therefore, it is possible that the stronger effect of H_2O_2 is due to stimulating of AA release that in turn additionally reduces the A-current. The effect of H_2O_2 on the maximal conductance was abolished by antioxidants only in CA1 pyramidal neurons, whereas entorhinal cortex neurons showed no recovery.

On the other hand H_2O_2 shifted voltage-dependence of inactivation to the same extent as AA.

Unlike AA, H_2O_2 also reduced the maximal conductance of the delayed rectifier current $I_{K(V)}$ in a GSH_i-sensitive way, further supporting that the interaction of AA with I_A is highly specific.

Culture vs. Slices

The reduction of I_A by extremely low concentrations of intracellular arachidonic acid or by H_2O_2 is in agreement with experiments, conducted with cultured hippocampal neurons (Bittner and Muller, 1999; Muller and Bittner, 2002). Therefore, it was expected antioxidants to block arachidonic acid effects in acute slices, as it was reported for neurons from primary hippocampal culture (Bittner and Muller, 1999; Muller and Bittner, 2002). Unexpectedly, enhancement and acceleration of arachidonic acid effect by several antioxidative agents in brain slice were observed. This suggests fundamental differences of oxidative regulation of the A-current and Ikv in cultured hippocampal neurons, compared to neurons from brain slice.

It is possible that GSH is oxidized to GSSG that, in turn, more effectively oxidizes cystein, methionine or histidine residues in the channel protein that are not accessible to GSSG in cultured neurons because of subunit composition or differential expression of other interacting proteins. This may have implications for the relevance of excitotoxicity and oxidative stress research using neuronal cultures.

Neuronal cultures are criticized for abnormal neuronal behaviour that may result from developmental maturation under artificial conditions, leading many to favour acute brain slice preparations or *in vivo* recording. For example, inhibitory synapses in dissociated neuronal cultures exhibit abnormal physiology from postnatal day 6–15, continuing to show properties of early (postnatal day 1–5) postnatal synapses even after 13–21 days *in vitro* (Henneberger et al., 2005). Cortical oscillatory behaviour *in vivo* does not require GABA A-ergic transmission and disappears at postnatal day 6–7 (Garaschuk et al., 2000), but develops much more slowly in cortical cultures only after days 9–15 *in vitro* and requires GABAA receptor activation (Opitz et al., 2002).

In one hand, brain slices are usually maintained in a 95% O_2 atmosphere in order to avoid O_2-dependent cell damage at a depth of 90–150 μm below both surfaces of the slice, as observed for an interface slice configuration at 20% O_2 with histology (Bingmann and Kolde, 1982). On the other hand, in experiments concerning oxidative modulation of channel in brain slice neurons, 95% O_2 is an important issue. Actually, with an O_2 partial pressure of 600 mmHg (79%) in the perfusion, microelectrode measurements have shown steep gradients of O_2 partial pressure in the bath adjacent to the slice surface, with an O_2 pressure gradient inside brain tissue of 400-μm slices at 24°C from 60 to 15 mmHg, i.e. in a normal physiological range for neurons only 50 μm below the surface and a hypoxic range in the centre of the slice, with observations of vacuolization of cytoplasm even in 300-μm-thick slices (Bingmann and Kolde, 1982).

The work of Bingmann and Kolde (1982), comprising data from 300–1000-μm thick slices at temperatures from 24 to 35 °C, shows somewhat lower O_2 pressure at the submerged side of slices in comparison to the gas interface side, indicating even less efficient O_2 supply in the submerged configuration. In order to avoid tissue hypoxia, recordings from submerged slices are usually performed at temperatures of 24–32°C, significantly below 37°C (Colbert and Pan, 1999; Garaschuk et al., 2000; Henneberger et al., 2005). This appears to be essential for healthy brain slice electrophysiology and histology, typically showing excellent agreement with *in vivo* findings.

Role of membrane fluidity

Lipid molecules surround an ion channel in its native environment of cellular membranes. However, the importance of the lipid bilayer and the role of lipid/protein interactions in ion channel structure and function are not well understood. Rod MacKinnon group the presence of negatively charged lipids is required for ion conduction through the potassium channel, suggesting that the lipid bound to the channel protein is important for ion channel function (Valiyaveetil et al., 2002). They also recently demonstrated that the bacterial potassium channel KcsA binds a negatively charged lipid molecule and that lipids are required for the *in vitro* refolding of the channel tetramer from the unfolded monomeric state.

Moreover, in my experiments Trolox, that is known to be a potent antioxidant against lipid peroxidation, had the strongest effects in reduction of AA-induced reduction of I_A, particularly when applied on both sides of the membrane. Therefore, it is not excluded that arachidonic acid/ROS influence channel protein functions through changing annular and/or bulk fluidity of the membrane, although the hypothesis that arachidonic acid may affect Kv channels in *oocytes* by affecting the membrane fluidity was rejected by Villaroel and Schwarz in 1996 (Villarroel and Schwarz, 1996).

Arachidonic acid as a retrograde messenger

The participation of arachidonic acid and its metabolites in retrograde signaling and in other forms of local modulation of neuronal activity has been proposed (Kandel and O'Dell, 1992; Williams et al., 1989). It is well known that stimulation of glutamate receptors evokes arachidonic acid release in a variety of neural cell preparations. In agreement to that, nonselective PLA_2 inhibitors prevent induction of LTP, while application of arachidonic acid (or other unsaturated fatty acids) to hippocampal slices causes a slow-onset enhancement of synaptic transmission that resembles LTP. It is known that the fatty acid may increase glutamate release from hippocampal nerve terminals, block glutamate uptake, or potentiate NMDA receptor current (Freeman et al., 1990). Alternatively, it may act by enabling presynaptic glutamate receptors to produce enhanced glutamate release. After the discovery of the prostaglandins (PGs) in the CNS, much attention has been given to the role the eicosanoids may play in modulating neurotransmission, by interacting with presynaptic or with postsynaptic PG receptors. The existence of such receptors is well-demonstrated, and, in the brain, high-affinity binding sites have been described for both PGE2 and PGD2 (Yumoto et al., 1986).

On one hand, direct AA retrograde messaging is most likely not an issue, as the applied concentration of AA is extremely low (1 pM) and apparently not sufficient for building a gradient, that could facilitate AA diffusion through the neuronal membrane. On the other hand, various enzymes stay alert for immediate conversion of AA to one of its many metabolites, which had also been shown to play some role in induction of LTP.

1 pM AA most probably exert effects on synaptic transmission by attenuating the maximal conductance and diminishing the number of open A-type channels.

Kv4.2 and Kv1.4 are known to be substrates for all 4 enzymes, which participate in LTP: PKA, PKC, CaMKII and erk MAPK. On one hand, arachidonic acid can stimulate MAPK, probably through PKC (Hii et al., 1995). On the other hand it has been shown, that ROS could activate erk-s (Baas and Berk, 1995) and PKC (Gopalakrishna and Anderson, 1989). It is not excluded, that arachidonic acid modulates phosphorylation of channel proteins by these kinases via ROS production. However, the exact role of arachidonic acid in enhancing neurotransmission remains to be established. If AA is released in presynaptic terminals and suppresses I_A then Ca^{2+} influx into presnypatic terminals may be augmented and transmitter release subsequently increased. Expression of I_A has been described for mossy fiber terminals in CA3 and 4-AP has a strong effect on presynaptic Ca^{2+} uptake and on glutamate release.

Significance of potassium channel modulation by ROS

Oxidation-derived radical species were once considered to be metabolic by-products that have mostly negative function. In continuously growing body of evidence, ROS are recognized to have roles in cell signalling and to take part in number of cellular functions, such as O_2 sensing, cell proliferation, and apoptosis (Schafer and Buettner, 2001). Numerous K^+-channels and other transport mechanisms are in fact redox-regulated (Kourie, 1998). Redox response of K^+-channels may be a regulation mechanism to changes in the cellular metabolism.

Oxidizing and reducing agents produce functional changes, mostly of the channel protein itself. Typically, the gating characteristics are altered while the permeation properties remain largely unchanged.

Furthermore, each channel complex may contain multiple oxidation targets that determine the effect specificity. It is possible that different experimental reagents attack distinct target residues.

For example, cysteine oxidation decreases the overall channel activity by decreasing the number of channels available to open by driving the channels to a very long-lived closed state (Soto et al., 2002). Additional complexity in the oxidant sensitivity of K^+-channel is conferred by oxidation of methionine residues. Reversible oxidation of methionine has been suggested to play a role both as a regulatory mechanism and also as an endogenous oxidant scavenger system (Hoshi and Heinemann, 2001).

The pore-forming subunits Kv1.4 and Kv4.2 contain many different situated cysteine and methionine residues, and differential oxidation of these residues in HEK-293 cells may account for the diverse results reported here.

Oxidative regulation is also reported for many Kv channels both in native and heterologous systems (Rozanski and Xu, 2002). N-type inactivation of Kv1.4 is reversibly redox-modulated by means of a cysteine in the distal part of the N-terminal inactivating ball domain (Ruppersberg et al., 1991). Auxiliary subunits which specifically co-assemble with Kv-α, also provide cysteine-containing N-terminal ball domains to equip Kv-α with redox-dependent inactivation. Potentially, this may allow for greater precision in regulation, as thus metabolic and electric events are coupled. Still, experimental evidence to support this idea is not yet available.

Arachidonic acid, oxidative stress and neurodegenerative diseases

Oxidative stress has met continuously growing interest for its roles in the physiology and pathophysiology of immune defense, ischemia, and neurodegenerative disease. Reactive oxygen species modify ion channels and other transport mechanisms (Kourie, 1998).

In this study, entorhinal cortex (EC) layer II stellate neurons (that show neuronal loss early in AD) and layer III pyramidal neurons (are shown to be damaged early in TLE) are compared to hippocampal CA1 pyramidal neurons (that are damaged late in TLE and AD).

Furthermore, the present study supported the finding that antioxidants in particular cases could affect ion channel functions alone or by increasing the AA-induced reduction. Clearly, AA as well as H_2O_2, particularly in older age or in neurodegenerative disease (Auerbach and Segal, 1997), will strongly affect K^+-currents and, via depolarization and inactivation of Na^+-channels, dendritic excitability and spike-timing-dependent synaptic plasticity / learning (Giese et al., 1998). Antioxidative therapy as a part of neurodegenerative condition treatment program may then have negative effects in this context.

Mechanism of arachidonic acid modulation of Kv channels still remain to be discovered

Members from the same Kv families can co-assemble to form functional channels. Functionally, this has crucial implications for both physiology and pharmacology of the final K^+-channel expressed in the cell membrane. Therefore, one must exercise considerable caution when extrapolating data for a single channel subunit to a “real” channel in a “real” cell membrane. The complexity increases further, as K^+-channels can associate with a large number of 'accessory subunits', which can alter the properties of the resulting oligomeric channel even more.

Indeed, the total number of different subunits is even larger since many of the subunit genes undergo RNA processing, such as alternative splicing resulting in multiple protein products from each gene. Additionally, the diversity of K^+ channels is magnified by alternative splicing, RNA editing and posttranslational modifications (Coetzee et al., 1999).

A difficult question that is yet to be addressed adequately is where and how arachidonic acid and/or ROS could modulate Kv channel function.

CONCLUSION

Novel findings

The present study was undertaken to investigate the mechanism of modulation of transient potassium channels by arachidonic acid and possible involvement/contribution of free radicals to this process. Based on the presented results, the following novel findings could be briefly summarized as:

1) The transient potassium current (I_A) is extremely sensitive to intracellular arachidonic acid in neurons from acute slices. 1 pM AA was sufficient to reduce A-current by about 50 % in CA1 pyramidal neurons, by ~60 % in ELCIII pyramidal neurons and Kv4.2-transfected HEK293 cells, and by ~70% in ECLII stellate cells and Kv1.4-transfected HEK 293 cells.

2) The effect of AA on the transient potassium currents in ECLII stellate neurons, ECLIII pyramidal neurons and CA1 pyramidal neurons is mimicked by the polyunsaturated fatty acid ETYA. However, ETYA required 100-fold higher concentration. 3) The delayed rectifier current is in general (with exception of ECLII neurons) insensitive to 1 pM arachidonic acid. 4) AA-mediated modulation of I_A involves ROS formation, as some of the AA effects are blocked by antioxidants. 5) Existence of more than one modulation sites for arachidonic acid and H_2O_2 on potassium channel complex molecules is possible. 6) Neurons from the entorhinal cortex (LII and LIII) tend to be more sensitive to oxidative stress than CA1 pyramidal neurons. 7) Both delayed rectifier and transient potassium channels reacted to exogenously applied H_2O_2 with strong reduction of their conductivity. 8) In contrast to primary cultured neurons, H_2O_2 effects in acute brain slices were not always abolished by antioxidants, which reveal different mechanisms in current modulation in neurons from acute brain slices compared to neurons in culture. 9) Antioxidants by themselves may affect functionality of potassium channels.

Significance

The results from this study provided evidence that endogenously generated free radical processes contribute significantly to the regulation of Kv channels in entorhinal cortex and the hippocampus.

Outlook

The functional properties of many Kv channels are clearly altered by oxidizing and reducing treatments. How these oxidative modifications contribute to neuron and other cell function needs to be investigated. The results presented in this study, together with the recent findings in the field suggested, that we are just at the beginning of the revolution of the ROS-and O_2-signalling research that may shed light not only on normal biological functions of the brain, but on disease mechanisms that are so far poorly understood, as Alzheimer's, Parkinson's, schizophrenia, etc. Future research should focus on: 1) discovering molecular, physiological and pharmacological features of missing key elements of the functional channels; 2) their precise cellular and subcellular localization ; 3) biochemical machinery involved in channel modulation; 4) roles played by ROS in channel modulation in various neurological and psychiatric disorders; 5) novel ROS signalling pathways.

REFERENCES

Akil,M., and Lewis,D.A. (1997). Cytoarchitecture of the entorhinal cortex in schizophrenia. Am. J. Psychiatry *154*, 1010-1012.

An,W.F., Bowlby,M.R., Betty,M., Cao,J., Ling,H.P., Mendoza,G., Hinson,J.W., Mattsson,K.I., Strassle,B.W., Trimmer,J.S., and Rhodes,K.J. (2000). Modulation of A-type potassium channels by a family of calcium sensors. Nature *403*, 553-556.

Anderson,K.M., Roshak,A., Winkler,J.D., McCord,M., and Marshall,L.A. (1997). Cytosolic 85-kDa phospholipase A2-mediated release of arachidonic acid is critical for proliferation of vascular smooth muscle cells. J. Biol. Chem. *272*, 30504-30511.

Angelova,P., and Muller,W. (2006). Oxidative modulation of the transient potassium current IA by intracellular arachidonic acid in rat CA1 pyramidal neurons. Eur. J. Neurosci. *23*, 2375-2384.

Arnold,S.E., Franz,B.R., Gur,R.C., Gur,R.E., Shapiro,R.M., Moberg,P.J., and Trojanowski,J.Q. (1995). Smaller neuron size in schizophrenia in hippocampal subfields that mediate cortical-hippocampal interactions. Am. J. Psychiatry *152*, 738-748.

Auerbach,J.M., and Segal,M. (1997). Peroxide modulation of slow onset potentiation in rat hippocampus. J. Neurosci. *17*, 8695-8701.

Baas,A.S., and Berk,B.C. (1995). Differential activation of mitogen-activated protein kinases by H2O2 and O2- in vascular smooth muscle cells. Circ. Res. *77*, 29-36.

Bahring,R., Boland,L.M., Varghese,A., Gebauer,M., and Pongs,O. (2001). Kinetic analysis of open- and closed-state inactivation transitions in human Kv4.2 A-type potassium channels. J. Physiol *535*, 65-81.

Bast,A., Wolf,G., Oberbaumer,I., and Walther,R. (2002). Oxidative and nitrosative stress induces peroxiredoxins in pancreatic beta cells. Diabetologia *45*, 867-876.

Baxter,D.A., and Byrne,J.H. (1991). Ionic conductance mechanisms contributing to the electrophysiological properties of neurons. Curr. Opin. Neurobiol. *1*, 105-112.

Beck,E.J., Bowlby,M., An,W.F., Rhodes,K.J., and Covarrubias,M. (2002). Remodelling inactivation gating of Kv4 channels by KChIP1, a small-molecular-weight calcium-binding protein. J. Physiol *538*, 691-706.

Bevan,S., and Wood,J.N. (1987). Arachidonic-acid metabolites as second messengers. Nature *328*, 20.

Bingmann,D., and Kolde,G. (1982). PO2-profiles in hippocampal slices of the guinea pig. Exp. Brain Res. *48*, 89-96.

Bittner,K., and Muller,W. (1999). Oxidative downmodulation of the transient K-current IA by intracellular arachidonic acid in rat hippocampal neurons. J. Neurophysiol. *82*, 508-511.

Blaine,J.T., and Ribera,A.B. (2001). Kv2 channels form delayed-rectifier potassium channels in situ. J. Neurosci. *21*, 1473-1480.

Braak,H., and Braak,E. (1992). The human entorhinal cortex: normal morphology and lamina-specific pathology in various diseases. Neurosci. Res. *15*, 6-31.

Braak,H., and Braak,E. (1995). Staging of Alzheimer's disease-related neurofibrillary changes. Neurobiol. Aging *16*, 271-278.

Braak,H., and Braak,E. (1996). Evolution of the neuropathology of Alzheimer's disease. Acta Neurol. Scand. Suppl *165*, 3-12.

Campomanes,C.R., Carroll,K.I., Manganas,L.N., Hershberger,M.E., Gong,B., Antonucci,D.E., Rhodes,K.J., and Trimmer,J.S. (2002). Kv beta subunit oxidoreductase activity and Kv1 potassium channel trafficking. J. Biol. Chem. *277*, 8298-8305.

Carmody,R.J., McGowan,A.J., and Cotter,T.G. (1999). Reactive oxygen species as mediators of photoreceptor apoptosis in vitro. Exp. Cell Res. *248*, 520-530.

Chakraborti,S., and Michael,J.R. (1993). Role of protein kinase C in oxidant--mediated activation of phospholipase A2 in rabbit pulmonary arterial smooth muscle cells. Mol. Cell Biochem. *122*, 9-15.

Coetzee,W.A., Amarillo,Y., Chiu,J., Chow,A., Lau,D., McCormack,T., Moreno,H., Nadal,M.S., Ozaita,A., Pountney,D., Saganich,M., Vega-Saenz,d.M., and Rudy,B. (1999). Molecular diversity of K+ channels. Ann. N. Y. Acad. Sci. *868*, 233-285.

Colbert,C.M., and Pan,E. (1999). Arachidonic acid reciprocally alters the availability of transient and sustained dendritic K(+) channels in hippocampal CA1 pyramidal neurons. J. Neurosci. *19*, 8163-8171.

Connor,J.A., and Stevens,C.F. (1971). Voltage clamp studies of a transient outward membrane current in gastropod neural somata. J. Physiol *213*, 21-30.

Cooper,E.C., Milroy,A., Jan,Y.N., Jan,L.Y., and Lowenstein,D.H. (1998). Presynaptic localization of Kv1.4-containing A-type potassium channels near excitatory synapses in the hippocampus. J. Neurosci. *18*, 965-974.

Covarrubias,M., Wei,A.A., and Salkoff,L. (1991). Shaker, Shal, Shab, and Shaw express independent K+ current systems. Neuron *7*, 763-773.

Danthi,P., Tosteson,M., Li,Q.H., and Chow,M. (2003). Genome delivery and ion channel properties are altered in VP4 mutants of poliovirus. J. Virol. *77*, 5266-5274.

Davi,G., Ciabattoni,G., Consoli,A., Mezzetti,A., Falco,A., Santarone,S., Pennese,E., Vitacolonna,E., Bucciarelli,T., Costantini,F., Capani,F., and Patrono,C. (1999). In vivo formation of 8-iso-prostaglandin f2alpha and platelet activation in diabetes mellitus: effects of improved metabolic control and vitamin E supplementation. Circulation *99*, 224-229.

Dolorfo,C.L., and Amaral,D.G. (1998). Entorhinal cortex of the rat: organization of intrinsic connections. J. Comp Neurol. *398*, 49-82.

Du,F., Eid,T., Lothman,E.W., Kohler,C., and Schwarcz,R. (1995). Preferential neuronal loss in layer III of the medial entorhinal cortex in rat models of temporal lobe epilepsy. J. Neurosci. *15*, 6301-6313.

Du,F., Whetsell,W.O., Jr., bou-Khalil,B., Blumenkopf,B., Lothman,E.W., and Schwarcz,R. (1993). Preferential neuronal loss in layer III of the entorhinal cortex in patients with temporal lobe epilepsy. Epilepsy Res. *16*, 223-233.

Duerson,K., White,R.E., Jiang,F., Schonbrunn,A., and Armstrong,D.L. (1996). Somatostatin stimulates BKCa channels in rat pituitary tumor cells through lipoxygenase metabolites of arachidonic acid. Neuropharmacology *35*, 949-961.

Duprat,F., Guillemare,E., Romey,G., Fink,M., Lesage,F., Lazdunski,M., and Honore,E. (1995). Susceptibility of cloned K+ channels to reactive oxygen species. Proc. Natl. Acad. Sci. U. S. A *92*, 11796-11800.

Eberhart,C.E., and Dubois,R.N. (1995). Eicosanoids and the gastrointestinal tract. Gastroenterology *109*, 285-301.

Eder,C., Klee,R., and Heinemann,U. (1996). Modulation of A-currents by [K+]o in acutely isolated pyramidal neurones of juvenile rat entorhinal cortex and hippocampus. Neuroreport *7*, 1565-1568.

Freeman,E.J., Damron,D.S., Terrian,D.M., and Dorman,R.V. (1991). 12-Lipoxygenase products attenuate the glutamate release and Ca2+ accumulation evoked by depolarization of hippocampal mossy fiber nerve endings. J. Neurochem. *56*, 1079-1082.

Freeman,E.J., Terrian,D.M., and Dorman,R.V. (1990). Presynaptic facilitation of glutamate release from isolated hippocampal mossy fiber nerve endings by arachidonic acid. Neurochem. Res. *15*, 743-750.

Frisoni,G.B., Laakso,M.P., Beltramello,A., Geroldi,C., Bianchetti,A., Soininen,H., and Trabucchi,M. (1999). Hippocampal and entorhinal cortex atrophy in frontotemporal dementia and Alzheimer's disease. Neurology *52*, 91-100.

Garaschuk,O., Linn,J., Eilers,J., and Konnerth,A. (2000). Large-scale oscillatory calcium waves in the immature cortex. Nat. Neurosci. *3*, 452-459.

Giese,K.P., Fedorov,N.B., Filipkowski,R.K., and Silva,A.J. (1998). Autophosphorylation at Thr286 of the alpha calcium-calmodulin kinase II in LTP and learning. Science *279*, 870-873.

Gomez-Isla,T., Price,J.L., McKeel,D.W., Jr., Morris,J.C., Growdon,J.H., and Hyman,B.T. (1996). Profound loss of layer II entorhinal cortex neurons occurs in very mild Alzheimer's disease. J. Neurosci. *16*, 4491-4500.

Gong,M.C., Kinter,M.T., Somlyo,A.V., and Somlyo,A.P. (1995). Arachidonic acid and diacylglycerol release associated with inhibition of myosin light chain dephosphorylation in rabbit smooth muscle. J. Physiol *486 (Pt 1)*, 113-122.

Gopalakrishna,R., and Anderson,W.B. (1989). Ca2+- and phospholipid-independent activation of protein kinase C by selective oxidative modification of the regulatory domain. Proc. Natl. Acad. Sci. U. S. A *86*, 6758-6762.

Graham,F.L., and van der Eb,A.J. (1973). A new technique for the assay of infectivity of human adenovirus 5 DNA. Virology *52*, 456-467.

Gulbis,J.M., Mann,S., and MacKinnon,R. (1999). Structure of a voltage-dependent K+ channel beta subunit. Cell *97*, 943-952.

Hampson,A.J., and Grimaldi,M. (2002). 12-hydroxyeicosatetrenoate (12-HETE) attenuates AMPA receptor-mediated neurotoxicity: evidence for a G-protein-coupled HETE receptor. J. Neurosci. *22*, 257-264.

Hatano,N., Ohya,S., and Imaizumi,Y. (2002). Functional interaction between KChIP1 and GFP-fused Kv4.3L co-expressed in HEK293 cells. Pflugers Arch. *444*, 80-88.

Heinemann,S.H., Rettig,J., Graack,H.R., and Pongs,O. (1996). Functional characterization of Kv channel beta-subunits from rat brain. J. Physiol *493 (Pt 3)*, 625-633.

Heinemann,S.H., Rettig,J., Wunder,F., and Pongs,O. (1995). Molecular and functional characterization of a rat brain Kv beta 3 potassium channel subunit. FEBS Lett. *377*, 383-389.

Henneberger,C., Juttner,R., Schmidt,S.A., Walter,J., Meier,J.C., Rothe,T., and Grantyn,R. (2005). GluR- and TrkB-mediated maturation of GABA receptor function during the period of eye opening. Eur. J. Neurosci. *21*, 431-440.

Hii,C.S., Ferrante,A., Edwards,Y.S., Huang,Z.H., Hartfield,P.J., Rathjen,D.A., Poulos,A., and Murray,A.W. (1995). Activation of mitogen-activated protein kinase by arachidonic acid in rat liver epithelial WB cells by a protein kinase C-dependent mechanism. J. Biol. Chem. *270*, 4201-4204.

Hille,B. (1992). G protein-coupled mechanisms and nervous signaling. Neuron *9*, 187-195.

Hille,B. (1992) Ionic Channels of Excitable Membranes. Sinauer Associates Inc., Sunderland, Massachusetts.

Hoffman,D.A., Magee,J.C., Colbert,C.M., and Johnston,D. (1997). K+ channel regulation of signal propagation in dendrites of hippocampal pyramidal neurons. Nature *387*, 869-875.

Holmqvist,M.H., Cao,J., Hernandez-Pineda,R., Jacobson,M.D., Carroll,K.I., Sung,M.A., Betty,M., Ge,P., Gilbride,K.J., Brown,M.E., Jurman,M.E., Lawson,D., Silos-Santiago,I., Xie,Y., Covarrubias,M., Rhodes,K.J., Distefano,P.S., and An,W.F. (2002). Elimination of fast inactivation in Kv4 A-type potassium channels by an auxiliary subunit domain. Proc. Natl. Acad. Sci. U. S. A *99*, 1035-1040.

Hoshi,T., and Heinemann,S. (2001). Regulation of cell function by methionine oxidation and reduction. J. Physiol *531*, 1-11.

Hoshi,T., Zagotta,W.N., and Aldrich,R.W. (1990). Biophysical and molecular mechanisms of Shaker potassium channel inactivation. Science *250*, 533-538.

Hoshi,T., Zagotta,W.N., and Aldrich,R.W. (1991). Two types of inactivation in Shaker K+ channels: effects of alterations in the carboxy-terminal region. Neuron *7*, 547-556.

Hsueh,Y.P., and Sheng,M. (1998). Eph receptors, ephrins, and PDZs gather in neuronal synapses. Neuron *21*, 1227-1229.

Hwang,C., Sinskey,A.J., and Lodish,H.F. (1992). Oxidized redox state of glutathione in the endoplasmic reticulum. Science *257*, 1496-1502.

Isacoff,E.Y., Jan,Y.N., and Jan,L.Y. (1991). Putative receptor for the cytoplasmic inactivation gate in the Shaker K+ channel. Nature *353*, 86-90.

Isbrandt,D., Leicher,T., Waldschutz,R., Zhu,X., Luhmann,U., Michel,U., Sauter,K., and Pongs,O. (2000). Gene structures and expression profiles of three human KCND (Kv4) potassium channels mediating A-type currents I(TO) and I(SA). Genomics *64*, 144-154.

Jan,Y.N., and Jan,L.Y. (1990). Genes required for specifying cell fates in Drosophila embryonic sensory nervous system. Trends Neurosci. *13*, 493-498.

Jelsema,C.L., and Axelrod,J. (1987). Stimulation of phospholipase A2 activity in bovine rod outer segments by the beta gamma subunits of transducin and its inhibition by the alpha subunit. Proc. Natl. Acad. Sci. U. S. A *84*, 3623-3627.

Johnston,D., Hoffman,D.A., and Poolos,N.P. (2000). Potassium channels and dendritic function in hippocampal pyramidal neurons. Epilepsia *41*, 1072-1073.

Kandel,E.R., and O'Dell,T.J. (1992). Are adult learning mechanisms also used for development? Science *258*, 243-245.

Keros,S., and McBain,C.J. (1997). Arachidonic acid inhibits transient potassium currents and broadens action potentials during electrographic seizures in hippocampal pyramidal and inhibitory interneurons. J. Neurosci. *17*, 3476-3487.

Keyser,D.O., and Alger,B.E. (1990). Arachidonic acid modulates hippocampal calcium current via protein kinase C and oxygen radicals. Neuron *5*, 545-553.

Kim,D., and Clapham,D.E. (1989). Potassium channels in cardiac cells activated by arachidonic acid and phospholipids. Science *244*, 1174-1176.

Kim,D., and Duff,R.A. (1990). Regulation of K+ channels in cardiac myocytes by free fatty acids. Circ. Res. *67*, 1040-1046.

Klee,R., Ficker,E., and Heinemann,U. (1995). Comparison of voltage-dependent potassium currents in rat pyramidal neurons acutely isolated from hippocampal regions CA1 and CA3. J. Neurophysiol. *74*, 1982-1995.

Kourie,J.I. (1998). Interaction of reactive oxygen species with ion transport mechanisms. Am. J. Physiol *275*, C1-24.

Krimer,L.S., Herman,M.M., Saunders,R.C., Boyd,J.C., Hyde,T.M., Carter,J.M., Kleinman,J.E., and Weinberger,D.R. (1997). A qualitative and quantitative analysis of the entorhinal cortex in schizophrenia. Cereb. Cortex *7*, 732-739.

Kuo,H.C., Cheng,C.F., Clark,R.B., Lin,J.J., Lin,J.L., Hoshijima,M., Nguyen-Tran,V.T., Gu,Y., Ikeda,Y., Chu,P.H., Ross,J., Giles,W.R., and Chien,K.R. (2001). A defect in the Kv channel-interacting protein 2 (KChIP2) gene leads to a complete loss of I(to) and confers susceptibility to ventricular tachycardia. Cell *107*, 801-813.

Leslie,C.C. (1997). Properties and regulation of cytosolic phospholipase A2. J. Biol. Chem. *272*, 16709-16712.

Leslie,C.C. (2004). Regulation of the specific release of arachidonic acid by cytosolic phospholipase A2. Prostaglandins Leukot. Essent. Fatty Acids *70*, 373-376.

Lin,L.L., Lin,A.Y., and Knopf,J.L. (1992). Cytosolic phospholipase A2 is coupled to hormonally regulated release of arachidonic acid. Proc. Natl. Acad. Sci. U. S. A *89*, 6147-6151.

Liss,B., and Roeper,J. (2001). Molecular physiology of neuronal K-ATP channels (review). Mol. Membr. Biol. *18*, 117-127.

Liu,Y., and Gutterman,D.D. (2002). The coronary circulation in diabetes: influence of reactive oxygen species on K+ channel-mediated vasodilation. Vascul. Pharmacol. *38*, 43-49.

Loo,R.W., Conde-Frieboes,K., Reynolds,L.J., and Dennis,E.A. (1997). Activation, inhibition, and regiospecificity of the lysophospholipase activity of the 85-kDa group IV cytosolic phospholipase A2. J. Biol. Chem. *272*, 19214-19219.

Machlin,L.J., and Bendich,A. (1987). Free radical tissue damage: protective role of antioxidant nutrients. FASEB J. *1*, 441-445.

MACLEAN,P.D. (1952). Some psychiatric implications of physiological studies on frontotemporal portion of limbic system (visceral brain). Electroencephalogr. Clin. Neurophysiol. Suppl *4*, 407-418.

Maletic-Savatic,M., Lenn,N.J., and Trimmer,J.S. (1995). Differential spatiotemporal expression of K+ channel polypeptides in rat hippocampal neurons developing in situ and in vitro. J. Neurosci. *15*, 3840-3851.

Mathern,G.W., Babb,T.L., Micevych,P.E., Blanco,C.E., and Pretorius,J.K. (1997). Granule cell mRNA levels for BDNF, NGF, and NT-3 correlate with neuron losses or supragranular mossy fiber sprouting in the chronically damaged and epileptic human hippocampus. Mol. Chem. Neuropathol. *30*, 53-76.

McCormack,K., McCormack,T., Tanouye,M., Rudy,B., and Stuhmer,W. (1995). Alternative splicing of the human Shaker K+ channel beta 1 gene and functional expression of the beta 2 gene product. FEBS Lett. *370*, 32-36.

McCormack,T., and McCormack,K. (1994). Shaker K+ channel beta subunits belong to an NAD(P)H-dependent oxidoreductase superfamily. Cell *79*, 1133-1135.

Meves,H. (1994). Modulation of ion channels by arachidonic acid. Prog. Neurobiol. *43*, 175-186.

Muller,W., and Bittner,K. (2002b). Differential oxidative modulation of voltage-dependent K+ currents in rat hippocampal neurons. J. Neurophysiol. *87*, 2990-2995.

Muller,W., and Misgeld,U. (1990). Inhibitory role of dentate hilus neurons in guinea pig hippocampal slice. J. Neurophysiol. *64*, 46-56.

Muller,W., and Misgeld,U. (1991). Picrotoxin- and 4-aminopyridine-induced activity in hilar neurons in the guinea pig hippocampal slice. J. Neurophysiol. *65*, 141-147.

Nadal,M.S., Ozaita,A., Amarillo,Y., Vega-Saenz de,M.E., Ma,Y., Mo,W., Goldberg,E.M., Misumi,Y., Ikehara,Y., Neubert,T.A., and Rudy,B. (2003a). The CD26-related dipeptidyl aminopeptidase-like protein DPPX is a critical component of neuronal A-type K+ channels. Neuron *37*, 449-461.

Nakamura,T.Y., Nandi,S., Pountney,D.J., Artman,M., Rudy,B., and Coetzee,W.A. (2001). Different effects of the Ca(2+)-binding protein, KChIP1, on two Kv4 subfamily members, Kv4.1 and Kv4.2. FEBS Lett. *499*, 205-209.

Nelson, D.L. & Cox, M.M. (2005) Lehninger Principles of Biochemistry. W.H. Freeman, New York.

Nishiyama,M., Okamoto,H., Watanabe,T., Hori,T., Hada,T., Ueda,N., Yamamoto,S., Tsukamoto,H., Watanabe,K., and Kirino,T. (1992). Localization of arachidonate 12-lipoxygenase in canine brain tissues. J. Neurochem. *58*, 1395-1400.

Nishiyama,M., Watanabe,T., Ueda,N., Tsukamoto,H., and Watanabe,K. (1993). Arachidonate 12-lipoxygenase is localized in neurons, glial cells, and endothelial cells of the canine brain. J. Histochem. Cytochem. *41*, 111-117.

O'Keefe,J., and Conway,D.H. (1978). Hippocampal place units in the freely moving rat: why they fire where they fire. Exp. Brain Res. *31*, 573-590.

Opitz,T., De Lima,A.D., and Voigt,T. (2002). Spontaneous development of synchronous oscillatory activity during maturation of cortical networks in vitro. J. Neurophysiol. *88*, 2196-2206.

Ordway,R.W., Singer,J.J., and Walsh,J.V., Jr. (1991). Direct regulation of ion channels by fatty acids. Trends Neurosci. *14*, 96-100.

Pak,M.D., Baker,K., Covarrubias,M., Butler,A., Ratcliffe,A., and Salkoff,L. (1991). mShal, a subfamily of A-type K+ channel cloned from mammalian brain. Proc. Natl. Acad. Sci. U. S. A *88*, 4386-4390.

Pardo,L.A., Heinemann,S.H., Terlau,H., Ludewig,U., Lorra,C., Pongs,O., and Stuhmer,W. (1992). Extracellular K+ specifically modulates a rat brain K+ channel. Proc. Natl. Acad. Sci. U. S. A *89*, 2466-2470.

Petersen,K.R., and Nerbonne,J.M. (1999). Expression environment determines K+ current properties: Kv1 and Kv4 alpha-subunit-induced K+ currents in mammalian cell lines and cardiac myocytes. Pflugers Arch. *437*, 381-392.

Petroni,A., Blasevich,M., Salami,M., Papini,N., Montedoro,G.F., and Galli,C. (1995). Inhibition of platelet aggregation and eicosanoid production by phenolic components of olive oil. Thromb. Res. *78*, 151-160.

Piomelli,D. (1993). Arachidonic acid in cell signaling. Curr. Opin. Cell Biol. *5*, 274-280.

Piomelli,D., Shapiro,E., Feinmark,S.J., and Schwartz,J.H. (1987). Metabolites of arachidonic acid in the nervous system of Aplysia: possible mediators of synaptic modulation. J. Neurosci. *7*, 3675-3686.

Po,S., Roberds,S., Snyders,D.J., Tamkun,M.M., and Bennett,P.B. (1993). Heteromultimeric assembly of human potassium channels. Molecular basis of a transient outward current? Circ. Res. *72*, 1326-1336.

Pomposiello,S., Rhaleb,N.E., Alva,M., and Carretero,O.A. (1999). Reactive oxygen species: role in the relaxation induced by bradykinin or arachidonic acid via EDHF in isolated porcine coronary arteries. J. Cardiovasc. Pharmacol. *34*, 567-574.

Pomposiello,S.I., Carroll,M.A., Falck,J.R., and McGiff,J.C. (2001). Epoxyeicosatrienoic acid-mediated renal vasodilation to arachidonic acid is enhanced in SHR. Hypertension *37*, 887-893.

Pongs,O. (1992). Molecular biology of voltage-dependent potassium channels. Physiol Rev. *72*, S69-S88.

Pongs,O. (1999). Voltage-gated potassium channels: from hyperexcitability to excitement. FEBS Lett. *452*, 31-35.

Pouzet,B., Welzl,H., Gubler,M.K., Broersen,L., Veenman,C.L., Feldon,J., Rawlins,J.N., and Yee,B.K. (1999). The effects of NMDA-induced retrohippocampal lesions on performance of four spatial memory tasks known to be sensitive to hippocampal damage in the rat. Eur. J. Neurosci. *11*, 123-140.

Pusch,M., and Neher,E. (1988). Rates of diffusional exchange between small cells and a measuring patch pipette. Pflugers Arch. *411*, 204-211.

Rettig,J., Heinemann,S.H., Wunder,F., Lorra,C., Parcej,D.N., Dolly,J.O., and Pongs,O. (1994). Inactivation properties of voltage-gated K+ channels altered by presence of beta-subunit. Nature *369*, 289-294.

Roshak,A., Sathe,G., and Marshall,L.A. (1994). Suppression of monocyte 85-kDa phospholipase A2 by antisense and effects on endotoxin-induced prostaglandin biosynthesis. J. Biol. Chem. *269*, 25999-26005.

Rozanski,G.J., and Xu,Z. (2002). Glutathione and K(+) channel remodeling in postinfarction rat heart. Am. J. Physiol Heart Circ. Physiol *282*, H2346-H2355.

Rudy,B. (1988). Diversity and ubiquity of K channels. Neuroscience *25*, 729-749.

Rudy,B., Chow,A., Lau,D., Amarillo,Y., Ozaita,A., Saganich,M., Moreno,H., Nadal,M.S., Hernandez-Pineda,R., Hernandez-Cruz,A., Erisir,A., Leonard,C., and Vega-Saenz de,M.E. (1999). Contributions of Kv3 channels to neuronal excitability. Ann. N. Y. Acad. Sci. *868*, 304-343.

Ruppersberg,J.P., Stocker,M., Pongs,O., Heinemann,S.H., Frank,R., and Koenen,M. (1991). Regulation of fast inactivation of cloned mammalian IK(A) channels by cysteine oxidation. Nature *352*, 711-714.

Ruth,R.E., Collier,T.J., and Routtenberg,A. (1982). Topography between the entorhinal cortex and the dentate septotemporal axis in rats: I. Medial and intermediate entorhinal projecting cells. J. Comp Neurol. *209*, 69-78.

Ruth,R.E., Collier,T.J., and Routtenberg,A. (1988). Topographical relationship between the entorhinal cortex and the septotemporal axis of the dentate gyrus in rats: II. Cells projecting from lateral entorhinal subdivisions. J. Comp Neurol. *270*, 506-516.

Salkoff,L., Baker,K., Butler,A., Covarrubias,M., Pak,M.D., and Wei,A. (1992). An essential 'set' of K+ channels conserved in flies, mice and humans. Trends Neurosci. *15*, 161-166.

Samad,T.A., Moore,K.A., Sapirstein,A., Billet,S., Allchorne,A., Poole,S., Bonventre,J.V., and Woolf,C.J. (2001). Interleukin-1beta-mediated induction of Cox-2 in the CNS contributes to inflammatory pain hypersensitivity. Nature *410*, 471-475.

Schafer,F.Q., and Buettner,G.R. (2001). Redox environment of the cell as viewed through the redox state of the glutathione disulfide/glutathione couple. Free Radic. Biol. Med. *30*, 1191-1212.

Schoppa,N.E., and Westbrook,G.L. (1999). Regulation of synaptic timing in the olfactory bulb by an A-type potassium current. Nat. Neurosci. *2*, 1106-1113.

Schweitzer,P., Madamba,S., and Siggins,G.R. (1990). Arachidonic acid metabolites as mediators of somatostatin-induced increase of neuronal M-current. Nature *346*, 464-467.

Serodio,P., Kentros,C., and Rudy,B. (1994). Identification of molecular components of A-type channels activating at subthreshold potentials. J. Neurophysiol. *72*, 1516-1529.

Serodio,P., Vega-Saenz,d.M., and Rudy,B. (1996). Cloning of a novel component of A-type K+ channels operating at subthreshold potentials with unique expression in heart and brain. J. Neurophysiol. *75*, 2174-2179.

Sheng,M., Liao,Y.J., Jan,Y.N., and Jan,L.Y. (1993). Presynaptic A-current based on heteromultimeric K+ channels detected in vivo. Nature *365*, 72-75.

Sheng,M., Tsaur,M.L., Jan,Y.N., and Jan,L.Y. (1992). Subcellular segregation of two A-type K+ channel proteins in rat central neurons. Neuron *9*, 271-284.

Shi,G., Nakahira,K., Hammond,S., Rhodes,K.J., Schechter,L.E., and Trimmer,J.S. (1996). Beta subunits promote K+ channel surface expression through effects early in biosynthesis. Neuron *16*, 843-852.

Sobey,C.G., Heistad,D.D., and Faraci,F.M. (1997). Mechanisms of bradykinin-induced cerebral vasodilatation in rats. Evidence that reactive oxygen species activate K+ channels. Stroke *28*, 2290-2294.

Soto,M.A., Gonzalez,C., Lissi,E., Vergara,C., and Latorre,R. (2002). Ca(2+)-activated K+ channel inhibition by reactive oxygen species. Am. J. Physiol Cell Physiol *282*, C461-C471.

Spencer,S.S., and Spencer,D.D. (1994). Entorhinal-hippocampal interactions in medial temporal lobe epilepsy. Epilepsia *35*, 721-727.

Squire,L.R. (1992). Memory and the hippocampus: a synthesis from findings with rats, monkeys, and humans. Psychol. Rev. *99*, 195-231.

Steward,O., and Scoville,S.A. (1976). Cells of origin of entorhinal cortical afferents to the hippocampus and fascia dentata of the rat. J. Comp Neurol. *169*, 347-370.

Stuhmer,W., Ruppersberg,J.P., Schroter,K.H., Sakmann,B., Stocker,M., Giese,K.P., Perschke,A., Baumann,A., and Pongs,O. (1989). Molecular basis of functional diversity of voltage-gated potassium channels in mammalian brain. EMBO J. *8*, 3235-3244.

Taglialatela,M., Castaldo,P., Iossa,S., Pannaccione,A., Fresi,A., Ficker,E., and Annunziato,L. (1997). Regulation of the human ether-a-gogo related gene (HERG) K+ channels by reactive oxygen species. Proc. Natl. Acad. Sci. U. S. A *94*, 11698-11703.

Trevisi,L., Bova,S., Cargnelli,G., Ceolotto,G., and Luciani,S. (2002). Endothelin-1-induced arachidonic acid release by cytosolic phospholipase A2 activation in rat vascular smooth muscle via extracellular signal-regulated kinases pathway. Biochem. Pharmacol. *64*, 425-431.

Valiyaveetil,F.I., Zhou,Y., and MacKinnon,R. (2002). Lipids in the structure, folding, and function of the KcsA K+ channel. Biochemistry *41*, 10771-10777.

Vane,J.R. (1976). Prostaglandins as mediators of inflammation. Adv. Prostaglandin Thromboxane Res. *2*, 791-801.

Vega-Saenz de,M.E., and Rudy,B. (1992). Modulation of K+ channels by hydrogen peroxide. Biochem. Biophys. Res. Commun. *186*, 1681-1687.

Villarroel,A., and Schwarz,T.L. (1996). Inhibition of the Kv4 (Shal) family of transient K+ currents by arachidonic acid. J. Neurosci. *16*, 2522-2532.

Wang,F.C., Parcej,D.N., and Dolly,J.O. (1999). alpha subunit compositions of Kv1.1-containing K+ channel subtypes fractionated from rat brain using dendrotoxins. Eur. J. Biochem. *263*, 230-237.

Watanabe,S., Hoffman,D.A., Migliore,M., and Johnston,D. (2002). Dendritic K+ channels contribute to spike-timing dependent long-term potentiation in hippocampal pyramidal neurons. Proc. Natl. Acad. Sci. U. S. A *99*, 8366-8371.

Wei,A., Covarrubias,M., Butler,A., Baker,K., Pak,M., and Salkoff,L. (1990). K+ current diversity is produced by an extended gene family conserved in Drosophila and mouse. Science *248*, 599-603.

Weiss,J.L., and Burgoyne,R.D. (2001). Voltage-independent inhibition of P/Q-type Ca2+ channels in adrenal chromaffin cells via a neuronal Ca2+ sensor-1-dependent pathway involves Src family tyrosine kinase. J. Biol. Chem. *276*, 44804-44811.

Williams,J.H., Errington,M.L., Lynch,M.A., and Bliss,T.V. (1989). Arachidonic acid induces a long-term activity-dependent enhancement of synaptic transmission in the hippocampus. Nature *341*, 739-742.

Witter,M.P., Groenewegen,H.J., Lopes da Silva,F.H., and Lohman,A.H. (1989). Functional organization of the extrinsic and intrinsic circuitry of the parahippocampal region. Prog. Neurobiol. *33*, 161-253.

Witter,M.P., Wouterlood,F.G., Naber,P.A., and van,H.T. (2000). Anatomical organization of the parahippocampal-hippocampal network. Ann. N. Y. Acad. Sci. *911*, 1-24.

Wong,W., Newell,E.W., Jugloff,D.G., Jones,O.T., and Schlichter,L.C. (2002). Cell surface targeting and clustering interactions between heterologously expressed PSD-95 and the Shal voltage-gated potassium channel, Kv4.2. J. Biol. Chem. *277*, 20423-20430.

Yasuda,Y., Yoshinaga,N., Murayama,T., and Nomura,Y. (1999). Inhibition of hydrogen peroxide-induced apoptosis but not arachidonic acid release in GH3 cell by EGF. Brain Res. *850*, 197-206.

Yu,M., onso-Galicia,M., Sun,C.W., Roman,R.J., Ono,N., Hirano,H., Ishimoto,T., Reddy,Y.K., Katipally,K.R., Reddy,K.M., Gopal,V.R., Yu,J., Takhi,M., and Falck,J.R. (2003). 20-hydroxyeicosatetraenoic acid (20-HETE): structural determinants for renal vasoconstriction. Bioorg. Med. Chem. *11*, 2803-2821.

Yumoto,N., Hatanaka,M., Watanabe,Y., and Hayaishi,O. (1986). Involvement of GTP-regulatory protein in brain prostaglandin E2 receptor and separation of the two components. Biochem. Biophys. Res. Commun. *135*, 282-289.

Zagotta,W.N., Hoshi,T., and Aldrich,R.W. (1990). Restoration of inactivation in mutants of Shaker potassium channels by a peptide derived from ShB. Science *250*, 568-571.

Zahradnik,H.P., Schafer,W., Neulen,J., Wetzka,B., Gaillard,T., Tielsch,J., and Casper,F. (1992). The role of eicosanoids in reproduction. Eicosanoids *5 Suppl*, S56-S59.

Zhang,L., and McBain,C.J. (1995). Voltage-gated potassium currents in stratum oriens-alveus inhibitory neurones of the rat CA1 hippocampus. J. Physiol *488 (Pt 3)*, 647-660.

Zhu,X.R., Wulf,A., Schwarz,M., Isbrandt,D., and Pongs,O. (1999). Characterization of human Kv4.2 mediating a rapidly-inactivating transient voltage-sensitive K+ current. Receptors. Channels *6*, 387-400.

Zola-Morgan,S.M., and Squire,L.R. (1990). The primate hippocampal formation: evidence for a time-limited role in memory storage. Science *250*, 288-290.

Zona,C., Palma,E., Pellerin,L., and Avoli,M. (1993). Arachidonic acid augments potassium currents in rat neocortical neurones. Neuroreport *4*, 359-362.

ERKLÄRUNG

Entsprechend der Promotionsordnung der Mathematisch-Naturwissenschaftlichen Fakultät I der Humboldt Universität zu Berlin erkläre ich, Plamena Angelova, geboren am 4 Juli 1977, an Eides Statt dass:

-ich mich an keinem anderen Ort um einen Doktorgrad beworben habe oder bereits einen solchen besitze,

-mir die genannte Promotionsordnung bekannt ist,

-ich die vorliegende Arbeit selbständig erarbeitet und verfasst habe und hierfür ausschließlich die angegebenen Quellen und Hilfsmittel verwendet habe.

Plamena Angelova Palo Alto, den 29. September 2006

DANKSAGUNG

The experimental work was performed in the Neuroscience Research Center, Department of Neurophysiology at Charité-Medical School, Humboldt University of Berlin during the years 2002 - 2005. Data analysis and manuscript writing were accomplished in Biblioteka National-Santiago de Chile and Lane Medical Library at Stanford University, CA, USA.

First of all, I am greatly indebted to Prof. Dr. Uwe Heinemann for giving me the opportunity to work in Johannes Müller Institute of Neurophysiology and to join Graduate School (GRK) 283. I truly appreciate his valuable criticism and encouragement during my work in Berlin.
I would like to thank Prof. Dr. Wolfgang Müller for accepting me in his group, his guidance during my work in NWFZ and expert comments for improving the manuscript.
Thanks to all my colleagues from the former AG Müller: Dr. Philppe Alix, Dr. Scott Adams, Dr. Ivan Raginov, Dr. Jochen Winterer, Siarhei Kirko, Adrij Volynets, Dr. Denis Bragin, Pamela Liebig and Sabrina Rötger for the unbelievable working atmosphere, helpful discussions and support at everyday work.
I thank PD Dr.Stephan Baader, Institute for Anatomy, Friedrich Wilhelm University of Rhein, Bonn for generously providing the Kv1.4, Kv4.2 and EGFP cDNAs.
I would also like to thank our administrative assistants - Mrs. Sonja Frosinski, Dr. Katrin Schultze and Mrs. Margaret Franke for their essential help through the years.
Thanks belong to all my student colleagues and friends from GRK 238 for their collaboration and ever friendly attitude.
I'm grateful to Ass. Prof. Dr.Virjinia Doltchinkova from Sofia University and Prof. Dr. Hermann Berg from Saxonian Academy of Sciences for encouraging me to start PhD and for continuous moral support.
I thank my family for their years-long patience and support.
Finally, but not last, I owe my warmest thanks to Dr. Albrecht Stroh for his everlasting support and encouragement during these years.

Herzlichen Dank!

EIGENE PUBLIKATIONEN

29.9.2006

- Traytcheva, N., **Angelova, P**., Radeva, M. and H. Berg; ELF Fields and Photooxidation Yelding Lethal Effects on Cancer Cells. In *Bioelectromagnetics 24: 148-150 (2003)*

- Doltchinkova, V., **Angelova, P**., Ugrinov, K.; Effect of bee venom melittin on biological membranes III. Electrokinetic properties of rat liver mitochondria. In *Annuaire de l'universite de Sofia'St.Kliment Ohridski' (2003)*

- Egorov, A., **Angelova, P**., Heinemann, U. and W.Müller, Ca^{2+} -independent muscarinic excitation of rat medial entorhinal cortex layer V neurons. In *Eur.J.Neuroscience 18: 3343-3351(2003)*

- Radeva, M.**,** Lambreva, M., **Angelova, P**., Traytcheva, N. and H. Berg; Synergisms of Electric or Electromagnetic fields and Photodynamic Effects Induce Apoptosis and Necrosis of Cancer Cells. In *Electrochemistry 10: 260-270 (2004)*

- **Angelova, P**. and W. Müller; Oxidative modulation of transient potassium current I_A by intracellular arachidonic acid in rat CA1 pyramidal neurons. In *Eur.J.Neuroscience 23: 2375-2384(2006)*

- Doltchinkova, V., **Angelova, P**., Parvanova, D.; Light-induced changes of surface electric charge in freezing tolerant tobacco thylakoids. *Under revision*

- **Angelova, P**. and W. Müller; Differential oxidative modulation of potassium currents by arachidonic acid and hydrogen peroxide in entorhinal cortex LII, LIII and CA1 hippocampal neurons. *In preparation*

Konferenzbeiträge

- **Angelova, P**., V. Doltchinkova - Oxygen Evolution, Electrokinetic and Light Scattering Properties of Pea Thylakoids, 2000, *Tribuna Medica*, vol. 2, pp. 58-59.

- Doltchinkova, V., **P. Angelova,** K. Ugrinov **-** Surface Electrical Properties of Rat Liver Mitochondria. Effect of Melittin, 2001, *5th National Congress of Biochemistry, Biophysics and Molecular Biology*, 29.-31. März, Sofia, Bulgarien.

- **Angelova, P.**, V. Doltchinkova, P. Ivanova, Sv. Dimov- Low Temperature Stress in Transgenic Tobacco Plants. Electrokinetic, Structural and Functional Studies, 2001, *National Scientific Students' Session*, 4.-5. Mai, Sofia, Bulgarien.

- Berg, H., **P. Angelova** – The synergism of Electromagnetic Field and Photodynamic Effect on Cancer Cells, 2002, *International Symposium : Endogenous Physical Fields in Biology*, 1.-3. Juli, Prag, Tschechische Republik

- **Angelova, P.**, W. Müller.– Modulation of transient potassium current by arachidonic acid of rat central neurons in brain slices, 2004, *International Symposium : Hippocampal function and dysfunction*, 19.-22. Februar, Schloss Blankensee, Deutschland

- **Angelova, P.,** W. Müller -Modulation of transient K^+-current by intracellular arachidonic acid in rat hippocampal pyramidal neurons, 2004, *83 Annual Meeting of The German Physiological Society,* 14.-17. März, Leipzig, Deutschland

- **Angelova, P.**, W. Müller-Direct modulation of transient K^+-current by arachidonic acid in rat CA1 and entorhinal cortex pyramidal neurons, 2004, *Berlin Neuroscience Forum,* 22.-24. April, Liebenwalde, Deutschland

- **Angelova, P.**, W. Müller -Modulation of the transient potassium current I_A by intracellular arachidonic acid in rat central neurons in brain slice, 2004, *34 Annual Meeting of Society for Neuroscience,* 23.-28. Oktober, San Diego, USA

- **Angelova, P.**, W. Müller -Oxidative modulation of transient potassium current I_A by intracellular arachidonic acid in rat pyramidal CA1 neurons, 2005, *35 Annual Meeting of Society for Neuroscience,* 12.-16. November, Washington DC, USA

- Doltchinkova, V., **P. Angelova**, D. Parvanova, E. Ivanova- Genetically-modified osmoprotectant accumulation alters thylakoid surface charge under cold stress , 2006, *31st FEBS Congress*, 24.-29. Juni, Istanbul, Türkei

- **Angelova, P.**, W. Müller -Differential oxidative modulation of potassium currents by arachidonic acid and hydrogen peroxide in rat entorhinal cortex LII, LIII and CA1 hippocampal neurons , 2006, *36 Annual Meeting of Society for Neuroscience,* 14.-18. Oktober, Atlanta, USA